ISAS - INTERNATIONAL SCHOOL FOR ADVANCED STUDIES

Academic year 1985 - 86

NON-LOCAL OVERSHOOTING AND THE EVOLUTION OF SINGLE STARS

Thesis for the title of
"Doctor Philosophiae"

Candidate:
ALESSANDRO BRESSAN

Supervisor:
Prof. CESARE CHIOSI

Trieste 5 - 12 - 1986

TABLE OF CONTENTS

A

ISAS-INTERNATIONAL SCHOOL FOR ADVANCED STUDIES

Academic year 1985-86

NON-LOCAL OVERSHOOTING AND THE EVOLUTION OF SINGLE STARS

Thesis for the title of
"Doctor Philosophiae"

Candidate:
ALESSANDRO BRESSAN

Supervisor:
Prof. CESARE CHIOSI

Trieste 5 - 12 - 1986

Introduction

In this thesis I will discuss the possibility of removing unexpected features which arise when comparing theoretical predictions of standard stellar evolution with observational data, assuming that convection in stellar interiors is to be treated in a more consistent way. In standard model computations the determination of the sole acceleration field is performed, while several theoretical and observational aspects suggest that this may lead to a severe underestimate of the true convective field.

For this purpose several criteria have been recently developed, which account for a velocity field and thus provide a more physical description of convection, but none of them is free from arbitrary parameters.

The determination of the parameter in my non local treatment of convection, through an extensive comparison of model predictions and observed features in the whole HR diagram, will be performed in this thesis along the following sequence.

In chapter I after a brief discussion of the standard criterion for determining the extension of the central convective region, I will introduce a new criterion which accounts for the velocity field and, consequently, for the penetration of convective motions inside surrounding stable layers (overshooting). In chapter II the results of the comparison of a set of new models

computed with the above prescriptions, with the observational scenario in the domain of massive stars, will be presented.

In chapter III the same convective criterion will be tested in the range of intermediate mass stars and it will be shown that a new panorama emerges from these models that better agrees with several observational facts among which I recall the width of the main sequence band of galactic clusters, the morphology of populous young clusters in LMC (NGC1866 as a prototype) and the absence, there, of luminous Asymptotic Giant Branch stars (a problem which is related to the determination of M_{UP}) and finally the disagreement between evolutionary and pulsational mass of Cepheid stars.

In chapter IV the same analysis will be performed for low mass stars and it will be shown that models computed with the new criterion better reproduce the observational transition mass between low and intermediate mass stars.

In chapter V, I will enter the domain of globular clusters through the comparison of a theoretical lifetime ratio, provided by a new set of models of Horizontal Branch stars, and an observed number ratio, which is particularly sensitive to the interior mixing in a star. This last investigation provide one with the most reliable value of the above parameter which turns out to be about equal to the one used in previous chapters of this thesis. On the contrary I will show that other convective criteria (like semiconvection plus breathing convection) which

may alleviate same discrepancies in a different area of the HR diagram (but not other discrepances), are unlikely to be correct in this domain of stellar evolution.

Finally chapter VI contains the conclusions, from which one sees that non local convective overshooting is the most suitable model for treats stellar convective cores, as it turns out that with the same parameter a variety of different and independent aspects of observed stellar evolution may be explained.

CHAPTER I

1.1 Convection inside stellar cores

The standard treatment of convection in stellar interiors rests upon the simple analysis which leads to the so-called Schwarzschild's criterion. For a chemically homogeneous medium simple considerations (Cox and Giuli 1968 p. 262) show that the sufficient condition for stability against convection may be expressed in terms of the temperature gradient as follows:

$$\partial T/\partial r_{matter} > \partial T/\partial r_{adiabatic}$$

which may also be written as :

$$\nabla_{radiative} < \nabla_{adiabatic}$$

where $\nabla = \partial \ln T/\partial \ln P$; T,P are the local values of the temperature and pressure of the medium and r is its radial coordinate in the usual approximation of spherical symmetry.

It is important to realize that this criterion defines the zones that are convectively stable or unstable; but it cannot say anything about the nature of the convective medium. This requires the solution of the full system of fluidodynamic equations which, by itself, is one of the greatest task of physics. To avoid the excessive complexity , a number of approximations are introduced

which lead to very simple models of convection and the one which is mostly employed in stellar evolution is that of the Mixing Length Theory (Bohm-Vitense 1958). In this approximation convection is described by means of eddies that maintain their own identity along a mean free path l ,before dissolving and mixing with the surrounding matter. l is a free parameter in the theory and usually it is expressed as a fraction of a characteristic scale height, say the pressure scale height H_p:

$$(H_p)^{-1} = P^{-1} \partial P/\partial r$$

$$l = \lambda \cdot H_p \quad ;$$

λ is the so called mixing length parameter. When this theory is applied to the convective cores of stellar models it, turns out that the efficiency of convection (defined as the ratio between the excess heat content of the eddies when they dissolve and the energy they lose during the motion), is so high that convective elements may be treated as adiabatic (Cox and Giuli 1968). Moreover convective velocities are high enough to ensure complete mixing during the main evolutionary phases. Therefore standard evolutionary computations adopt the following scheme to deal with the convective cores:

i) first the extension of the unstable region is determined by means of the Schwarzschild criterion.

ii) then one assumes that convection extends and instantaneously mixes over the whole unstable region.

iii) the run of the temperature is determined by the adiabatic temperature gradient.

This description is said to be a local one because only local quantities (temperature, pressure and their derivatives with respect to the radial coordinate) enter the determination of extension of the convective region; the inertia of motions which require a non-local description is completely neglected. In other words only the acceleration field is considered (the unstable region) and nothing is said about the velocity field inside convective cores. Thus it is implicitly assumed that the extension of convective motions inside stable regions, which in advance we will call "overshooting", is negligibly small. However, as we will see, to neglect this phenomenon may lead to important consequences in stellar evolution.

1.2 Non-local treatment of convection.

In the last few years non-local approaches in the treatment of convective cores aimed to the determination of the extension of the velocity field, have been the subject of a great amount of theoretical work. First attempts to evaluate the extension of the overshooting region lead to the conclusion that overshooting was negligibly small. (Roxburgh 1965, Saslow and Schwarzschild 1965). Contrary to what believed, recent studies about this phenomenon show that the scale length of the overshooting region is a non negligible fraction of the mixing length itself (Shaviv and

Salpeter 1973 , Maeder 1975 , Maeder and Mermilliod 1981, Xiong 1985). Most of the recent studies rest upon some parameters that introduce a degree of arbitrariness which may be eliminated only through a careful comparison between model predictions and observations. Although based on rather arbitrary assumptions about this parameterization, some works clearly illustrate the model response to a variation of the mass size of the mixed region (Massevitch et al. 1979, Doom 1982 a,b) More realistic treatments rest upon some extension of the Mixing Length Theory (Maeder 1975, Bressan et al. 1981, Matraka et al. 1982) thus having as a free parameter the mixing length itself. Further investigations describe convection in terms of turbulence, introducing the characteristic scale length of turbulence as a free parameter. However, Roxburghh (1975) has derived a particular formulation to treat convective overshooting which is intended to improve upon other previous descriptions of this physical phenomenon ,mainly because its final formulation does not contain arbitrary free parameters.

However this formulation has been questioned by Eggleton (1983) on the basis of general arguments such that of the case of a completely convective star. Recently Doom (1984) revisited Roxburgh's criterion and gave it a physical interpretation in terms of kinetic energy flux.

Owing to the relevance of the Roxburgh's criterion for determining the extension of the convective region, due to its

independence of any parameter, Bressan (1984) performed a careful reexamination of the whole problem (see appendix), showing that Roxburgh' relation rests upon an incorrect approximation in the averaged equation of fluidodynamics. That analysis has been independently performed by Baker and Kuhfuss (1986) who arrived to the same conclusions.

It is important to stress here the need of some arbitrary parameter for a non local description of convection; moreover, as we are dealing with something which, by itself is not directly "observable" from outside, we are left with the hard task of evaluating this parameter from the effects it produces as the models evolve. Then a series of evolutionary sequences has to be computed varying such a parameter, and model predictions have to be compared with observations. This requires a lot of computational effort, even if convection is treated locally; when a non local criterion is introduced the situation gets much worse. In fact one of the most serious difficulties in dealing with overshooting is that iterative procedures are usually required which enormously increase the computing time (20 time longer using Maeder's algorithm). Therefore when evolutionary sequences were calculated ,the amount of overshooting was tested only in some models and then fixed during subsequent evolution. However recently, Bressan et al.(1981) have developed a new method which, in the framework of the mixing length theory, enables one to calculate overshooting from convective cores in a

simple way and with a reasonable amount of computational effort. New investigations on stellar evolution described in the following sections will mainly rest upon this criterion.

1.3 The overshooting model of Bressan, Bertelli and Chiosi (1981)

The method proposed for evaluating the layer reached by convective elements which overshoot from the unstable core rests on the following scheme. It seems reasonable (Shaviv and Salpeter 1973, Maeder 1975) that, independently from the theory adopted to follow convective motions, the temperature distribution in deep interiors of the stars can be the one characterized by the adiabatic gradient up to the region where velocities of convective elements vanish. To determine the border of the convective region one may proceed in the following way. In the framework of the mixing length theory the acceleration given to a rising convective element is expressed by:

$$v_r \frac{\partial v_r}{\partial r} = -g \frac{\Delta \rho}{\rho} \qquad (1)$$

where g,r,v are the gravitational acceleration,density and velocity. Dρ is the density defect and it is given by:

$$\Delta \rho(r) = \int_{r_1}^{r} \left[\frac{\partial \rho^*}{\partial r'} - \frac{\partial \rho}{\partial r'} \right] dr' \qquad (2)$$

where r_1 is the starting level ,asterisk refers to convective

elements and other quantities to the surrounding matter. By means of equation of state eq. (2) may be written as:

$$\Delta\rho = -\int_{r_1}^{r} \frac{\rho}{T}\,\frac{\chi_T}{\chi_\rho}\left(\frac{\partial T^*}{\partial r'} - \frac{\partial T}{\partial r}\right) dr' + \int_{r_1}^{r} \frac{\rho}{\mu}\,\frac{\chi_\mu}{\chi_\rho}\,\frac{\partial \mu}{\partial r'}\,dr' \qquad (3)$$

here T and m are the temperature and molecular weight and

$$\chi_T = \left.\frac{\partial \ln P}{\partial \ln T}\right|_{\rho,\mu}$$

$$\chi_\rho = \left.\frac{\partial \ln P}{\partial \ln \rho}\right|_{T,\mu}$$

$$\chi_\mu = \left.\frac{\partial \ln P}{\partial \ln \mu}\right|_{\rho,T}$$

The convective flux Fc at a level r carried by elements originating at level r_1 is given by:

$$F_c = K C_p \rho v_r \int_{r_1}^{r} \left[\frac{\partial T^*}{\partial r'} - \frac{\partial T}{\partial r'}\right] dr' \qquad (4)$$

where C_p is the specific heat at constant pressure and the factor K takes into account some average between rising and falling elements. From equation (3) and equation (4) one can see that it is possible to express the quantity Dr in equation (2) if some average values $\langle \rho/T, \chi_T/\chi_\rho \rangle$ and $\langle \rho/\mu, \chi_\mu/\chi_\rho \rangle$ over the distance $r - r_1$ are assumed, by means of the convective flux F_c and the

molecular weight m. Then equation (2) becomes:

$$v\frac{\partial v}{\partial r} = \frac{g}{\rho}\left\langle\frac{\chi_T}{\chi_\rho}\frac{\rho}{T}\right\rangle\frac{F_c}{\kappa c_p \rho v} - \frac{g}{\rho}\left\langle\frac{\chi_\mu}{\chi_\rho}\frac{\rho}{\mu}\right\rangle\Delta\mu \qquad (5)$$

where $D\mu = \mu(r) - \mu r_1)$.

The convective flux Fc can be derived from the equality

$$F_{tot} = F_R + F_c \qquad (6)$$

where F_{tot} is the total available energy flux (generated by nuclear sources). It has to be stressed that this treatment holds only in convective cores, where the real gradient is known to be approximately given by the adiabatic one; in this way the radiative flux F_R is known and then from equation (6) one gets the convective flux F_c. This does not hold in outer convective layers in which the real gradient strongly depends on the convective flux itself or even in the deep interiors if the real gradient significantly deviates from the adiabatic one. All quantities being known, integration of equation (5) is carried out from an initial level r_i out to the level r_i+l (where l is the mixing length), or out to the level at which velocity vanishes (inside the stable region). Integration is repeated in such a way that r_i scans the whole unstable region and the highest level at which velocity is not zero is chosen to be the border of the convective core. Some comments are needed about equation (5). Viscosity has been neglected at all; this is because of the high Reynolds number characterizing stellar interiors (due to large dimensions of eddies = l), which is a

dimensionless measure of the ratio between inertial and viscosity terms in the momentum conservation equation of fluidodynamics. However, viscosity may be introduced in equation (5) through a term proportional to some power of the velocity. The average quantities in equation (5) may also be substituted by local ones without affecting significantly the results (numerical experiments have been performed). With all these simplifications equation (5) is easily adapted to numerical computation on a Henyey scheme; the required time is only a factor of two or less greater than the one of standard models and comparable or even less with respect to models that account for semiconvection.

As far as the term involving the molecular weight difference Dm is concerned, order of magnitude estimates show that when $Dm \neq 0$ the convective motions abruptly stops. In fact, the negative contribution given by this term is by several orders of magnitude greater than that of the temperature excess. However if the mixing process is assumed to be very efficient (the timescales of convective motions 1/v are much smaller than nuclear timescales), then arguments invoked by Castellani et al (1971), indicate that in a very short time, barriers of molecular weight might be eroded. Therefore the term containing the molecular weight can be treated a part from the main equation, for instance by comparing the characteristic time scale of the erosion with the nuclear time scale. The influence of the molecular weight barrier turns out to be important only at the end of central Helium burning,

where the models undergo periodic variations of the convective region (breathing pulses of convection Castellani et al 1985) in a time scale comparable and even shorter than that of the mixing of the fresh fuel itself.

Chapter II

2.1 Massive stars

In this chapter I summarize the results of the study of the effect of convective overshooting on the evolution of luminous massive stars during both the Hydrogen and Helium burning phases. However as there are other important phenomena which strongly affect the evolution of massive stars and their appearance in the HR diagram, like mass loss or enhanced outer layers opacity, it will be difficult to constraint the amount of overshooting from the statistics of luminous stars only.

First I will describe some general features of models with overshooting and compare them with standard models or with models with overshooting computed with other algorithms. Then after a brief description of the evolution of massive stars with constant mass (conservative case) I will consider the more plausible case of evolution with mass loss and overshooting. Finally the amount of observational data available for luminous stars will be analysed in order to get a consistent comparison with the panorama proposed by the new models.

2.2 The initial homogeneous model

Some results of the application of the new criterion for convective cores described in the previous chapter, to

homogeneous models are shown in Figure (2.1) and they are compared with a model of different stellar mass obtained by Maeder(1975) who employed a different non local criterion - Figure (2.2a). The mixing length inside the convective core in all the following models is chosen to be one pressure scale height; that is the overshooting parameter is chosen to be $\Lambda = 1$. If other values are used they are explicitly given in the text.

I stress here that standard models do not require any specification of the mixing length in deep interiors, because there the convection is treated locally. In Figure (2.1) the velocity curves for three homogeneous models of mass 100, 60, 20 M_o and chemical composition X,Y,Z =0.7,0.28,0.02 are shown. Vertical dashed lines indicate the point where the usual Schwarschild's criterion holds, showing that the overshooting region extends far beyond this point. The percentage amount in mass of overshooting region for the above models is respectively 6%, 14% and 38%; that is the percentage amount of overshooting increases as the mass decreases and, as we will see, it reaches 100% or more in the domain of low mass stars. No important differences in the internal structure between models with and without overshooting exist, as can be seen from Figure (2.2b) (Maeder 1975). The only main difference when overshooting is accounted for is in the size of the mixed region. This however will have important effects in the subsequent evolution.

2.3 Overshooting in massive stars

Massive stars are defined to be those stars that never experience a condition of degeneracy in the core and then undergo quiescent ignition of all nuclear fuels . In the standard theory the minimum mass for this range is of about 10-12 Mo. A number of evolutionary tracks for this range of masses may be found in the literature (Chiosi and Summa 1971; Chiosi et al. 1978; Maeder 1982 a,b; Doom 1982a,b Doom 1985; Doom et al. 1986; Sybesma 1985,1986) and a very recent review of massive star evolution in Chiosi and Maeder 1986; the results presented here rest on the work of Bressan, Bertelli and Chiosi (1981) and Bertelli, Bressan and Chiosi (1984 a). Tables (2.1) and (2.2) show some characteristic quantities of the models of 20, 60, 100 M_o (chemical composition X,Z=0.7,0.02) during the phase of central H burning on the Zero Age Main Sequence (ZAMS) -point a)- and at the minimum effective temperature -point b)-. Also models with mass loss are included as it will be discussed in the following section.

i) Evolution at constant mass.

There are only slight differences in the luminosity and effective temperature (Teff) between models with overshooting (Λ=1) and standard ones on the ZAMS (set A and A' respectively). As evolution proceeds the effects of an enlarged size of the convective core cause the models with overshooting to be cooler

and more luminous. The 100 Mo model reaches the red zone in the H-R diagram while burning Hydrogen in the center. The larger luminosity is more than compensated by the extended convective region so that these models have a Hydrogen burning lifetime which is longer than that of the standard ones -about 30%,15%,11% for 20,60,100 M_o models. For more massive stars this fraction is lower because they are already characterized by a very large convective core. Because of the strong evidence of mass loss from massive stars we keep the discussion of this case very short; I only notice that the widening of the higher main sequence band is strongly at variance with the observations, so that overshooting alone does not reproduce even the morphology of the HR diagram of massive stars.

ii) Evolution with mass loss.

Recently a variety of formulations have been proposed to account for mass loss during the evolution of the more massive stars (see Chiosi and Maeder 1986 for an exhaustive review on the subject). All of them contain some free parameters to be adjusted in order to represent the increasing amount of observational data; up to date the only model in which a consistent picture between the external atmosphere and the internal structure of the star has been approached is that by Calvani Nobili and Turolla (1986) but it only applies to extreme cases in which a super Eddington luminosity appears. In the models I present here mass loss has been included according to the formalism of Castor,Abbot and

Klein (1975):

$$dM/dt = (L/cV_{th})\cdot(\alpha/\Gamma)\cdot (1-\alpha)/(1-\Gamma)^{(1-\alpha)/\alpha} \cdot(K\Gamma)^{1/\alpha}$$

where c = light velocity; V_{th} = thermal velocity; Γ = ratio of luminosity L to the Eddington luminosity; α κ parameters chosen to be 0.83 and 0.01 respectively (Chiosi et al. 1978).

Under the effects of mass loss and overshooting the main sequence band widens at lower masses more than in the case of overshooting alone. On the contrary, for more massive stars (about 100 Mo) the main sequence band shrinks toward the ZAMS. This behaviour can be attributed to the pealing off of the envelope which ,in the case of overshooting, is very efficient due to the increased lifetime. The 100 Mo and 60 Mo models show at their surfaces, during Hydrogen burning, highly CNO processed material (the Hydrogen abundance by mass at the surface is X_s = 0.360 and 0.504 respectively) as the pealing has already reached the molecular weight profile generated by the receding convective core.

Figure (2.3) show how the main sequence band is affected by different prescriptions in model computations.

iii) He burning phase

As far as central Helium burning is concerned, all models with overshooting alone spend this part of their life near the Hayashi line in the H-R diagram. For the models having both overshooting and mass loss the behaviour depends critically on their initial mass and on the rate of mass loss in the red. More massive stars have already a low Hydrogen content at their surfaces so that

they stay on the Helium main sequence from the beginning of the Helium burning; less massive stars start burning Helium as red giants and only if mass loss is able to peal off the Hydrogen rich envelope they will spend the last phase of He burning in the blue region.

All models burn helium with a considerably higher luminosity, due to the enlarged inert Helium core left out after Hydrogen burning, and overshooting during this phase does not compensate for this effect, so that lifetimes are shorter than that of the standard case.

2.4 Comparison with observations.

A great effort has been recently made to infer some constraints on evolution of massive stars from observational data. A fairly complete set of luminous stars with Mb < -7 and within 2.5 Kpc around the Sun, is now available from the works of Humphreys(1978), Humphreys and Davidson(1979), Garmany et al.(1982). The H-R diagram for supergiant stars in young clusters and associations in the solar vicinity shows the following mean features, Figure (2.4):

i) a group of very luminous O and B stars with $M_{bol} < -10$

ii) an envelope of decreasing temperature with declining luminosity for the hottest stars, with an upper limit for M supergiants at about $-10 < M_{bol} < -9.5$

iii) A continuous distribution of stars in the luminosity range

$-9.5 < M_{bol} < -7$, up to spectral type A0 with a remarkable crowding in the range B0-B2, a gap for spectral types F,G,K and a clump of M type stars.

The standard theory of massive star evolution predicts a zone in the H-R diagram in which models evolve in a Kelvin time scale after the end of Hydrogen burning and the beginning of Helium burning. However no gap of this type exists among stars more massive than about 15 M_o. The inclusion of mass loss somewhat relaxes this discrepancy for stars more massive than about 40-50 Mo, but the problem still remains for less massive stars. As can be seen from Figure (2.3) this situation may not be improved by models with overshooting alone because they predict too many bright stars in the region of more luminous supergiants (moreover mass loss is an "observed" phenomenon). This discrepancy between theory and observations has been also noticed by Meylan and Maeder(1982). They have performed a comparative analysis of the colour-magnitude diagrams of 23 young clusters (age $< 2*10^7$ years) in the Galaxy, Large and Small Magellanic Clouds. The observations of galactic clusters (11) were compared with theoretical evolutionary tracks accounting for a moderate mass loss rate but not for overshooting (Maeder 1981a,b). In Table (2.3) the lifetime ratios over the total one are compared with observed frequencies for each spectral type. The inescapable conclusion is that about 30% more stars are observed out of the predicted main sequence. Models with overshooting and mass loss,

on the contrary, greatly improve upon the agreement between theory and observations. In the highest part of the H-R diagram they predict a narrow main sequence band (as it is observed), while in the lowest part they predict a widening up to $LogT_{eff}=4.3$ with a lifetime in this extended region comparable with that of the Helium burning. Furthermore Bertelli, Bressan and Chiosi(1984) isolated among the Humphreys catalogue a strip at limiting magnitudes $-7 < M_{bol} < -9$ and improved this set with the help of the Garmany et al. (1982) catalogue of bright O stars and with the Van der Hutcht et al. (1981) catalogue of Wolf Rayet stars (which current scenario explains as post red supergiant stars). Table (2.4) shows observed absolute numbers N and number ratios N/N_t for three different groupings. Each of these follow a scenario proposed by the theoretical evolution which rests upon the previous models; standard evolution, standard plus mass loss, overshooting plus mass loss. These scenarios predict a main sequence widening, respectively, up to the spectral types O9.5, B0.5, B1. If a continuous star formation is assumed, then the number ratio inside the main sequence band has to match the lifetime ratio of the corresponding phase. The last is given approximately by the Q values involved in the Hydrogen and Helium nuclear reaction energy release (slightly modified by the core mass extent); one may guess that the Helium burning lifetime is at most 10% of the total lifetime (our models give about 6%). This is the number of stars one expects to escape the observed

main sequence band. It is soon evident that a great discrepancy exists between theory and observation, as suggested from the number ratios of Table (2.4). For the most favourable case still a 20% of stars are out of the main sequence band which corresponds at more than two times the Helium burning lifetime. Moreover this case was obtained with an intermediate mass loss rate while current observations indicate that in the domain of this comparison a much lower mass is lost (Garmany et al.1981). This means that an overshooting parameter is required higher than $\Lambda = 1$ used for those computations, as shown by Figure (2.4) (Bertelli, Bressan and Chiosi 1984). However other effects might be responsible for the main sequence widening. The above authors investigated on the role played by radiative opacities and on that of non hydrostatic atmospheres. They came to the conclusion that opacities with features like those proposed by Carson(1976) could lead to theoretical results in good agreement with the observed scenario. These opacities, having a relative maximum around CNO ionization regions, provide more extended envelopes for stars which leave the ZAMS; however these features have been shown to be physically unrealistic by more recent calculations (Carson et al.1984). Stothers and Chin (1984) have provided further evidence of a main sequence widening. They have compared theoretical isochrones which rest upon a rough parameterization of the overshooting, with very young star cluster turnups (the observed vertical part of the main

sequence). The outcoming suggestion is that a substantial amount of overshooting (or another form of mixing) occurs in cores of massive stars; the quoted value of Λ corresponds to about 1.5. In conclusion different investigations based on a variety of observational material, agree in stating that standard evolutionary models, even with mass loss, cannot explain some basic features of the H-R diagram for the most luminous stars. In particular star counts for different spectral types coupled with observed turnup morphologies, indicate a much wider main sequence band than that suggested by standard model computations. A more extended internal mixing and eventually new enhanced opacities can bring theory and observation, in the domain of massive stars, into agreement.

TABLE 2.1

Mass[a]	20	60	100	20	60	100
Model	a			Set A b		
$t(10^6 ys)$	0.	0.	0.	9.813	3.899	2.999
$Lg\ L/L_\odot$	4.611	5.702	6.101	5.077	6.029	6.376
$Lg\ T_e$	4.537	4.680	4.717	4.368	4.265	3.614
q_c	0.558	0.779	0.850	0.373	0.522	0.567
X_c	0.700	0.700	0.700	0.017	0.004	0.019
Model	a			Set A' b		
$t(10^6 ys)$	0.	0.	0.	7.459	3.378	2.69
$Lg\ L/L_\odot$	4.640	5.720	6.119	4.935	5.964	6.307
$Lg\ T_e$	4.542	4.683	4.721	4.444	4.506	4.507
q_c	0.438	0.684	0.813	0.241	0.403	0.455
X_c	0.700	0.700	0.700	0.032	0.017	0.012

[a] in solar units

q_c: fractionary mass of the convective core
X_c: central by mass abundance of hydrogen

TABLE 2.2

Mass	20	60	100	20	60	100
Model	a			Set B b		
$t(10^6 ys)$	0.	0.	0.	10.758	4.015	2.862
$Lg\ L/L_\odot$	4.594	5.967	6.098	4.977	5.945	6.235
$Lg\ T_e$	4.535	4.679	4.718	4.295	4.462	4.665
$\dot{M}$	2.1(-7)	3.1(-6)	8.5(-6)	8.4(-7)	9.7(-6)	1.6(-5)
M	19.74	59.62	99.32	16.00	40.83	67.81
q_c	0.558	0.772	0.852	0.412	0.662	0.799
X_c^c	0.700	0.700	0.700	0.011	0.014	0.120
X_e^c	0.700	0.700	0.700	0.700	0.504	0.360
Model	a			Set B' b		
$t(10^6 ys)$	0.	0.	0.	8.020	3.396	2.760
$Lg\ L/L_\odot$	4.625	5.717	6.120	4.798	5.839	6.220
$Lg\ T_e$	4.540	4.683	4.721	4.406	4.433	4.482
$\dot{M}$	2(-7)	3.3(-6)	1.(-5)	4.5(-7)	6.8(-6)	1.5(-5)
M	19.90	59.74	99.80	18.20	45.27	68.39
q_c	0.427	0.680	0.806	0.237	0.441	0.574
X_c^c	0.700	0.700	0.700	0.027	0.011	0.033
X_e^c	0.700	0.700	0.700	0.700	0.700	0.566

$\dot{M}$: rate of mass loss in units of $M_\odot/yr$
M : current total mass of the model
q_c : fractionary mass of the convective core
X_c^c : central by mass abundance of hydrogen
X_e^c : surface by mass abundance of hydrogen

TABLE 2.3

. Results of models and of counts for four "track-shaped" bands centered around the evolutionary tracks of 9, 15, 30, and 60 $M_\odot$. The values of the ratios of the different lifetimes (respectively different number of stars) to the total lifetime (respectively total number of stars) are given

$t_{tot}=t_{OB}+t_A+t_{FG}+t_{KM}$ / $N_{tot}=N_{OB}+N_A+N_{FG}+N_{KM}$	Models				Observations				
	A	B	C		GC	GAC	Galaxie	LMC	SMC
60 $M_\odot$ t_{KM}/t_{tot}	0.015	0.007	0.002	N_{KM}/N_{tot}	0.00	0.00	0.00	0.00	0.00
60 $M_\odot$ t_{FG}/t_{tot}	0.029	0.001	0.000	N_{FG}/N_{tot}	0.00	0.00	0.00	0.00	0.00
60 $M_\odot$ t_A/t_{tot}	0.022	0.000	0.000	N_A/N_{tot}	0.00	0.00	0.00	0.00	0.00
60 $M_\odot$ t_{OBA}/t_{tot}	0.955	0.946	0.929	N_{OBA}/N_{tot}	1.00	1.00	1.00	1.00	1.00
60 $M_\odot$ t_{OB}/t_{tot}	0.934	0.946	0.929	N_{OB}/N_{tot}	1.00	1.00	1.00	1.00	1.00
60 $M_\odot$ t_{MS}/t_{tot}	0.927	0.929	0.923	N_{MS}/N_{tot}	0.50	1.00	0.73	1.00	1.00
30 $M_\odot$ t_{KM}/t_{tot}	0.002	0.024	0.013	N_{KM}/N_{tot}	0.00	0.00	0.00	0.00	0.00
30 $M_\odot$ t_{FG}/t_{tot}	0.000	0.027	0.002	N_{FG}/N_{tot}	0.00	0.17	0.08	0.03	0.00
30 $M_\odot$ t_A/t_{tot}	0.000	0.018	0.001	N_A/N_{tot}	0.06	0.17	0.11	0.00	0.00
30 $M_\odot$ t_{OBA}/t_{tot}	0.998	0.949	0.930	N_{OBA}/N_{tot}	1.00	0.83	0.92	0.98	1.00
30 $M_\odot$ t_{OB}/t_{tot}	0.998	0.931	0.929	N_{OB}/N_{tot}	0.94	0.67	0.82	0.98	1.00
30 $M_\odot$ t_{MS}/t_{tot}	0.921	0.928	0.921	N_{MS}/N_{tot}	0.59	0.33	0.47	0.94	0.68
15 $M_\odot$ t_{KM}/t_{tot}	0.014	0.036	0.098	N_{KM}/N_{tot}	0.02	0.08	0.05	0.08	0.12
15 $M_\odot$ t_{FG}/t_{tot}	0.001	0.002	0.001	N_{FG}/N_{tot}	0.02	0.04	0.03	0.03	0.12
15 $M_\odot$ t_A/t_{tot}	0.001	0.004	0.000	N_A/N_{tot}	0.02	0.06	0.04	0.01	0.03
15 $M_\odot$ t_{OBA}/t_{tot}	0.985	0.961	0.894	N_{OBA}/N_{tot}	0.96	0.88	0.92	0.89	0.76
15 $M_\odot$ t_{OB}/t_{tot}	0.984	0.958	0.894	N_{OB}/N_{tot}	0.95	0.81	0.89	0.88	0.73
15 $M_\odot$ t_{MS}/t_{tot}	0.895	0.894	0.893	N_{MS}/N_{tot}	0.70	0.35	0.54	0.75	0.54
9 $M_\odot$ t_{KM}/t_{tot}	0.085	0.124	-	N_{KM}/N_{tot}	0.07	0.08	0.07	0.08	0.20
9 $M_\odot$ t_{FG}/t_{tot}	0.010	0.032	-	N_{FG}/N_{tot}	0.03	0.06	0.04	0.17	0.40
9 $M_\odot$ t_A/t_{tot}	0.013	0.000	-	N_A/N_{tot}	0.00	0.05	0.02	0.06	0.00
9 $M_\odot$ t_{OBA}/t_{tot}	0.905	0.844	-	N_{OBA}/N_{tot}	0.90	0.86	0.88	0.75	0.40
9 $M_\odot$ t_{OB}/t_{tot}	0.893	0.843	-	N_{OB}/N_{tot}	0.90	0.81	0.86	0.68	0.40
9 $M_\odot$ t_{MS}/t_{tot}	0.843	0.835	-	N_{MS}/N_{tot}	0.82	0.55	0.70	0.50	0.20

TABLE 2.4

Star counts in different spectral types for stars with luminosity in the range $-7 \geqq M_b \geqq -9$

Sp [a]	O	B	A	F	G	K	M	WR
N	138	201	10	4	1	1	29	20
N/Nt	0.342	0.498	0.025	0.010	0.002	0.002	0.072	0.050
Sp [b]	O - B0.5	B1 - B9	A	F	G	K	M	WR
N	259	80	10	4	1	1	29	20
N/Nt	0.640	0.198	0.025	0.010	0.002	0.002	0.072	0.050
Sp [c]	O - B1	B2 - B9	A	F	G	K	M	WR
N	290	49	10	4	1	1	29	20
N/Nt	0.718	0.121	0.025	0.010	0.002	0.002	0.072	0.050
Sp [a']	O	B	A	F	G	K	M	WR
N	280	201	10	4	1	1	29	20
N/Nt	0.513	0.368	0.018	0.007	0.002	0.002	0.053	0.037
Sp [b']	O - B0.5	B1 - B9	A	F	G	K	M	WR
N	401	80	10	4	1	1	29	20
N/Nt	0.734	0.147	0.018	0.007	0.002	0.002	0.053	0.037
Sp [c']	O - B1	B2 - B9	A	F	G	K	M	WR
N	432	49	10	4	1	1	29	20
N/Nt	0.791	0.09	0.018	0.007	0.002	0.002	0.053	0.037

Figure 2.1) Curves of maximum velocity for the Z.A.M.S. models of 20,60,100 Mo ; vertical dashed lines indicate the point where the Schwarzschild criterion holds $\nabla_{AD} = \nabla_{RAD}$ (Bressan et al. 1981)

Figure 2.2a) Values of the various function v (velocity), f= Fr/(Fr+Fc) , and excess temperature T inside a 2 Mo model (Maeder 1975).

Figure 2.2b) Changes between the structure of a homogeneous model computed with the Schwarzschild's criterion and with overshooting (Maeder 1975)

Figure 2.3) Theoretical H-R diagram for the sets of models of tables 1) and 2) (Bressan et. al 1981):

- A' standard
- A with overshooting
- B' whit mass loss
- B with mass loss and overshooting

Figure 2.4) The "theoretical" H-R diagram for the most luminous stars in the solar vicinity (Humphreys 1978)

Figure 2.5) Theoretical widening for the main sequence band with various overshooting parameters without mass loss (Bertelli et al. 1984).

2.1

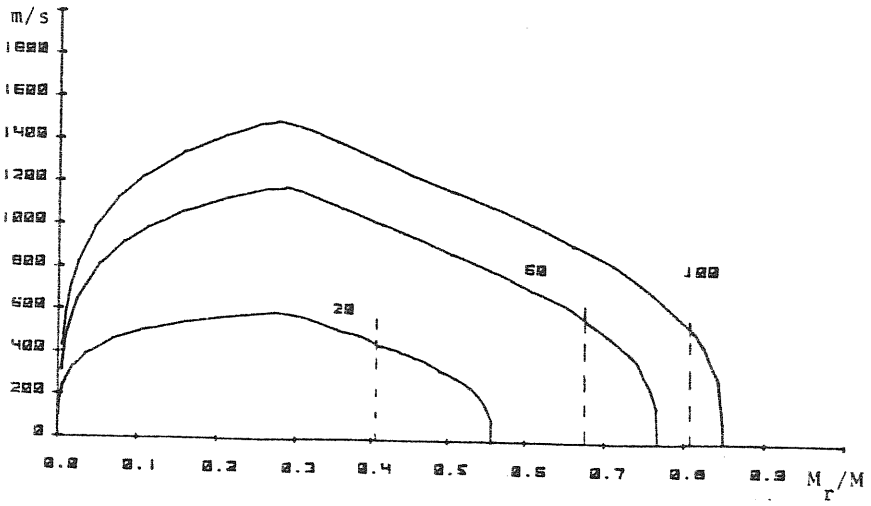

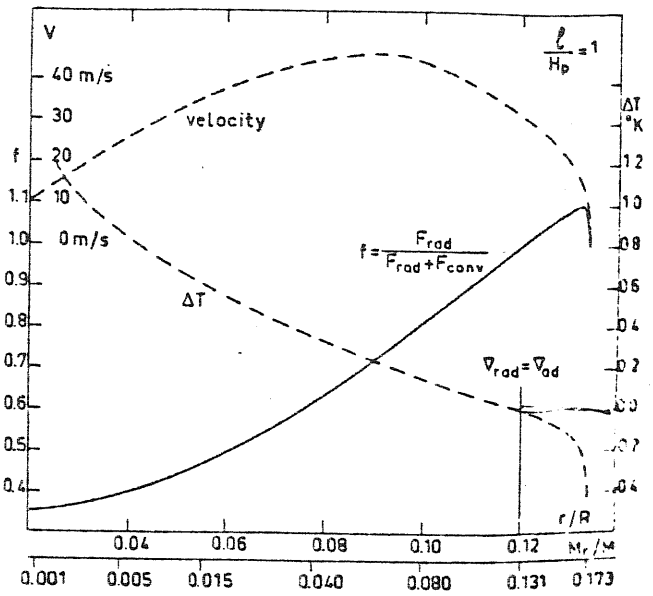

2.2 a

2.2 b

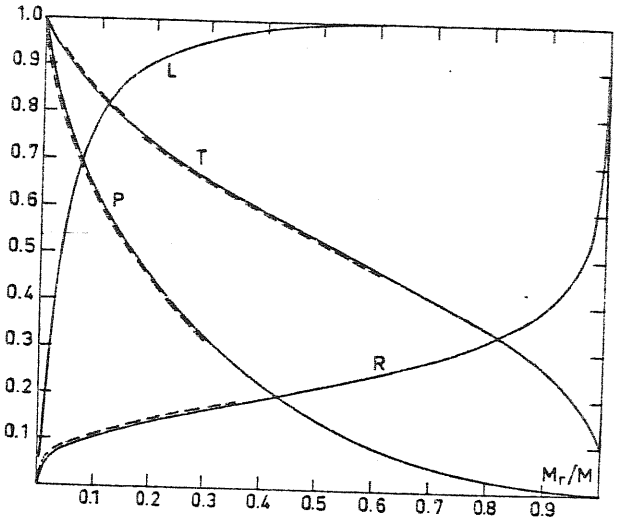

Changes between the structure of a homogeneous 2 $M_\odot$ star computed with Schwarzschild's criterion (continuous line) and criterion $v=0$ for $\ell/H_p=1$ (broken line)

2.3

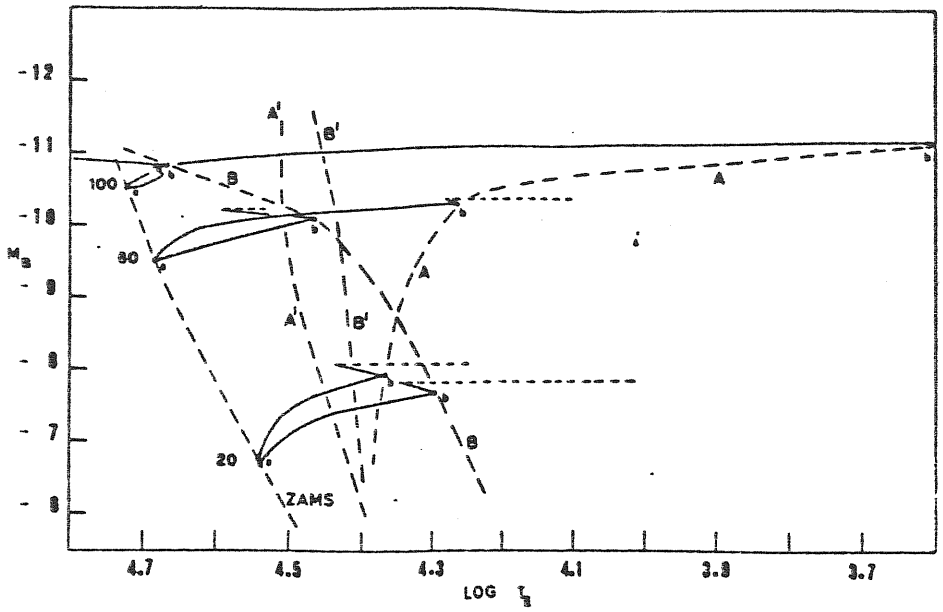
A'
B'
100
B
A
80
A'
B'
A
B
20
ZAMS
4.7
4.5
4.3
4.1
3.8
3.7
LOG

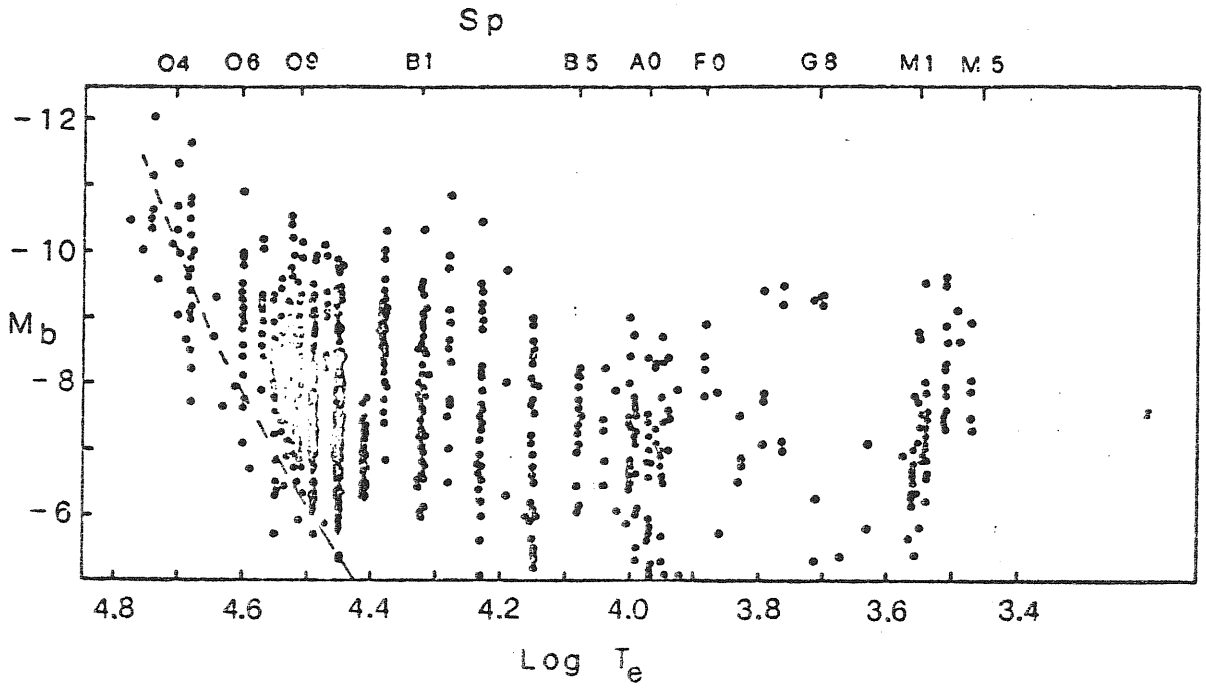
Sp
O4 O6 O9 B1 B5 A0 F0 G8 M1 M5
-12
-10
-8
-6
Mb
4.8
4.6
4.4
4.2
4.0
3.8
3.6
3.4
Log Te

2.4

2.5

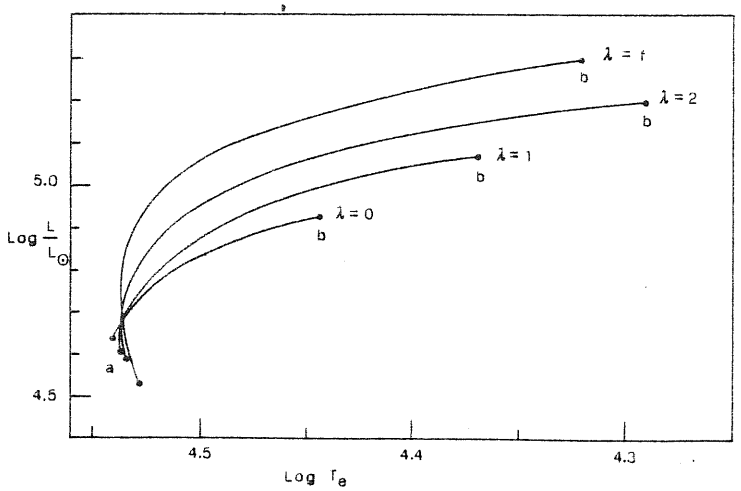
λ = 1
λ = 2
λ = 1
λ = 0
5.0
Log L/L⊙
4.5
4.5
4.4
4.3
Log Te

Chapter III

3.1 Intermediate mass stars.

Intermediate mass stars are those that ignite Helium non degenerately, but develop a highly electron-degenerate carbon-oxygen core after central Helium exhaustion. In standard models these stars are confined in the range 2.2/8-9 Mo for the chemical composition characteristic of the Population I, while those limits are slight lower if one considers the Population II chemical composition. The lower limit (thereafter called M_{HEF}) is set by the maximum mass which experiences central Helium flash and the upper limit (thereafter M_{UP}) corresponds to the stars in which carbon ignition starts off center in a mildly degenerate core with an energy release that is high enough to remove degeneracy. This nominal definition is however very dependent on details of stellar model computations and, ultimately, it is the critical core mass for non degenerate ignition that defines this class of models. The critical mass is about 0.31 Mo for non degenerate Helium ignition and 1.06 Mo for non degenerate Carbon ignition. All stars that develop a Helium core of about 0.31 Mo before undergoing high degeneracy, and that undergo high degeneracy before developing a carbon-oxygen core of 1.06 Mo, belong to this class. As far as the lower limit is concerned, we will see in the next chapter that it is coupled with the

stability of an isothermal non-degenerate Helium core, while the relation between the higher critical mass and the initial mass of the star Mi depends on a variety of inputs in model computations, like mass loss ,size of convective core , neutrino loss rates, etc.. . Then it is not surprising that changing one of the above conditions will primarily change the nominal definition of intermediate mass stars ,and of course of other mass ranges.

In this chapter I will be mainly concerned with the effect of overshooting during almost the entire evolution of these stars. They will be followed from the phase of Hydrogen burning, through Helium burning up to the Asymptotic Giant Branch (A.G.B.). Each phase will be treated separately and the major qualitative results of both the standard and non standard models will be outlined with the purpose of looking for observable effects which possibly may discriminate between the two proposed scenarios. The properties of intermediate mass stars from the standpoint of classical evolution have been extensively reviewed by Iben (1974) and Iben and Renzini (1983,1984); among the several models already existing in the literature only a few of them account for overshooting and mainly during Hydrogen burning phase (Maeder 1976 ; Maeder and Mermilliod 1981 ; Matraka et al. 1982 ; Huang and Weigert 1983).

Recently Bertelli, Bressan and Chiosi (1985) and Bertelli, Bressan, Chiosi and Angerer (1986) have computed a complete set of evolutionary tracks for intermediate mass stars tacking into

account overshooting from convective core, mass loss and other updated input physics. With the help of this new set of models I will show that several important discrepancies, that arise when comparing classical models predictions with the observations, disappear, so that a more extended convective mixing seems effectively to take place inside real stars. Moreover it will be interesting to show that, even if other theoretical approach are possible which partly alleviate the discrepancies encountered in the domain of intermediate mass stars, only a full non local overshooting, as that used by the above authors, can match observations in different domains of the HR diagram.

In the following I will first report on the physical details of models construction; then I will discuss the main nuclear burning phases together with the constraints imposed by the observations and subsequently I will describe the Asymptotic Giant Branch Phase where several important differences arise between these models and classical ones.

3.2 The input Physics

Evolutionary tracks for intermediate mass stars are displayed in Figures (3.1a,b) and have been computed for the following set of initial parameters:

Z=0.02, X=0.700, Y=0.280

M = 9.0, 7.0, 6.0, 5.0, 4.5, 4.0, 3.0, 2.0*, 1.7*, 1.6* M_o

Z=0.001, X=0.700, Y=0.299

$M = 9.0,\ 7.0,\ 6.0,\ 5.0,\ 4.0,\ 3.0,\ 2.0,\ 1.7^{*},\ 1.6^{*},\ 1.5^{*},\ 1.4^{*}\ M_{o}$

Asterisked models belong to the domain of low mass stars in standard evolution, but behave as intermediate mass stars if overshooting is accounted for; they will be discussed in the chapter of low mass stars.

The models are calculated under the following physical assumptions (Bertelli et al. 1986)

1) Overshooting from the convective core as described at the beginning and for a value of $\Lambda = 1$ (other values are explicitly given in the text)

2) Models have been evolved at constant mass; however for investigating on the effects of mass loss in this domain of masses some tracks have been repeated with mass loss introduced according to the formalism of Reimers (1975):

$$dm/dt = 4\ 10^{-3}\ \eta L/gR$$

where the rate is expressed in $M_{o}\ yr^{-1}$ and L,g,R are respectively surface luminosity, gravity and radius of the star; the parameter η is uncertain by a factor of ten - from 0.3 to 3.0 - but according to Fusi-Pecci and Renzini (1976) and Renzini (1981), the morphology of the H-R diagram of globular clusters put stringent limits on it -η=0.4 ± 0.05-. This same value led to an underestimate of the rate for the more luminous red giants and supergiants (de Jong 1983, Bertelli et al. 1984) so that a relation with a slightly higher dependence on the luminosity may be more appropriate for these stars (Bertelli et al. 1985)

3) The radiative opacities are taken from Cox & Stewart (1970) interpolated by bicubic splines, whereas the conductive opacities are from Hubbard & Lampe (1969) and Canuto (1970).

4) The nuclear energy generation rates are derived from Fowler et al (1975). The abundances of CNO elements are the same as in the mixture used for the opacity and equilibrium is assumed only for the CN cycle. The abundances of ^{14}N, ^{16}O, ^{17}O are followed and modified according to the importance of the ON cycle. Finally, the rate of the $^{12}C(\alpha,\gamma)^{16}O$ reaction is according to the new measurement of the cross section by Kettner et al (1982) or equivalently the reduced width of the α particle (θ_α^2) is in the range 3 to 4 times the classical value (0.078).

5) The neutrino energy losses by Beaudet et al (1967) for plasma, photo and pair production are adopted.

5) The mixing length in the outer layers is chosen to be 1.5 time the pressure scale height.

6) Particular care is devoted to the mass spacing in order to define the border of the convective core as accurately as possible. In the vicinity of this border the mass interval is less than $\Delta m/m_{tot} = 0.001$. The number of mesh points range from about 500 during the central Hydrogen and Helium burning phases to about 900 in the double shell phase.

3.3 Core Hydrogen burning phase.

As for the massive stars, the zero age main sequence (Z.A.M.S.) is only slightly affected by convective overshooting. The effect

of varying the free parameter Λ on the extension of the mixed region is shown in Figure (3.2), where are also displayed the results of Matraka et al. (1982) for Λ = 0.25 and 0.5 but for a different chemical composition (X,Z =0.602, 0.044) and a different computational procedure. From the computations of Bressan et al.(1981) and Bertelli et al.(1985) it appears that the same overshooting parameter implies a relative growth of the size of the convective core which increases as the model mass decreases. The relative increase of the fractionary mass $\Delta q/q$ $\left(q = M_r/M_{tot}\right)$ of the convective core ranges from about 0.30 for a 9 M_o, to 0.75 for a 5 M_o and reaches about 1.8 for the 1.6 M_o model for the metal abundance Z = 0.02 and has about the same values for Z = 0.001. Furthermore an inspection of the above models and of the results obtained by Matraka et al. shows that with decreasing metallicity, both the standard and overshooting cores get larger : 19% for Λ = 0.5 and Mi= 5 Mo , while 15% for Λ = 0 and the same mass. The more extended convective core makes the models to evolve at higher luminosities during Hydrogen burning, this effect being growing during evolution , and at lower effective temperatures, causing the widening of the main sequence band. The lifetime of the phase is controlled by both the higher luminosity and the fact that more fuel is available, but the last effect largely overwhelms the first, so that the lifetime increases consistently.

During this phase the main characteristic of the models directly

comparable with observational data is the widening of the main sequence band as for massive stars. A composite Mv-(U-B)o diagram of galactic clusters (from Maeder and Mermilliod 1981) is shown in Figure (3.3) together with the main sequence band obtained from the models described above for Z = 0.02. The transformation from Log L - Log Te to Mv-(U-B)o plane is based on the relationships given by Buser and Kurucz (1978). This diagram shows, only qualitatively, that standard models cannot account for the widening of the main sequence band even in the case of intermediate mass stars. One may speculate about uncertainty in experimental data when constructing composite diagrams; in fact a more rigorous analysis has to be based on systematic comparisons between observed and synthetic star clusters. However here it is worth mentioning that when a comparison is made as in Figure (3.3) one has to keep in mind that about 50% of the H burning lifetime is spent in a very narrow region along the Z.A.M.S. and this clearly stresses the discrepancy obtained from standard evolution.

3.4 Core Helium burning.

Following central Hydrogen exhaustion the stars move to the red region of the H-R diagram in a Kelvin-Helmoltz time scale and then, climb along the Hayashi line, while central Helium core heats due to the gravitational contraction and Hydrogen burning proceeds in a shell. At the same time the external convective

envelope moves inward and eventually reaches layers left out by the receding H burning core, thus starting the so called "first dredge up" of nuclear processed material. When central density and temperature reach the critical value for Helium ignition this proceeds quiescentely because the core is not degenerate. Central convection is initiated, driven by the high temperature dependence of Helium burning. During subsequent evolution the Helium inert core continuously grows in mass, because of the Hydrogen shell burning, and this makes the convective core to become greater and greater. The model luminosity decreases slightly down to a minimum after that a blue loop is started in the H-R diagram. In this phase standard models face with the so called problem of semiconvection. Due to the growth of the convective core a steep discontinuity in molecular weight appears at its border , where opacity is very dependent on the Helium, Carbon and Oxygen content. Helium rich regions slightly outside the convective core are strongly unstable with respect to perturbation in molecular weight: if for some reason (penetration of convective elements, shear, diffusion) these regions are partially mixed with the core, their opacity considerably increases owing to the injection of carbon and oxygen rich material. The radiative gradient thus overcomes the adiabatic one and the region becomes completely convective. This process propagates outward giving rise to a series of gradient profiles like those shown in Figure (3.4), so that the question arises of

where the convective border actually is.

The difficulty is overcome by assuming that in those regions mixing is only partially efficient (semiconvection) and so well regulated to give rise to a zone of varying molecular weight in which the neutrality condition against convection exactly holds. This has been the subject of a great deal of theoretical work aimed to determine the true process of mixing and the consequent neutrality condition. The problem is not yet solved and both the Scwarzschild and Ledoux criteria for convective neutrality are found in the literature. It is worth mentioning that some authors refer to this mixing process as to "overshooting and semiconvection during Helium burning", (Renzini 1977) because, in reality, the inner full convective region moves slightly outward; it is however a "local overshooting", because no full penetration of convective motions in radiatively stable regions is considered. On the contrary, models with overshooting parameter $\Lambda = 1$ never experience this phenomenon while, for $\Lambda = 0.5$ it is marginally present at the end of Helium burning phase only. This reflects the fact that when $\Lambda \rightarrow 0$ one expects to recover the standard results.

Turning now to the H-R diagram morphology it is well known that when the loop crosses the Cepheid instability strip the star starts pulsating with a well known relation between the period and the average density. Although one of the major goals of the stellar evolution theory is the prediction of the existence of

these very typical objects still some problems exist, as we will see in the following.

3.5 Overshooting and the Cepheid stars

As noticed by Matraka et al.(1982) and by Huang and Weigert(1983) overshooting strongly affects the morphology of the H-R diagram during Helium burning. The models evolve at a higher luminosity, with a $\Delta LogL/L_{\odot}$ which is about 0.5 for $M = 5M_{\odot}$ and 0.3 for $M = 9M_{\odot}$ and $\Lambda = 1$. Furthermore the extension of the blue loop is reduced as the size of the overshooting region increases. Matraka et al.(1982) argued that this would constitute a strong difficulty for models with overshooting and in fact, their calculations showed that only stars more massive than about 6 Mo would be able to cross the instability strip. This in turn would mean that no Cepheids with periods shorter than about 8 days could be explained by theory. They were also able to show that the morphology of the loops is greatly affected by other agents, among which one of the most important is the treatment of the external convective envelope. If the mixing length ratio decreases, the Hayashi line gets redder but the hottest point of the loop moves to the blue. A later work of Huang and Weigert (1983) confirmed this finding as may be seen in Figure (3.5), where their case for $M = 5M_{\odot}$ and $\Lambda = 0.5$ is shown. Against such a decrease of the external mixing length parameter (down to 0.5) I report that recently Vandenberg and Bridges(1984) claimed that

the standard value of α = 1.5 should be preferred. Furthermore other important inputs in the model computations are known to modify the appearance of the loops in the H-R diagram. Apart from the effect of metal content (the lower the value of Z, the more extended the loop), or of mass loss (which has been discussed by Lauterborn et al. 1971), also the nuclear energy rates for Helium burning have a great impact on the H-R diagram morphology. In particular the parameter θ^2_α(7.12 Mev) of the reaction $^{12}C(\alpha,\gamma)^{16}O$ is determined with an uncertainty of about one order of magnitude and its effect on the occurrence of loops has been reviewed by Iben (1972) and it is illustrated in Figure (3.6). The probable values of this parameter range from 0.045 and 0.125. An increase of this parameter from the minimum value to the maximum (which would primarily affect the chemical composition of the final Carbon-Oxygen core changing the $^{12}C/^{16}O$ ratio from about one to zero) produces more extended loops in the H-R diagram in the region of less massive intermediate mass stars, while the luminosity of the models is not affected. Standard models, the ones of Matraka et al. and of Huang and Weigert were obtained assuming the value given by Flower(1975) of θ^2_α = 0.078. Recently however, new accurate measurements of cross section have increased its value of about three to five times (Kettner et al. 1982). The models computed with this new value (Bertelli et al 1984) confirm the finding of Iben (1972); the loops have about the same luminosity as in previous computations

but they are more extended. In such a way models with overshooting and the new value of the α particle reduced width, as proposed by Kettner et al.(1982), do not face the problem of the absence of blue loops for stars in the mass range 4 to 6 M_o.

3.6 The mass-luminosity relation for cepheid stars.

Another important problem arises when comparing theoretical predictions with observations in this phase. In the last few years it becomes evident that the mass of cepheids predicted by stellar evolution theory were larger than those inferred by pulsation theory by a non negligible factor. This so called "cepheid mass anomaly" appears more or less stressed in the different ways in which the comparison is made. The linear pulsation theory predicts relation between the period and the mean density of a cepheid, which may be written in terms of its mass and radius (or equivalently luminosity and effective temperature) :

$$Q = \Pi \cdot (M / R^3)^{1/2}$$

where Q is the pulsation constant, Π is the period, M the total mass and R the radius.

Cogan (1970) studied the 13 cepheid stars employed by Sandage and Tamman (1969) for calibrating the period-luminosity-color relation. From the well known mean luminosity and effective temperature he was able to show that the masses inferred from pulsation theory (with the help of the above relation) were too

low ,by a factor of 30%-40%, with respect to the masses inferred by evolutionary tracks crossing the instability strip at the same luminosity. Furthermore since the first application of hydrodynamic calculations to the cepheid pulsations, Christy (1968,1974), Stobie (1969,a,b,c), it was evident that the so called "bump cepheids" could not be modelled unless the masses used in the calculations were about 30% or 40% less than the evolutionary masses of the same luminosity. Since then a great amount of theoretical work has been performed to clarify if this mass anomaly is only apparent. A number of different agents was invoked to lower the evolutionary mass, like mass loss (the required amount however also modifies the extension of the loop and turns out to be too high) or increased envelope opacities (like those suggested by Carson 1976) whose effect is mainly directed to lower the luminosity of the loop (Carson and Sthoters 1984). On the other hand improved hydrodynamical calculations (Fricke et al. 1971,1972; Adams et al.1980) have demonstrated that a "bump cepheid" mass anomaly of about 40% exists, independently of numerical codes employed in the calculations.
As far as the "pulsational masses" are concerned, the discrepancy is displayed in Figure (3.7) (from Iben and Tuggle 1972). In that Figure the dots indicate the pulsational masses obtained for sixteen galactic cepheids and the shaded region represents the mass-luminosity relation of the blue loop for stars with chemical composition X,Z = 0.7,0.02 . The fitting line for cepheids has a

slope (LogL = 5.6 LogM) different from that drawn for the evolutionary models (LogL = 4 LogM). For a given luminosity the discrepancy ΔLog M is about 15%. It was noticed by Iben and Tuggle (1972 a,b) that an underestimate of the intrinsic luminosity of the cepheid stars by a factor of ΔLog L ≈ 0.1 and a slightly different slope of the P-L-C relation from that of Sandage and Tamman (used for the plot in Figure 13), would remove the discrepancy. This is not at variance with observations as the luminosity depends on the distance scale and for the sixteen cepheids of Figure (3.7) the last rests mainly on the Hyades distance modulus. An increase of ΔLog L ≈ 0.1 implies an increase of Δ(M-m) ≈ 0.3 mag.; in the last few years the Hyades distance modulus has grown from about 3.00 mag. to 3.18 mag (Flower 1979) and recently to about 3.4 (Hanson 1980). This possible overcoming of the pulsational mass anomaly (see also Cox 1980), has been recently questioned by Schmidt (1984) on the basis of a recent redetermination of the distance moduli of several open clusters containing cepheid stars. Schmidt derived a zero point for the period luminosity color relation which gives absolute magnitudes that are fainter by about 0.4 - 0.6 mag than those based on the above Hyades distance modulus. Moreover a significantly lower estimate of the luminosity of two cepheids - U Sgr and S Nor - is given in the revision made by Peel (1984). In Figure (3.8), which shows a plot of Log L/L_o vs. Mpul (pulsational masses) calculated with the new distance for the

Hyades (Hanson 1979) by Cox(1979), the effect of the revision by Peel is indicated by an arrow. If one applies the revision made by Schmidt, all other points shift almost of an equal quantity. As can be seen by the Figure, when distances are based on the new Hyades modulus, cepheid stars fall in between the relations Log L/L_o-Log M/M_o defined by standard models and by models with overshooting, while if the corrections suggested by Schmidt and Peel are adopted, the stars shift over and even behind the relation defined by models with overshooting for $\Lambda = 1$.

Thus the higher luminosity the new models have during central Helium burning - ΔLog $L/L_o \simeq 0.5$ - may offer an immediate explanation to the pulsational mass discrepancy.

From the standpoint of classical evolution, the bump mass anomaly may be eliminated postulating an overabundance of He - Y=0.75 Cox (1980)- in a very narrow region of mass inside the ionization region. This is not implausible but strongly conflicts with the immediate mixing that an outward decreasing molecular weight would imply. Even in this case models with overshooting offer an elegant possibility to overcome the difficulties encountered, because they fruitfully obey the requirement of providing the same luminous envelopes with a total mass about 30%-40% lower than in standard models.

To conclude this section dealing with Helium burning phase a remark on lifetimes is needed. Standard models predict that the Helium burning lifetime is about 30% 40% of Hydrogen burning

time. This is due primarily to the growth of the inert Helium core as the Hydrogen shell advances during evolution. On the contrary, in the new models, evolution at higher luminosity exactly balances the effects of an enlarged size of the core. Therefore they predict a Helium burning lifetime which is about 6% for $\Lambda = 1$ or 15% for $\Lambda = 0.5$ of the Hydrogen burning lifetime. This has a very clear observational counterpart in the number ratio between evolved and unevolved stars, and may be compared with theory, if one disposes of a good enough photometry for well populated young clusters.

3.7 The Asymptotic Giant Branch phase.

Following central Helium exhaustion the Carbon Oxygen core undergoes gravitational contraction while central density and temperature grow. In the H-R diagram the model is now climbing again along the Hayashi line which, for intermediate mass stars, asymptotically approaches the prolongation of the red giant branch of low mass stars, from which the name given to this phase. The convective envelope expands, cools and penetrates inward in mass. At the beginning both Hydrogen and Helium shells are active, but the first immediately quenches out owing to the cooling of the envelope. During this phase the luminosity is mostly provided by the gravitational core contraction and by the shell Helium burning. However when temperature and density enter the range in which neutrino losses become important, the core reaches an equilibrium configuration with neutrino losses exactly balancing gravitational energy input. Therefore the central temperature stops rising while density continuously grows up, driving the model toward central electron degeneracy. In the outer Carbon Oxygen core regions neutrino losses are much less efficient and there the temperature continuously increases. However the point where neutrino losses just balance gravitational heating progressively shifts outward, thus producing an off center maximum temperature. On the other hand, nuclear energy sources provided by carbon burning are not yet sufficient to overcome neutrino losses but grow with temperature

and experience the same off center shifting. Here the model faces with two different fates. If maximum temperature grows faster than it is pushed outward by neutrino cooling (this happens when enough Carbon Oxygen material is outside the maximum to significantly contribute in gravitational heating), then carbon burning starts off-center with a power that immediately overwhelms neutrino losses and forces the core to leave degeneracy. The limiting mass for a mildly degenerate C-O core to undergo this carbon ignition is about 1.06 Mo. On the other hand if there is not enough heating from the gravitational pool, neutrino losses make the temperature to drop, after a stage in which a maximum off center was reached; the central core becomes highly electron degenerate and only when the Carbon Oxygen mass reaches the critical value of 1.4 $M_{\odot}$, carbon ignition may occur, however with a destroying power. Subsequent evolution of models that ignite Carbon in a mild or non-degenerate material was investigated in a series of papers by Nomoto et al. (1984 and references therein). Briefly, after quiescent central Carbon burning, the star develops an highly degenerate Oxygen-Neon-Magnesium core and in a short time scale reaches the stage in which electron capture by ^{20}Ne and ^{24}Mg is dominant. The star then implodes giving rise to a deflagration type I1/2 supernova. Stars belonging to the second class (properly intermediate mass stars) follow a different evolution and, what is important, survive for a time significant to produce observable effects in

the H-R diagram. While the Carbon Oxygen core is contracting, the luminosity input and the effect of cooling force the radiative gradient in the envelope to overcome the adiabatic one in progressively more internal regions. Thus convection deeply penetrates inward and eventually shifts the Helium-Hydrogen discontinuity toward the Helium shell, as it may be seen in Figure (3.8) from Becker and Iben(1979). During this phase CNO processed material is brought to the surface and the star undergoes the so called second dredge up episode. As the location in mass of the Hydrogen-Helium discontinuity (M_H) approaches the location of the Helium shell, heating forces the Hydrogen to reignite in a thin shell.

This determines the end of the Early Asymptotic Giant Branch (EAGB) phase and the star enters the double shell phase which is characterized by a series of thermal pulses of the Helium shell (TPAGB). During this phase the Carbon-Oxygen core is highly degenerate and its mass increases due to the effect of the burning shells which, alternatively, process Hydrogen into Helium and Helium into Carbon and Oxygen (Neon is present in a very small quantity). Helium burning in the shell does not proceed regularly, but on the contrary, is characterized by subsequent periodic flashes of growing amplitude, soon followed by the appearance of convection and by the expansion of the surrounding layers. The expansion is so quick and mixing so efficient that Helium nuclear reactions cannot reach equilibrium and the main

product is ^{12}C. Expansion propagates outward like a wave quenching out the Helium shell first and subsequently the Hydrogen shell, and forcing the external convective envelope to advance in regions ^{12}C enriched by previous internal mixing. Through this mechanism newly made ^{12}C is brought to the surface during a series of flash episodes which constitute the so called third dredge up phase. When and, eventually if, surface Carbon abundance overwhelms Oxygen abundance, the star shows up as a carbon star, so called to distinguish it from normal stars in which Oxygen is more abundant.

The luminosity of the models along the A.G.B. is quite well represented by a relation involving the mass inside the Hydrogen burning shell (Paczynski 1970) :

$$L = 5.925\ 10^4\ (M_H - 0.495)$$

and it is mostly provided by Hydrogen burning. If gravitational energy release is important (as it is the case for more massive intermediate mass stars) the relation is slightly different, involving also the total mass M (Iben 1977) :

$$L = 6.34\ 10^4\ (M_H - 0.44)(M/7)^{0.19}$$

This luminosity refers to the interpulse phase which has a characteristic time duration given by :

$$\text{Log } \Delta t \text{ (Yr)} \simeq 3.05 - 4.50\ (M_H - 1.00)$$

and grows until Log Δt is about 25 % greater than the above

value. The number of pulses experienced by a model is an increasing function of the initial mass starting from 13 at Log M_i = 0, to about 840 at Log M_i = 0.6 and ending at about 9000 for Log M_i > 0.7 . Comparing the number of pulses with the interpulse time one can see that a considerable amount of time is spent during the thermal pulsing phase. The situation is summarized in Figure (3.9) (from Iben 1980). In that Figure several mass-luminosity properties are shown for a set of evolutionary models (including low mass stars) with chemical composition X,Y,Z = 0.7,0.28,0.02. The models begin the thermal pulsing phase along the line marked "begin", and end up in three different ways on the lines marked "end". For initial masses smaller than about 1.23 $M_\odot$, the models lose their envelope by stellar wind before developing a core mass of 1.4 Mo. Stars in the range 1.38 $M_\odot$ < M < 5 $M_\odot$ eject a planetary nebula and become white dwarfs. Stars more massive than 5 $M_\odot$ develop a degenerate Carbon-Oxygen core of Mc=1.4 $M_\odot$ before losing their envelopes, therefore presumably undergoing supernova explosion. Following a dredge-up law inferred by model computations, lines of constant ratio $^{12}C/^{16}O$ = 1, 2, 4 are drawn in Figure (3.9). As can be seen from that Figure, stars in the range 4 to 9 $M_\odot$ must appear as bright C stars with bolometric magnitudes in the range -6 < M_{bol} < -7.2. In addition, more detailed calculations (Iben 1980) show that using a birthrate derived from Salpeter's mass function, one may obtain a theoretical distribution for C and M stars, as

summarized in Figure (15 b). C stars are normalized to a total number of 100. The number of C stars versus magnitude indicator M(0.81), defined by a study of Blanco et al. (1980) for Magellanic Clouds, is also shown for comparison.

It is evident that theory is at variance with observations. The theoretical distribution of carbon stars, which ranges from M_{bol}=-5 to M_{bol}=-7.5 and has a maximum at about M_{bol}=-6.3, is completely "off center" with respect to the observed distribution which has a maximum at about M_{bol} = -4.7 and extends from M_{bol} ≃ -3.5 to M_{bol} ≃ -6. This means that where theory predicts that C star stage may be easily reached (M_i > 5 $M_\odot$), there are not real C stars, and where theory predicts that dredge-up mechanisms are not able to produce C stars, they actually exist !. Even if the dredge-up mechanism is supposed to be more efficient for low mass stars (Iben and Renzini 1982a,b and Renzini 1983), the theoretical distribution of C stars fails to predict the true one, giving too many stars above M_{bol} = -5.5. In conclusion if, on one hand, it is fairly well established that the C star phenomenon occurs along the A.G.B., above a certain luminosity, on the other hand, the observed distribution vs. magnitude is completely at variance with theoretical predictions. Surveys of selected fields in the Magellanic Clouds confirmed that C stars are confined within the magnitude range $-4<M_{bol}<-6$, and none is found brighter than this limit. Recently Frogel and Blanco (1983) claimed that young clusters in the Magellanic Clouds which

contain Cepheids (age less than 10^8 years), do not have C stars; on the contrary, stars in the range 4-6 Mo are expected to easily expose C rich material at their surfaces.

Several arguments have been invoked to explain such a paucity of bright C stars, among which the most convincing is the so called "envelope burning" (Renzini and Voli 1981). It is suggested that if the base of the convective envelope is sufficiently hot, then the fresh dredged-up ^{12}C may be directly converted into ^{14}N via the reaction $^{12}C(p,\gamma)^{13}N(\beta,\nu)^{13}C(p,\gamma)^{14}N$. If this is the case, then the star should appear as a M giant star. This however conflicts with the more surprising observational result that not only C stars are absent, but also M stars brighter than about M_{bol}=-6 are lacking (Frogel and Blanco 1983; Aaronson and Mould 1984, Renzini 1985). Therefore on the basis of observational evidences one is forced to conclude that a real luminous A.G.B. star leaves A.G.B. considerably before the critical mass of 1.4 Mo is reached.

Mass loss has been invoked to get out from this intriguing discrepancy but, as discussed by Renzini (1985), that mechanism seems to be rather ad hoc, because it requires rates two orders of magnitude greater for massive intermediate mass stars than for those of lower mass but of similar luminosity and temperature.

The most promising explanation (Chiosi et al. 1984; Bressan 1984; Bertelli, Bressan and Chiosi 1985; Renzini et al. 1985; Castellani et al. 1985) is related to the interior of the star

and in particular it concerns the correct treatment of the convective core.

3.8 Overshooting and M_{UP}

A number of evolutionary computations accounting for overshooting have been provided by Bertelli et al.(1985) and Bertelli et al. (1986) which span the entire domain of intermediate mass stars for two different metallicities. In those models the thermal pulsing phase is not followed as it requires considerable amount of computing time and very detailed grids of models. However a number of interesting results have been obtained concerning, in particular, the initial mass (M_{UP}) of those models that undergo C ignition before the beginning of the thermal pulsing phase. The main results may be better understood by looking at Figures (3.10) and (3.11) (Bertelli et al. 1985). In Figure (3.10) the size of convective core during Helium burning is plotted against central Helium content for two different values of the overshooting parameter (Λ = 0 :standard case; and Λ = 1). The core mass is much greater in models with overshooting owing to its effects during both the Hydrogen and Helium burning phases. Because of the continuous growth of the convective core, the region is completely mixed until Yc is as low as 10^{-3}; then the core starts receding and leaves a very flat Y profile (Y = 10^{-3}) which extends outward up where the maximum size of convective core generated the steep Carbon-Oxygen Helium discontinuity

(this maximum extension is shown in the right side of Figure (3.10) for different initial masses and for Z = 0.02).

After central Helium exhaustion, the core contracts and Helium starts burning in a shell which covers the whole flat profile and has its maximum efficiency around the discontinuity. For initial masses greater than about 6 $M_\odot$ for Z=0.02 and 5 $M_\odot$ for Z=0.001 the mass size inside this discontinuity already overwhelms the critical value of 1.06 $M_\odot$. The central temperature and density runs for some of the computed models and for Z=0.02, are shown in Figure (3.11) for this contracting phase, corresponding to the early A.G.B. phase. All models down to 6 M⊙ ignite carbon in a non degenerate core (for the 6 M⊙ model the ignition is off center and in a mildly degenerate core as can be seen in Figure (3.13 a,b,c,d). Thus when overshooting is taken into account (with $\Lambda = 1$), models of initial mass greater than about 5-6 M⊙ do not experience thermal pulses in a phase of degenerate Carbon Oxygen core and they climb along the A.G.B. in a characteristic time which is about a factor of ten less than that predicted by standard models.

The direct consequence of the overshooting is thus the lowering of the initial star mass for which Carbon starts burning quietly or, as otherwise said, the lowering of M_{UP}. In such a way stars more massive than say 5 or 6 $M_\odot$ will not contribute to the luminous tail of the AGB luminosity function. Therefore the new models predict quite straightforwardly that young clusters with

turnoff masse at about say 5-6 $M_{\odot}$ may contain cepheid stars but not C or M stars above $M_{bol} \simeq -6$. However the problem of luminous AGB stars is far from being solved by overshooting alone. It suffices to remember that, while on the A.G.B., the luminosity is strictly related to the mass inside the Hydrogen Helium discontinuity M_{HE}. Thus one expects less massive stars to continuously populate the bright part of the A.G.B. even with overshooting. For such stars the accompanying mechanism may be the mass loss, as suggested by Chiosi et al.(1986). The above authors computed different theoretical AGB luminosity functions based on the new models and on the usual parameterization of the mass loss rate (Reimers 1975) and were able to show that only a modest increase in the mass loss rate, compatible with the observational errors, is needed in order to reproduce the observations.

Non local overshooting of the kind I just described, is not the only way of getting a lower value of M_{UP}. Castellani et al. (1985) have investigated this problem focusing on the effects of local overshooting and semiconvection during central Helium burning. The difference between local and non local overshooting is that in the first the matter that surrounds an unstable region is locally perturbed in composition and then tested for stability while, as we have already seen, the second looks for the correct definition of the velocity field. During central Helium burning it happens that radiative surrounding regions become convective

when mixed with the Carbon and Oxygen rich matter which, for several reasons (Renzini 1977), overshoot from the convective core. However no investigation is made on the velocity field and on the possibility that mixing effectively takes place apart from timescale arguments. The main characteristic of this convective treatment is that it concerns central Helium burning only, because intermediate mass stars never present favorable internal conditions during Hydrogen burning. Moreover Helium burning lifetime is about twice that of standard models and finally, pulses of convection appear toward the end of Helium burning which again contribute to an enlarged Helium exhausted core. This argument will be touched again in the session of low mass stars, where it was noticed first.

For what concerns the problem of M_{UP}, it is clear that a more sized Helium exhausted core goes in the same direction of models with non local overshooting and indeed Castellani et al. have obtained a value for M_{UP} as low as 6 $M_{\odot}$ for a metallicity of Z=0.001.

Apart from the observational evidences presented in the next chapter, which strongly contradict the occurrence of convective pulses inside real low mass stars, I remember here that doubling the Helium lifetime while letting unchanged the Hydrogen one is strongly at variance with the observed number of evolved to unevolved stars in several clusters of the Magellanic Clouds. NGC1866 is a well studied prototype for which Becker and Mathews

(1983) have found the following ratios of $N_{evolved}/N_{unevolved}$, resting upon standard models and the Salpeter initial mass function:

Observed = 1/2 Theoretical = 2

Thus standard models already overestimate Helium burning lifetime with respect to the Hydrogen one at least of a factor of four. If local overshooting, semiconvection and breathing pulses are introduced the overestimate may easily reach one order of magnitude. Moreover incompleteness of the observations may only make worse the comparison as unevolved stars are the best missing candidates.

On the contrary non local overshooting reduces considerably the above theoretical ratio, so that it fully reproduces a variety of observational constraints and not only the tip of the iceberg.

Figure 3.1a) HR diagram for models with overshooting for the following parameters X = 0.700, Y = 0.28 Z = 0.02 Λ = 1 and initial mass (M_o) indicated on the Main sequence

Figure 3.1b) The same of a) but for X = 0.700, Y = 0.299 and Z = 0.001

Figure 3.2) Size of convective core (Mc/M) vs. model mass for several models on the Z.A.M.S. from Bertelli et al. (continuous line) and Matraka et al. 1982 (dashed lines)

Figure 3.3) Composite Mv-(B-V)o diagram for galactic star clusters. Shaded line corresponds to points b of the models with overshooting parameter Λ = 0.5 (Maeder and Mermilliod 1981)

Figure 3.4) Temperature gradient profiles caused by mixing during He-burning.

Figure 3.5) Evolutionary tracks for a 5 Mo model with Λ = 0.5 in the red giant region of the H-R diagram for different values of the mixing length in the outer convective zone (Huang et al. 1983).

Figure 3.6) Blue limits during He burning for different values of the parameter θ^2_α of the nuclear reaction $^{12}C(\alpha,\gamma)^{16}O$. (Iben 1972)

Figure 3.7) Mass-luminosity relationships from standard evolutionary tracks and from observed Cepheids (Iben and Tuggle 1972)

Figure 3.8) Luminosity versus mass relationship for Cepheid stars The full dots show the luminosities and pulsational masses of Cox (1980). The arrows indicate the revision made by Pel (1984). Standard models of Becker et al. (1977) and those of Bertelli et al. (1984) are shown.

Figure 3.9) The variation with time of the location of the base of the convective envelope and the center of the Helium burning shell during the second dredge up phase (model of 5 M_o, Y=0.28 Z=0.001 from Becker and Iben 1979)

Figure 3.10a) Mass-luminosity properties during A.G.B thermal pulsing phase.(from Becker and Iben 1979)

Figure 3.10b) Distribution in number versus bolometric magnitude for thermally pulsating M and C stars. Also shown is the Blanco and al.1980 observed distribution of C stars in the Magellanic Clouds (from Becker and Iben 1980)

Figure 3.11) Mass size of the convective core during He burning with overshooting parameters Λ = 0 and 1 (models of 9 and 5 M_o and X = 0.700, Y = 0.28 Z = 0.001 Bertelli et al. 1984).

Figure 3.12) Log ρ_c -Log T_c diagram for models with overshooting parameter Λ = 1. (Bertelli et al. 1984)

Figure 3.13) Run of temperature, density, gravitational energy release, nuclear energy release from the He shell, neutrino energy losses for different models along the early A.G.B. phase of a 6 Mo model and X = 0.700, Y = 0.28, Z = 0.001 and Λ = 1.
Also shown are the chemical profiles of Hydrogen, Helium, Carbon (Bertelli et al. 1984)

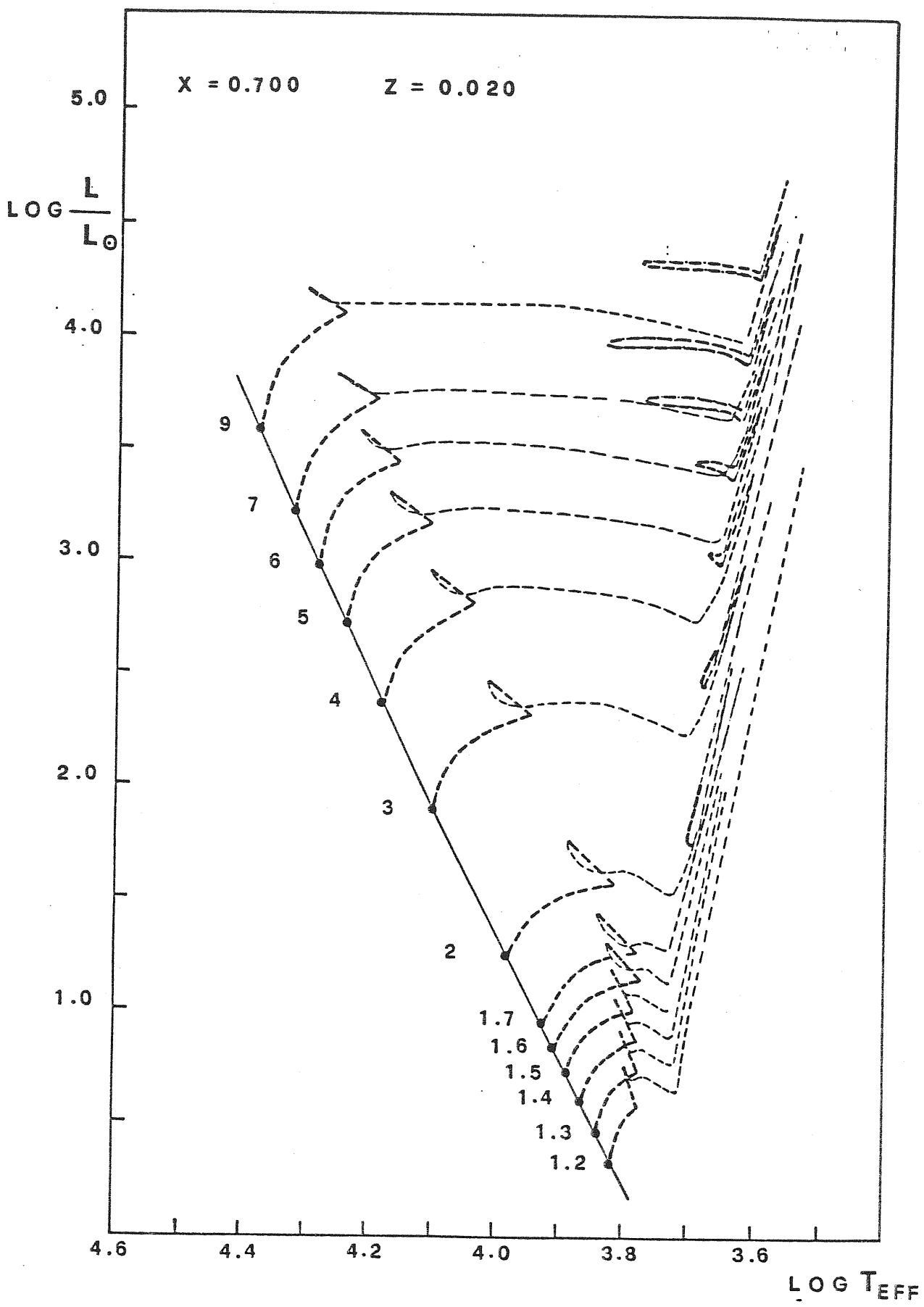
X = 0.700
Z = 0.020
LOG L/L⊙
5.0
4.0
3.0
2.0
1.0
9
7
6
5
4
3
2
1.7
1.6
1.5
1.4
1.3
1.2
4.6
4.4
4.2
4.0
3.8
3.6
LOG T_EFF

3.1 a

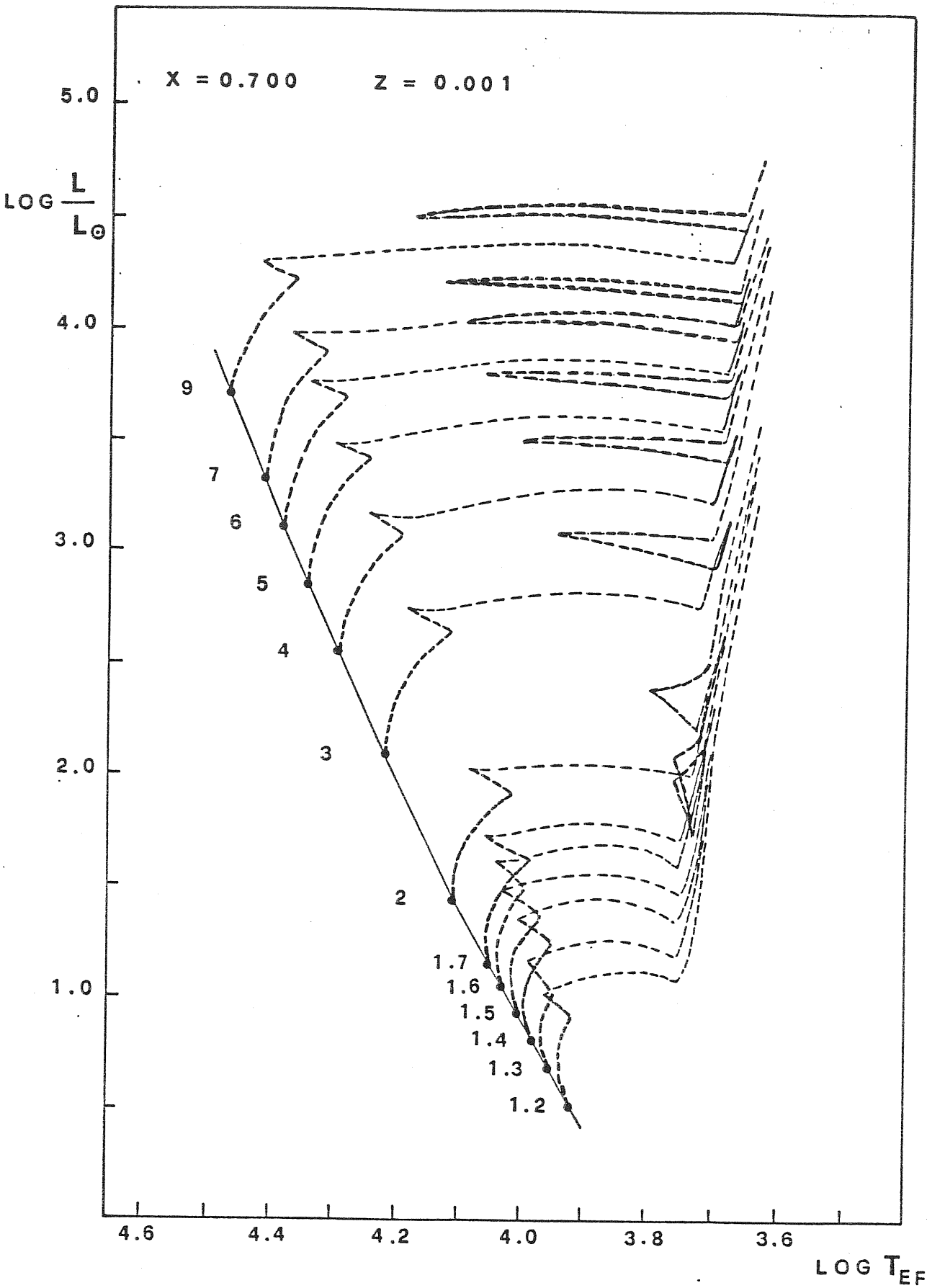
X = 0.700
Z = 0.001
5.0
4.0
3.0
2.0
1.0
LOG L/L⊙
9
7
6
5
4
3
2
1.7
1.6
1.5
1.4
1.3
1.2
4.6
4.4
4.2
4.0
3.8
3.6
LOG T_EFF

3.1 h

3.2

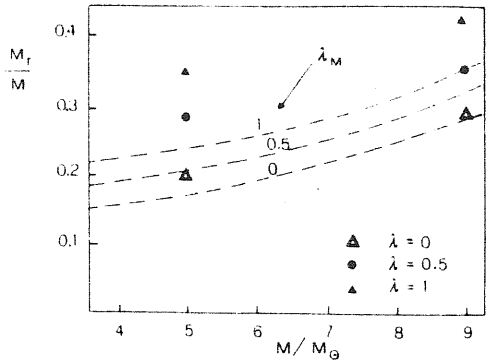

Fractionary mass of the convective core in homogeneous models as a function of the star mass and several values of λ. The same relation given by Matraka's et al. (1982) treatment of overshooting (λ_M) is shown for comparison

3.3

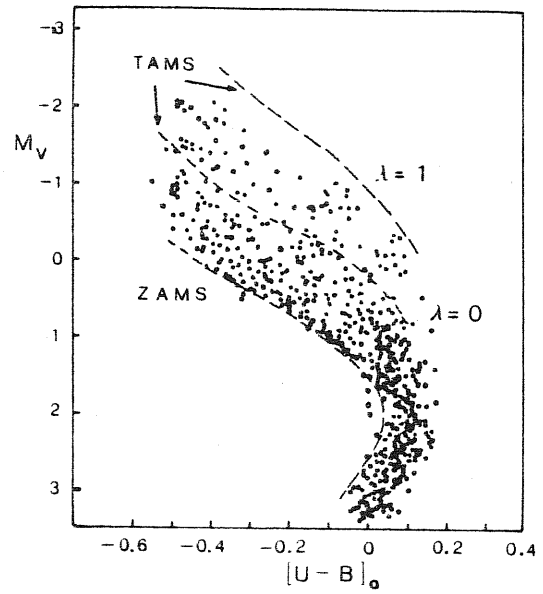

Composite HR diagram reproduced from Maeder and Mermilliod (1981). The widening of the core H-burning band produced by models with overshooting is shown by the TAMS lines obtained with $\lambda = 0$ and $\lambda = 1$

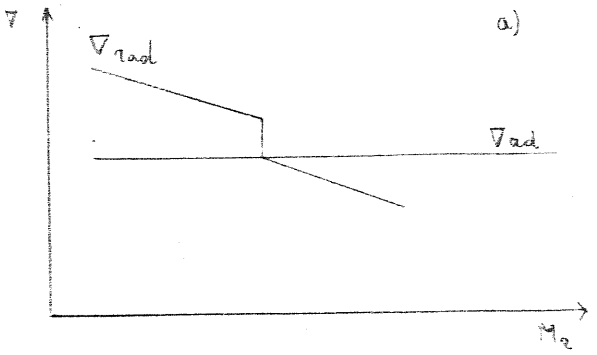
∇
a)
∇rad
∇ad
Mr

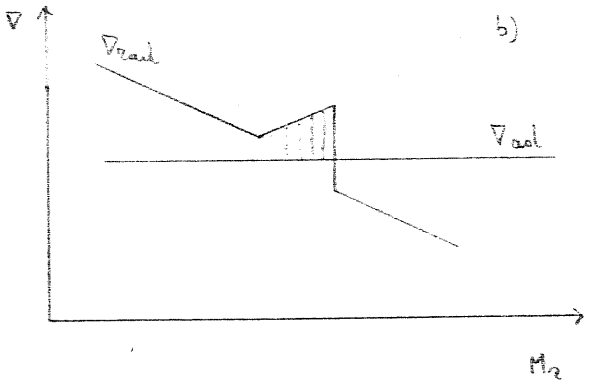
∇
b)
∇rad
∇ad
Mr

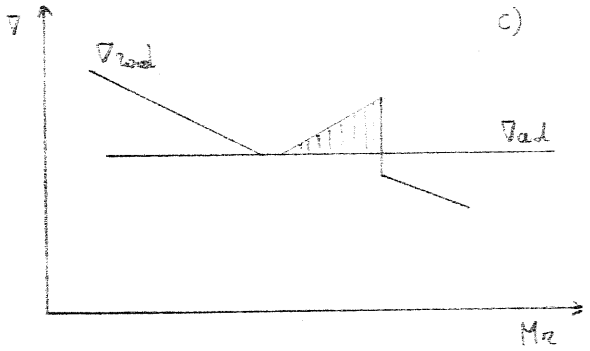
∇
c)
∇rad
∇ad
Mr

3.5

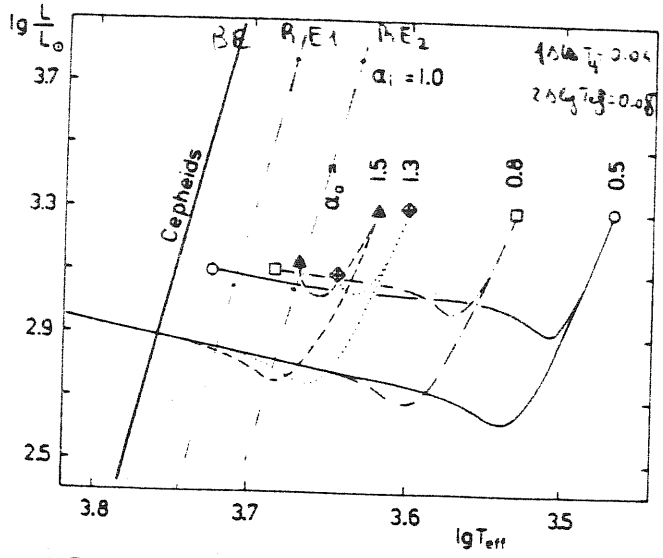

Evolutionary tracks for a $5\,M_\odot$ star in the red giant region of the HR diagram; the overshooting in the main-sequence phase was here calculated using $\alpha_i = 0.5$. The ratio of mixing length to pressure scale height in the outer convective zone is varied from $\alpha_0 = 0.5$ to 1.5. For each of these tracks, equal symbols denote the highest point at the Hayashi-line (deepest penetration of the outer convective zone) and the bluest point of the loop

3.6

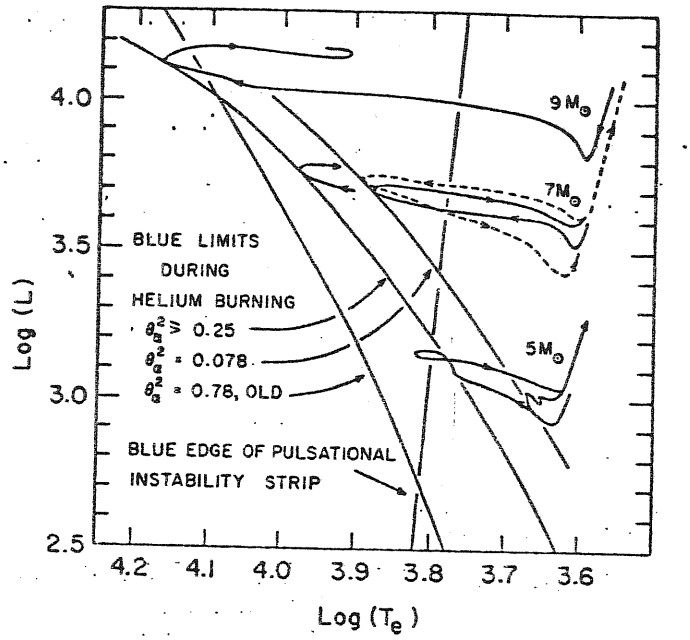

—Evolutionary tracks during core helium-burning, blue limits, and the blue edge of a theoretical instability strip for radial pulsation in the fundamental mode. Initial composition parameters are $X = 0.7$, $Y = 0.28$, $Z = 0.02$. Three choices of reduced width θ_a^2 are represented. For the $5\,M_\odot$ models, $\theta_a^2 = 0.078$ and 0.25; for the $7\,M_\odot$ models, $\theta_a^2 = 0.078$ and 0.78; for the $9\,M_\odot$ model, $\theta_a^2 = 0.25$. The blue limits connect, for different masses, the bluest points reached during the major core helium-burning phase. A blue limit defined by an earlier set of models (see Iben 1967) is also shown.

3.7

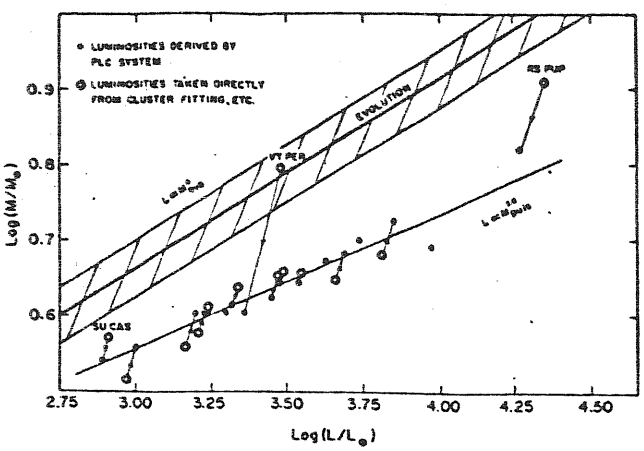

—Mass-luminosity relationships. The shaded region represents the $\mathcal{M}$-L relationship for stars of composition $(X, Z) = (0.71, 0.02)$ during the core-helium-burning stage. Circles are the consequence of comparing observed periods and colors and estimated luminosities with a theoretical relationship between period, surface temperature, luminosity, and mass for pulsation in the fundamental mode. The luminosity coordinates of the 13 open circles have been estimated by the main-sequence-fitting technique. The luminosity coordinates of the filled circles have been estimated by using the period-luminosity-color (*PLC*) relationship given by Sandage and Tammann (1969).

3.8

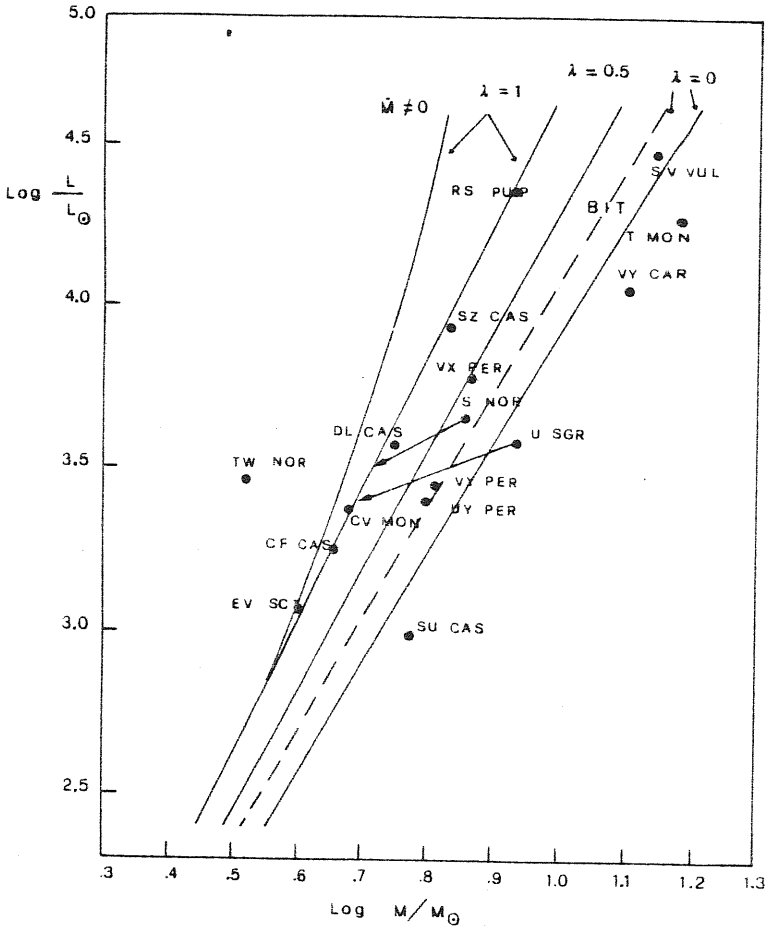

3.9

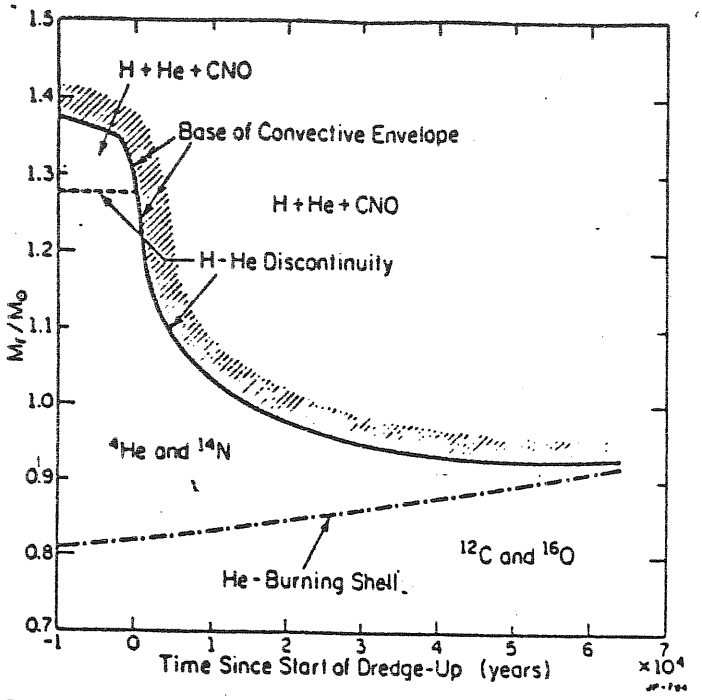

The variation with time of the location (in mass) of the base of the convective envelope and of the center of the helium-burning shell during the second dredge-up phase in a model of mass 5 $M_\odot$ and initial composition $(Y, Z) = (0.28, 0.001)$.

3.10 a

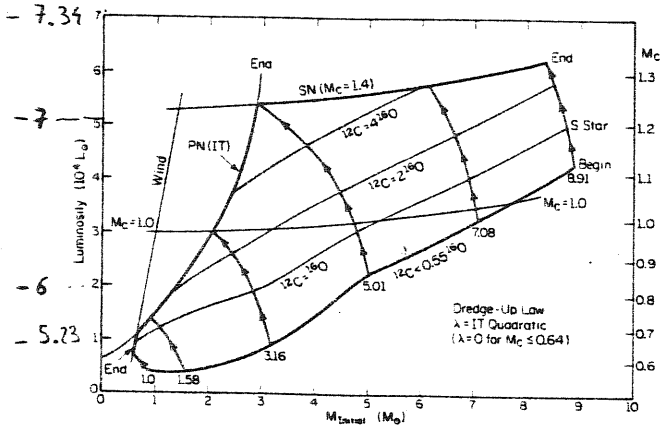

3.10 b

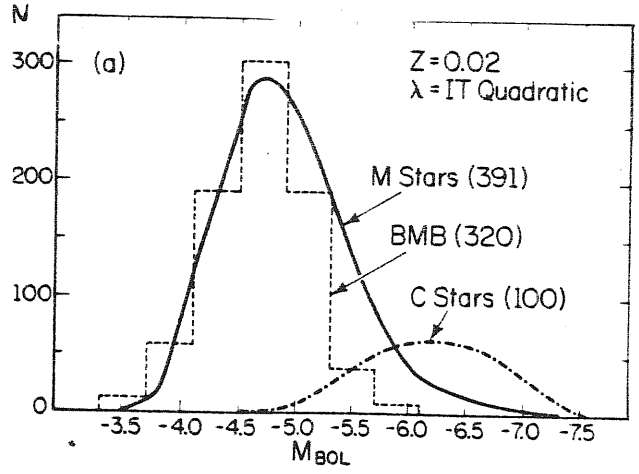

3.11

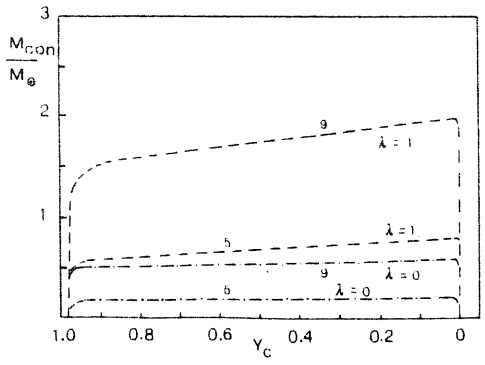
$\frac{M_{con}}{M_\odot}$
3
2
1
9
$\lambda = 1$
5
$\lambda = 1$
9
$\lambda = 0$
5
$\lambda = 0$
1.0
0.8
0.6
Y_c
0.4
0.2
0

3.12

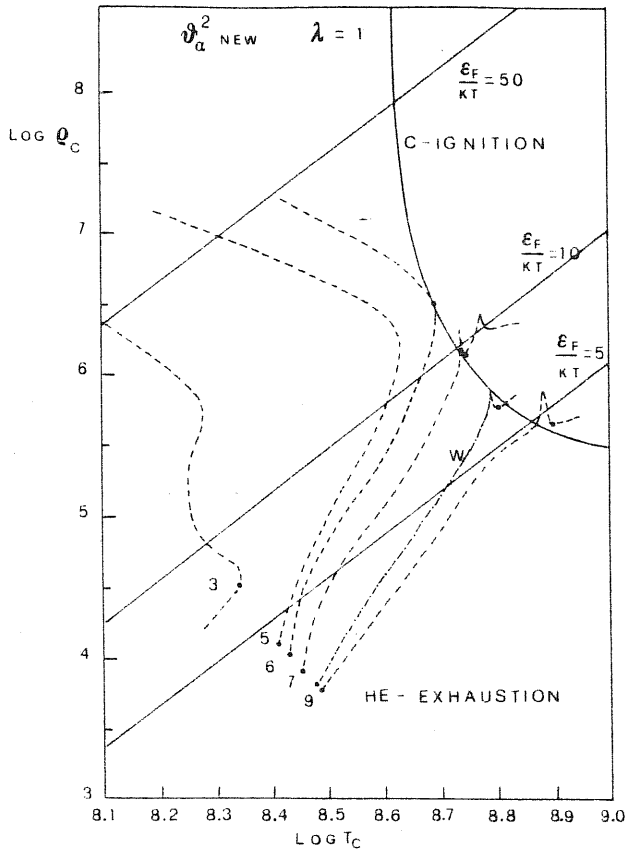
ϑ_α^2 NEW
$\lambda = 1$
$\frac{\varepsilon_F}{KT} = 50$
C-IGNITION
$\frac{\varepsilon_F}{KT} = 10$
$\frac{\varepsilon_F}{KT} = 5$
W
3
5
6
7
9
HE - EXHAUSTION
LOG ϱ_c
8
7
6
5
4
3
8.1
8.2
8.3
8.4
8.5
8.6
8.7
8.8
8.9
9.0
LOG T_c

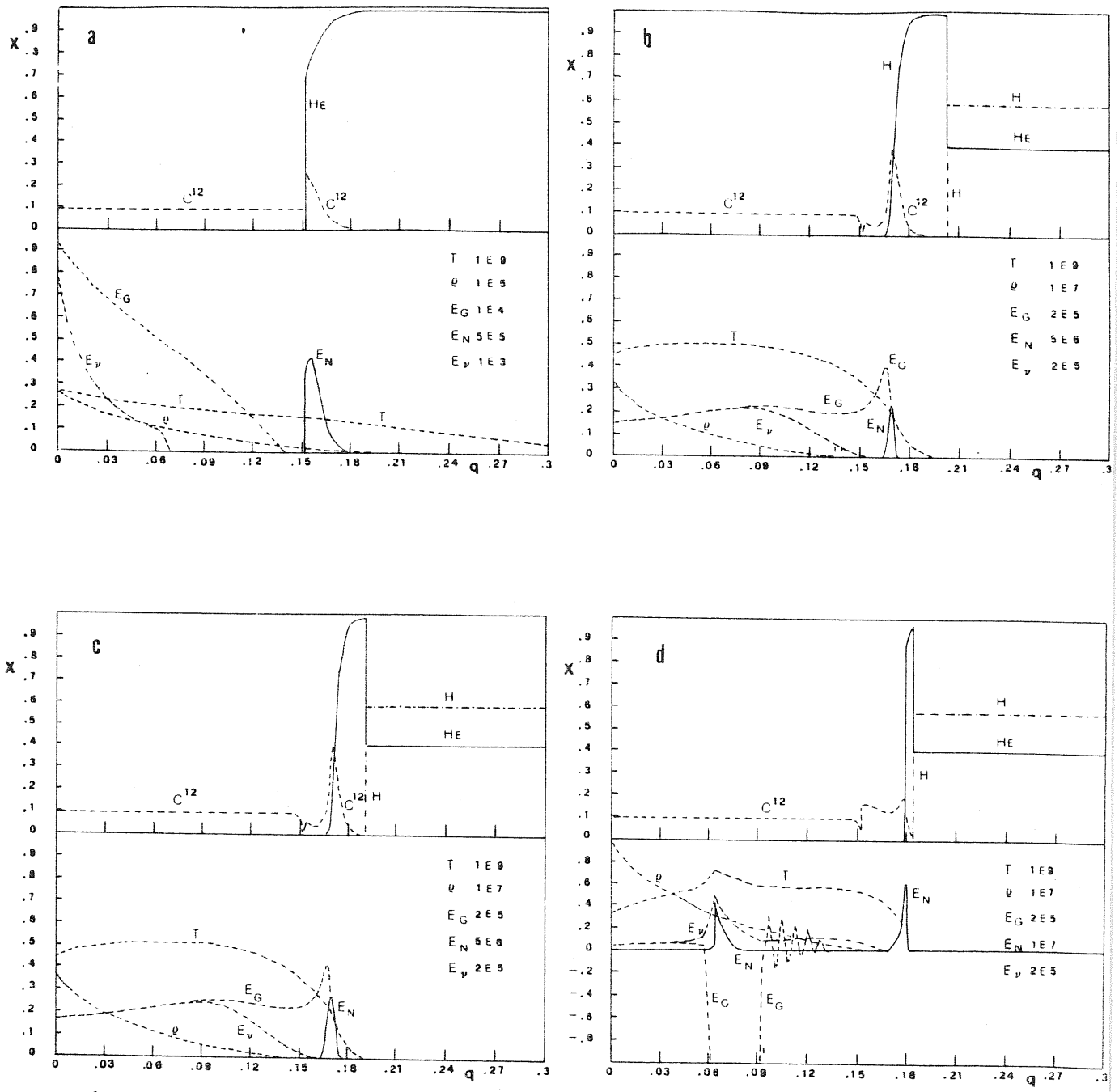

Internal structure of the 6 $M_\odot$ star of set C at various stages of the AGB phase: **a** beginning of AGB, **b** beginning of the 2nd dredge up, **c** during the 2nd dredge up, **d** stage of off-centre C-ignition. The abscissa shows the fractionary mass $q = M_r/M$, whereas the ordinate is normalized to the value indicated for each quantity at the right hand side of the diagrams. E_ν stands for the absolute value of the rate of neutrino energy losses.

CHAPTER IV

4.1 Low mass stars

The stars that after the Main Sequence phase ignite Helium in a highly electron degenerate core undergoing the Helium flash phenomenon, belong to the low mass stars category.

The appropriate mass range is defined on the side of the upper limit, by the ability of the models of building up an inert He core which encompasses the limit of Schonberg-Chandrasekhar before the degeneracy sets in and, on the side of the lower limit by their ability of ignite Helium.

The Schonberg-Chandrasekhar theory on the stability of an isothermal core is useful for understanding how the upper limit (M_{HEF}), which separates intermediate mass stars from low mass stars, depends on the assumed input physics. In this mass range the inert Helium core left out after central Hydrogen exhaustion, may reach an isothermal stable configuration because its mass is less than the Schonberg-Chandrasekhar limit; however owing to the continuous advancement of the Hydrogen burning shell its mass steadily grows and, when it encompasses the Schonberg-Chandrasekhar limit two different situations may arise, depending on the degree of the internal electron degeneracy.

For sufficient low degeneracy the core becomes unstable and enters a phase of rapid gravitational contraction so that heating

of the central regions drives the model toward quite He-ignition in a non-degenerate material.

On the contrary if degeneracy is already considerable, the core remains isothermal while being greater than the Schonberg-Chandrasekhar limit and the model enters a phase of slow growth of the degenerate core which is driven by the input of Helium provided by the Hydrogen burning shell. Contrary to the previous alternative where the characteristic lifetime of the phase was that of gravitational contraction, here the lifetime is defined by the velocity of the outward displacement of the Hydrogen shell and in turn by the luminosity of the model.

Ultimately the central temperature and density reach the Helium burning locus but, because of the strong electron degeneracy, ignition is violent and give rise to the so called Helium flash phenomenon.

These two alternatives generate two very different morphologies in the HR diagram. In both cases the model climbs along the Hayashi line but, both the time duration and the extension of the Red Giant phase is much shorter in the first case than in the second, so that only clusters with turnoff masses below M_{HEF} have very well populated and extended Read Giant Branches (RGB), which constitute one of the main characteristics of their HR diagrams. Existing models in the literature (Iben 1967, Sweigart and Gross 1978) have shown that M_{HEF} is a sensitive function of the initial chemical composition, being around 2.2 $M_{\odot}$ for a value typical of

the Pop. I , while being around 1.8 $M_{\odot}$ for the Pop. II.

Both these values are well above the minimum mass which possesses a convective core during central Hydrogen burning (around 1.2 - 1.1 $M_{\odot}$) so that it is straightforward to foresee the impact of the overshooting even in this range of masses. In particular the greater inert Helium core left out at the end of central Hydrogen burning, by a more extended convective region, immediately suggests a lower value of M_{HEF}.

Several observational implications would consequently follow and, among others, we recall that if the transition mass between intermediate and low mass stars shifts toward a lower value, the appearance of a well developed Red Giant Branch in star clusters shifts toward older ages.

Once the Helium flash had occurred the subsequent evolution of low mass stars is very similar to that of intermediate mass stars. Central Helium burning proceeds in a convective core so that here again overshooting may play a significant role.

To investigate on the effects of overshooting in the range of low mass stars I have computed evolutionary tracks which span the main sequence phase and the entire Red Giant phase, till to the violent Helium ignition; furthermore to complete the evolution of these stars I have constructed Zero Age Horizontal Branch models with suitable values of initial parameters (like Helium core mass, total mass ....) and I have evolved these models up to the appearance of the first major thermal pulse during the double

shell phase.

To better understand the result obtained with this new class of models and to facilitate the comparison with the observational counterpart it is useful to separate low mass stars in two different groups.

Stars in the range $M_{con} < M < M_{HEF}$ suffer overshooting during both central Hydrogen and Helium burning phases and observations of the oldest open clusters in the Galaxy and of their coeval in the Magellanic Clouds are very powerful in assessing the relevance of this phenomenon. Evolution of the stars in the range $M_{LOW} < M < M_{con}$, which possess radiative cores during central Hydrogen burning and for which overshooting is active only during central Helium burning, will be presented in the next chapter where, looking to the information collected in the domain of the Globular Clusters, we will be able to fix the mixing length scale with some confidence. Table 4.1 below resumes our computed sequences for the Hydrogen burning phase.

Table 4.1 **Hydrogen burning**

	Z = 0.02 Y = 0.280
M_i =	0.7,0.8,0.9,1.0,1.1,1.2,1.3,1.4,1.5,1.6*,1.7*,2.0*
	Z = 0.001 Y = 0.299
M_i =	0.7,0.8,0.9,1.0,1.1,1.2,1.3,1.4*,1.5*,1.6*,1.7*,2.0*
	Z = 0.001 Y = 0.200
M_i =	0.7,0.8,0.9

M_i = total mass in solar units
asterisked models does not undergo the Helium flash

4.2 Low mass stars with $M_{con} < M < M_{HEF}$

As can be seen from table 4.1 the major result concerning this class of stars is the strong dependence of M_{HEF} on the assumed amount of extramixing during the main sequence phase.

For a Pop. I chemical composition this value changes from about 2.2 $M_{\odot}$ in the classical case, to about 1.5-1.6 $M_{\odot}$ when overshooting is considered (with Λ=1); similarly for a Pop. II chemical composition M_{HEF} changes from about 1.8 $M_{\odot}$ to about 1.3-1.4 $M_{\odot}$ (Λ=1).

As for the other mass ranges this result confirms the finding that overshooting during the main sequence phase makes the model to behave like a more massive standard one.

From the observational standpoint the very different morphology of the red giant region in the HR diagrams of clusters with turnoff masses above and below M_{HEF} renders the analysis of their luminosity functions a powerful tool for investigating about the precise determination of the transition mass.

Recently Barbaro and Pigatto (1984) have analysed 38 among the oldest open clusters performing both a comparison of the HR diagram with isochrones and a statistical check of the fit between observed and theoretical luminosity functions of the red giant stars. Figure 4.1 (from Barbaro and Pigatto 1984) shows a set of luminosity functions constructed for a metallicity Z=0.01 and for the shown ages; the underlying evolutionary tracks are from Mengel (1979) and Sweigart and Gross (1976,1978) and are

based on the standard input physics, in particular without overshooting from convective core.

One clearly sees that the base of the red giant branch is well defined because a relative maximum of stars is expected there, and that the luminosity function has a bimodal character, because a second relative maximum is expected, some magnitudes brighter, in the region of helium burning stars. From the comparison of the theoretical and observed luminosity functions and from the analysis of other relevant parameters (like an independent estimate of the metal abundance, the absolute magnitude and the intrinsic color of the turnoff point and the position of the Red Giant Branch on the HR diagram) a consistent picture of the age and of the metal abundance should emerge for each cluster, with the accuracy permitted by the errors in the assumed distance modulus and reddening, and by the quality of the HR diagram itself.

Barbaro and Pigatto were able to show that their sample dichotomizes into two groups, that they called older and younger depending on the intrinsic color of the turnoff point. While older clusters - $(B-V)_o > 0.35$ - strictly fulfill standard theoretical expectations, for the group of younger clusters it is impossible to accept any of the theoretical luminosity functions constructed on the basis of the age (and chemical composition) suggested by other parameters of the HR diagram [$(B-V)_o$ and M_v at the turnoff]. In particular observed red giant luminosity

function shows up as a narrow clump of red stars, much brighter than the expected base of the Red Giant Branch.

This is illustrated in fig. 4.2 in which the magnitude of the faintest red star is plotted against the $(B-V)_o$ of the turnoff of the parent cluster. Continuous lines in the Figure are the theoretical relations between the $(B-V)_{o,t}$ and the magnitude of the base of the Red Giant Branch (where one expects a maximum of stars !) for different metallicities. The sample of clusters clearly dichotomizes at a $(B-V)_{o,t}$ of about 0.35, below which all clusters are well above the theoretical lines. A metallicity effect would produce an inverse tendency as can be seen from the relative positions of the theoretical lines.

Instead all happens as if younger clusters have missed the strong electron degenerate Helium core building phase, and have proceeded to a non violent Helium ignition; therefore no extended Red Giant Branch would be observed and the clump of stars would be in the central Helium burning phase, at a higher luminosity. In that case we would be looking at the transition mass between non degenerate and degenerate Helium ignition or between intermediate and low mass stars. However such a behaviour is expected to occur at a much lower $(B-V)_{o,t}$ in the standard theory, than that showed by Figure 4.2 and indeed the suggested turnoff mass at the transition (for a solar composition) is of only 1.4 - 1.5 M_o against the value of 2.2 M_o indicated by the theory. It is unlikely that errors in the observations of single

clusters combine in such a way to give the well defined trend in Figure 4.2, so that putting together also the information provided by the statistics on the luminosity functions, it seems natural to conclude that the trouble must lie in the theory.

With the help of the Schonberg-Chandrasekhar theory we have concluded at the beginning, that the branching between intermediate and low mass stars must come soon after central Hydrogen burning, when the subsequent fate of the star relies on the stability of its isothermal core.

Among those mechanisms which, at given initial mass, may result in an enlarged inert Helium core after the main sequence phase we recall mixing of whatever kind: overshooting, diffusion, meridional. As far as the last mechanism is concerned, one may object that it would require a significant rotation component, while for what concerns diffusion it suffices to remember that its efficiency increases with decreasing mass, in that contrary to what is suggested by the above observations.

As far as other possibilities are concerned that, beside mixing, may resolve the above discrepancy, we stress that observations put stringent limits to the space of parameters into which we may investigate.

First the physics underlying the formation of the Red Giant Branch is quite simple and the observation of Galactic Globular Clusters indicates that this phase is quite well understood. Second a relatively early phase of evolution is incriminate,

where incertitudes related to those phenomena like mass loss, neutrino emission, Helium burning reaction rates and conduction, which certainly enter more advanced phases, are completely excluded here.

Among the "known" phenomena, rotation may affect the future evolution of an inert Helium core, but one wonders if it can be so important that a significant range of masses (from 2.2 to about 1.5 $M_{\odot}$) avoid degeneracy.

Models with overshooting of table 4.1 have a better chance for explaining the discrepancy observed by Barbaro and Pigatto. Indeed with the calibrations obtained by Pigatto(1986), based on the new models, the discrepancy vanishes almost completely as can be seen from Figure 4.3 (Pigatto 1986) in which the same data of Figure 4.2 are displayed together with relations $M_{b,RG} - (B-V)_{o,t}$ obtained from models in table 4.1.

Looking now to the new models in more detail we see from Figures 4.4 and 4.5 the behaviour of the convective core during the evolution (indicated by the central Hydrogen abundance) for different initial masses and for the chemical compositions of Z=0.02 and Z=0.001 respectively. We first notice that the limiting mass for deep convection to be significant (M_{con}) is about 1.2 $M_{\odot}$ and about 1.0 $M_{\odot}$ for the above compositions. Therefore these are also the initial masses above which we expect overshooting during central Hydrogen burning to be an important phenomenon.

If lifetimes are considered instead of masses, we get that clusters older than about 2 and 4 billions years are unaffected by overshooting during Hydrogen burning depending on the above metallicities; this fact holds independently from the mixing length parameter -A- because it is the unstable region itself which disappears at lower masses as can be seen from Figure 4.5 for the 9 $M_{\odot}$ model.

Of particular interest is the behaviour of the convective core for initial masses slightly above M_{con}; the rapid growth in mass, which causes for some models an increase of the central Hydrogen abundance, can be interpreted as due to the transition from the PP to the CNO Hydrogen burning cycles during the evolution. While for lower masses this happens only when Hydrogen starts burning in the shell (Renzini 1977), here the transition comes early, during central Hydrogen burning.

At the beginning the convective core shrinks because of the effect that the increasing central temperature has on the opacity; however when the model enters the region where the CNO cycle is dominant the term L_r/M_r makes the radiative gradient to encompass the adiabatic one in more and more external regions, so that a relatively rapid growth of the convective core follows. The characteristic timescale of growth is however much longer than the scale of mixing so that the convective core may be treated as chemically homogeneous; for the same reason this rapid variation has not the characteristic of a pulse of convection

which I will describe later.

Differences in the HR diagram with respect to models without overshooting are the same as for other mass ranges, however as anticipated in the discussion of massive stars, they are enhanced by the large effects of the overshooting for decreasing masses. The following table gives the percentage of the overshooting region with respect to the unstable region on the ZAMS and at maximum core extension, (conv-cuns)/cuns :

$M/M_\odot$	P_{ZAMS}	P_{Max}	$M/M_\odot$	P_{ZAMS}	P_{Max}
	Z = 0.02			Z = 0.001	
1.0	-	-	1.0	1.36	1.54
1.1	1.36	2.16	1.1	1.49	1.73
1.2	1.38	2.21	1.2	1.34	1.90
1.3	1.57	2.17	1.3	1.44	1.64
1.4	1.68	2.09	1.4		
1.5	1.82	2.14	1.5	1.38	1.41

A comparison of the values given for massive and intermediate mass stars, bearing in mind that the same algorithm was used together with the same mixing scale, shows how this phenomenon depends on the initial star mass.

The main characteristic quantities of the models during evolution are contained in Table 4.2, where the symbols have the following meanings:

AGE the age of the models in years; $L/L_\odot$ logarithm of the luminosity in solar units; T_{eff} logarithm of the effective temperature; M_{con} mass of the convective core in solar units;

M_{Sch} mass of the unstable region in solar units; X_{cen} central Hydrogen abundance by mass; T_c logarithm of the central temperature; ρ_c logarithm of the central density; L_x logarithm of the luminosity of the Hydrogen shell in solar units. M, Z, Y give the total mass in solar units and the abundance by mass of the metals and Helium respectively. Te-m, Te-M, L-m indicate where a minimum or maximum in temperature and luminosity are found.

Figures 4.6 and 4.7 contain the HR diagram of the computed models for the metal abundance by mass Z = 0.02 and Z = 0.001 respectively.

Legend to table 4.2

AGE the age of the models in years; L/L_o logarithm of the luminosity in solar units; T_{eff} logarithm of the effective temperature; M_{con} mass of the convective core in solar units and when central Hydrogen is zero, the mass of Helium-Hydrogen discontinuity; M_{Sch} mass of the unstable region in solar units and when central Hydrogen is zero, the mass of the maximum temperature; X_{cen} central Hydrogen abundance by mass and for the last model, the logarithm of the Helium luminosity in solar units; T_c logarithm of the central temperature; ρ_c logarithm of the central density; L_x logarithm of the luminosity of the Hydrogen shell in solar units. M, Z, Y give the total mass in solar units and the abundance by mass of the metals and Helium respectively. Te-m, Te-M, L-m indicate where a minimum or maximum in temperature and luminosity are found.

TABLE 4.2

M=0.7 Z=0.001 Y=0.299

AGE	$L/L_\odot$	T_{eff}	M_{con}	M_{Sch}	X_{cen}	T_c	ρ_c	L_x
0.00000E+00	-0.468	3.760	0.000	0.006	0.700	7.0855	2.0304	-0.468
0.19818E+10	-0.430	3.765	0.000	0.000	0.600	7.1008	2.0931	-0.430
0.38548E+10	-0.390	3.769	0.000	0.000	0.500	7.1168	2.1618	-0.390
0.56864E+10	-0.347	3.774	0.000	0.000	0.400	7.1351	2.2390	-0.347
0.74986E+10	-0.299	3.778	0.000	0.000	0.300	7.1559	2.3288	-0.299
0.94373E+10	-0.240	3.783	0.000	0.000	0.200	7.1808	2.4451	-0.240
0.12056E+11	-0.134	3.790	0.000	0.000	0.100	7.2188	2.6478	-0.134
0.13960E+11	-0.027	3.796	0.000	0.000	0.050	7.2608	2.8427	-0.027
0.15137E+11	0.054	3.799	0.000	0.000	0.010	7.3089	2.9767	0.054
0.15667E+11	0.098	3.799	0.000	0.000	0.001	7.3149	3.0756	0.098
0.17193E+11	0.299	3.790	0.372	0.000	0.000	7.3440	3.6380	0.300
0.17451E+11	0.361	3.780	0.372	0.000	0.000	7.3643	3.8637	0.361
0.17597E+11	0.404	3.770	0.372	0.000	0.000	7.3861	4.0435	0.405
0.17700E+11	0.441	3.760	0.372	0.000	0.000	7.4087	4.2014	0.442
0.17792E+11	0.483	3.750	0.372	0.000	0.000	7.4313	4.3576	0.484
0.17944E+11	0.600	3.736	0.372	0.000	0.000	7.4609	4.6091	0.599
0.18033E+11	0.700	3.731	0.372	0.000	0.000	7.4730	4.7406	0.699
0.18106E+11	0.800	3.727	0.372	0.000	0.000	7.4827	4.8412	0.799
0.18168E+11	0.900	3.723	0.357	0.000	0.000	7.4923	4.9229	0.899
0.18219E+11	1.000	3.720	0.331	0.000	0.000	7.5030	4.9920	0.999
0.18261E+11	1.100	3.716	0.318	0.000	0.000	7.5150	5.0529	1.099
0.18296E+11	1.200	3.713	0.306	0.000	0.000	7.5281	5.1082	1.198
0.18325E+11	1.300	3.709	0.301	0.000	0.000	7.5422	5.1599	1.298
0.18349E+11	1.400	3.705	0.301	0.000	0.000	7.5568	5.2082	1.398
0.18369E+11	1.500	3.702	0.301	0.000	0.000	7.5716	5.2534	1.498
0.18385E+11	1.600	3.697	0.301	0.000	0.000	7.5869	5.2968	1.598
0.18399E+11	1.700	3.693	0.301	0.000	0.000	7.6027	5.3385	1.698
0.18410E+11	1.800	3.689	0.301	0.000	0.000	7.6189	5.3791	1.798
0.18419E+11	1.900	3.684	0.301	0.000	0.000	7.6357	5.4191	1.898
0.18429E+11	2.000	3.680	0.302	0.000	0.000	7.6581	5.4701	1.998
0.18435E+11	2.100	3.675	0.311	0.005	0.000	7.6731	5.5048	2.098
0.18440E+11	2.200	3.670	0.320	0.017	0.000	7.6883	5.5394	2.198
0.18444E+11	2.300	3.665	0.331	0.042	0.000	7.7041	5.5742	2.298
0.18447E+11	2.400	3.660	0.342	0.067	0.000	7.7207	5.6093	2.398
0.18450E+11	2.500	3.654	0.353	0.094	0.000	7.7379	5.6451	2.497
0.18453E+11	2.600	3.649	0.365	0.120	0.000	7.7558	5.6815	2.597
0.18455E+11	2.700	3.643	0.378	0.142	0.000	7.7743	5.7190	2.697
0.18456E+11	2.800	3.638	0.392	0.160	0.000	7.7932	5.7577	2.797
0.18458E+11	2.900	3.632	0.407	0.182	0.000	7.8125	5.7978	2.897
0.18459E+11	3.000	3.627	0.423	0.202	0.000	7.8322	5.8397	2.997
0.18460E+11	3.100	3.621	0.440	0.223	0.000	7.8523	5.8838	3.096
0.18461E+11	3.200	3.616	0.458	0.242	0.000	7.8725	5.9306	3.196
0.18462E+11	3.264	3.613	0.472	0.150	2.694	7.8810	5.9559	3.260

M=0.8 Z=0.001 Y=0.299

AGE	$L/L_\odot$	T_{eff}	M_{con}	M_{Sch}	X_{cen}	T_c	ρ_c	L_x	
0.00000E+00	-0.190	3.795	0.027	0.012	0.700	7.1279	2.0400	-0.190	
0.14722E+10	-0.146	3.799	0.010	0.004	0.600	7.1471	2.1048	-0.146	
0.26474E+10	-0.105	3.802	0.000	0.000	0.500	7.1645	2.1717	-0.105	
0.36765E+10	-0.067	3.805	0.000	0.000	0.400	7.1818	2.2443	-0.067	
0.47156E+10	-0.023	3.808	0.000	0.000	0.300	7.2008	2.3314	-0.023	
0.59018E+10	0.037	3.812	0.000	0.000	0.200	7.2240	2.4519	0.037	
0.74942E+10	0.140	3.819	0.000	0.000	0.100	7.2638	2.6540	0.140	
0.83088E+10	0.207	3.821	0.000	0.000	0.050	7.2989	2.7743	0.207	
0.88802E+10	0.258	3.823	0.000	0.000	0.010	7.3253	2.8765	0.258	
0.92582E+10	0.299	3.823	0.000	0.000	0.001	7.3298	2.9750	0.299	
0.93924E+10	0.316	3.823	0.000	0.000	0.000	7.3309	3.0149	0.316	Te-M
0.10031E+11	0.412	3.820	0.456	0.000	0.000	7.3412	3.2722	0.413	
0.10420E+11	0.499	3.810	0.456	0.000	0.000	7.3586	3.5507	0.499	
0.10575E+11	0.546	3.800	0.456	0.000	0.000	7.3738	3.7351	0.547	
0.10669E+11	0.579	3.790	0.456	0.000	0.000	7.3905	3.8888	0.580	
0.10734E+11	0.605	3.780	0.456	0.000	0.000	7.4093	4.0249	0.606	
0.10786E+11	0.624	3.770	0.456	0.000	0.000	7.4301	4.1535	0.626	
0.10832E+11	0.642	3.760	0.456	0.000	0.000	7.4517	4.2800	0.643	
0.10880E+11	0.666	3.750	0.456	0.000	0.000	7.4735	4.4170	0.668	
0.10997E+11	0.800	3.734	0.456	0.000	0.000	7.5043	4.7054	0.799	
0.11054E+11	0.900	3.729	0.456	0.000	0.000	7.5130	4.8219	0.899	
0.11101E+11	1.000	3.724	0.398	0.000	0.000	7.5217	4.9117	0.999	
0.11140E+11	1.100	3.721	0.363	0.000	0.000	7.5316	4.9862	1.099	
0.11172E+11	1.200	3.717	0.337	0.000	0.000	7.5428	5.0507	1.198	
0.11199E+11	1.300	3.713	0.322	0.000	0.000	7.5552	5.1079	1.298	
0.11221E+11	1.400	3.709	0.312	0.000	0.000	7.5686	5.1602	1.398	
0.11239E+11	1.500	3.705	0.309	0.000	0.000	7.5828	5.2089	1.498	
0.11254E+11	1.600	3.701	0.309	0.000	0.000	7.5977	5.2548	1.598	
0.11267E+11	1.700	3.697	0.308	0.000	0.000	7.6131	5.2986	1.698	
0.11277E+11	1.800	3.693	0.308	0.000	0.000	7.6292	5.3410	1.798	
0.11286E+11	1.900	3.688	0.308	0.000	0.000	7.6460	5.3824	1.898	
0.11293E+11	2.000	3.683	0.308	0.000	0.000	7.6637	5.4241	1.998	
0.11303E+11	2.100	3.679	0.312	0.000	0.000	7.6944	5.4956	2.098	
0.11308E+11	2.200	3.674	0.321	0.000	0.000	7.7084	5.5309	2.198	
0.11312E+11	2.300	3.669	0.331	0.006	0.000	7.7213	5.5674	2.298	
0.11315E+11	2.400	3.663	0.342	0.034	0.000	7.7357	5.6032	2.397	
0.11318E+11	2.500	3.658	0.353	0.058	0.000	7.7512	5.6396	2.497	
0.11321E+11	2.600	3.653	0.366	0.091	0.000	7.7675	5.6768	2.597	
0.11323E+11	2.700	3.647	0.378	0.116	0.000	7.7845	5.7147	2.697	
0.11324E+11	2.800	3.642	0.392	0.144	0.000	7.8021	5.7537	2.797	
0.11326E+11	2.900	3.636	0.407	0.168	0.000	7.8204	5.7942	2.897	
0.11327E+11	3.000	3.630	0.423	0.189	0.000	7.8391	5.8364	2.996	
0.11328E+11	3.100	3.625	0.440	0.214	0.000	7.8583	5.8808	3.096	
0.11329E+11	3.197	3.619	0.458	0.230	-0.803	7.8768	5.9257	3.193	

M=0.9 Z=0.001 Y=0.299

AGE	$L/L_\odot$	T_{eff}	M_{con}	M_{Sch}	X_{cen}	T_c	ρ_c	L_x
0.00000E+00	0.050	3.825	0.050	0.023	0.700	7.1667	2.0466	0.050
0.11335E+10	0.101	3.829	0.043	0.018	0.600	7.1890	2.1102	0.101
0.20959E+10	0.149	3.833	0.034	0.014	0.500	7.2118	2.1782	0.149
0.28692E+10	0.194	3.836	0.008	0.003	0.400	7.2333	2.2566	0.195
0.34510E+10	0.235	3.839	0.000	0.000	0.300	7.2497	2.3484	0.235
0.41051E+10	0.287	3.843	0.000	0.000	0.200	7.2705	2.4689	0.287
0.48330E+10	0.356	3.847	0.000	0.000	0.100	7.3035	2.6185	0.356
0.51716E+10	0.390	3.849	0.000	0.000	0.050	7.3245	2.6945	0.390
0.55217E+10	0.430	3.851	0.000	0.000	0.010	7.3382	2.7934	0.431
0.58185E+10	0.471	3.852	0.000	0.000	0.001	7.3408	2.8945	0.471
0.60238E+10	0.504	3.852	0.000	0.000	0.000	7.3427	2.9747	0.504
0.63972E+10	0.575	3.850	0.546	0.000	0.000	7.3504	3.1656	0.576
0.66951E+10	0.654	3.840	0.546	0.000	0.000	7.3642	3.4145	0.654
0.68104E+10	0.694	3.830	0.546	0.000	0.000	7.3748	3.5682	0.695
0.68825E+10	0.724	3.820	0.546	0.000	0.000	7.3861	3.6987	0.725
0.69334E+10	0.748	3.810	0.546	0.000	0.000	7.3990	3.8165	0.749
0.69723E+10	0.768	3.800	0.539	0.000	0.000	7.4142	3.9273	0.769
0.70036E+10	0.783	3.790	0.539	0.000	0.000	7.4315	4.0325	0.785
0.70306E+10	0.795	3.780	0.539	0.000	0.000	7.4506	4.1356	0.797
0.70552E+10	0.802	3.770	0.539	0.000	0.000	7.4708	4.2383	0.805
0.70794E+10	0.807	3.760	0.539	0.000	0.000	7.4916	4.3441	0.810
0.71076E+10	0.817	3.750	0.539	0.000	0.000	7.5125	4.4652	0.819
0.71701E+10	0.900	3.736	0.539	0.000	0.000	7.5370	4.6923	0.900
0.72149E+10	1.000	3.730	0.514	0.000	0.000	7.5445	4.8225	0.999
0.72511E+10	1.100	3.725	0.435	0.000	0.000	7.5514	4.9178	1.099
0.72814E+10	1.200	3.721	0.384	0.000	0.000	7.5597	4.9957	1.198
0.73065E+10	1.300	3.717	0.351	0.000	0.000	7.5698	5.0618	1.298
0.73274E+10	1.400	3.713	0.333	0.000	0.000	7.5814	5.1206	1.398
0.73447E+10	1.500	3.709	0.322	0.000	0.000	7.5940	5.1737	1.498
0.73591E+10	1.600	3.705	0.316	0.000	0.000	7.6078	5.2233	1.598
0.73711E+10	1.700	3.701	0.316	0.000	0.000	7.6225	5.2702	1.698
0.73810E+10	1.800	3.696	0.316	0.000	0.000	7.6379	5.3150	1.798
0.73893E+10	1.900	3.692	0.316	0.000	0.000	7.6541	5.3584	1.898
0.73963E+10	2.000	3.687	0.316	0.000	0.000	7.6709	5.4008	1.998
0.74023E+10	2.100	3.682	0.316	0.000	0.000	7.6888	5.4439	2.098
0.74115E+10	2.200	3.677	0.322	0.003	0.000	7.7212	5.5222	2.198
0.74154E+10	2.300	3.672	0.332	0.004	0.000	7.7350	5.5590	2.298
0.74187E+10	2.400	3.667	0.342	0.015	0.000	7.7484	5.5957	2.397
0.74215E+10	2.500	3.662	0.354	0.039	0.000	7.7627	5.6326	2.497
0.74239E+10	2.600	3.656	0.366	0.072	0.000	7.7778	5.6701	2.597
0.74259E+10	2.700	3.651	0.379	0.102	0.000	7.7939	5.7085	2.697
0.74275E+10	2.800	3.645	0.392	0.128	0.000	7.8106	5.7478	2.797
0.74290E+10	2.900	3.639	0.407	0.157	0.000	7.8280	5.7885	2.897
0.74302E+10	3.000	3.634	0.423	0.181	0.000	7.8460	5.8310	2.997
0.74313E+10	3.100	3.628	0.440	0.207	0.000	7.8644	5.8754	3.096
0.74322E+10	3.200	3.623	0.458	0.218	0.000	7.8830	5.9223	3.196
0.74325E+10	3.232	3.621	0.465	0.169	0.511	7.8875	5.9357	3.228

M=1.0 Z=0.001 Y=0.299

AGE	$L/L_\odot$	T_{eff}	M_{con}	M_{Sch}	X_{cen}	T_c	ρ_c	L_x	
0.00000E+00	0.260	3.855	0.085	0.036	0.700	7.2011	2.0492	0.259	
0.88664E+09	0.314	3.861	0.083	0.035	0.600	7.2251	2.1095	0.314	
0.16409E+10	0.368	3.866	0.071	0.031	0.500	7.2504	2.1766	0.368	
0.22218E+10	0.419	3.871	0.028	0.012	0.400	7.2752	2.2601	0.419	
0.26338E+10	0.461	3.876	0.007	0.002	0.300	7.2970	2.3542	0.461	
0.29933E+10	0.502	3.881	0.007	0.002	0.200	7.3209	2.4551	0.503	
0.32746E+10	0.535	3.882	0.023	0.009	0.135	7.3469	2.5209	0.535	Te-M
0.43871E+10	0.665	3.858	0.155	0.061	0.100	7.4055	2.4623	0.666	
0.45827E+10	0.695	3.849	0.146	0.059	0.050	7.4275	2.5128	0.696	
0.46575E+10	0.710	3.848	0.140	0.057	0.030	7.4413	2.5509	0.710	Te-m
0.47244E+10	0.733	3.854	0.133	0.054	0.010	7.4671	2.6294	0.732	
0.47529E+10	0.781	3.881	0.118	0.044	0.001	7.5147	2.8101	0.755	
0.47567E+10	0.843	3.900	0.614	0.000	0.000	7.5354	3.2396	0.769	Te-M
0.47568E+10	0.844	3.900	0.614	0.000	0.000	7.5344	3.2588	0.782	
0.47578E+10	0.859	3.890	0.614	0.000	0.000	7.5293	3.4703	0.888	
0.47588E+10	0.876	3.880	0.614	0.000	0.000	7.5259	3.5672	0.904	
0.47599E+10	0.890	3.870	0.614	0.000	0.000	7.5225	3.6495	0.912	
0.47613E+10	0.900	3.860	0.614	0.000	0.000	7.5191	3.7228	0.917	
0.47632E+10	0.907	3.850	0.614	0.000	0.000	7.5157	3.7917	0.920	
0.47656E+10	0.913	3.840	0.614	0.000	0.000	7.5127	3.8596	0.922	
0.47689E+10	0.918	3.830	0.614	0.000	0.000	7.5101	3.9289	0.925	
0.47736E+10	0.924	3.820	0.614	0.000	0.000	7.5089	4.0030	0.929	
0.47801E+10	0.929	3.810	0.614	0.000	0.000	7.5106	4.0845	0.933	
0.47882E+10	0.933	3.800	0.614	0.000	0.000	7.5161	4.1670	0.937	
0.47972E+10	0.936	3.790	0.614	0.000	0.000	7.5239	4.2473	0.940	
0.48074E+10	0.935	3.780	0.614	0.000	0.000	7.5318	4.3254	0.939	
0.48196E+10	0.929	3.770	0.614	0.000	0.000	7.5377	4.4043	0.933	
0.48360E+10	0.921	3.760	0.614	0.000	0.000	7.5419	4.4920	0.924	
0.48542E+10	0.918	3.752	0.614	0.000	0.000	7.5469	4.5769	0.920	L-m
0.48603E+10	0.919	3.750	0.614	0.000	0.000	7.5485	4.6031	0.921	
0.49266E+10	1.000	3.735	0.614	0.000	0.000	7.5519	4.8258	0.999	
0.49698E+10	1.100	3.729	0.532	0.000	0.000	7.5517	4.9353	1.099	
0.50031E+10	1.200	3.725	0.447	0.000	0.000	7.5566	5.0139	1.199	
0.50297E+10	1.300	3.721	0.395	0.000	0.000	7.5645	5.0778	1.299	
0.50515E+10	1.400	3.716	0.359	0.000	0.000	7.5752	5.1340	1.398	
0.50694E+10	1.500	3.712	0.340	0.000	0.000	7.5878	5.1849	1.498	
0.50840E+10	1.600	3.708	0.329	0.000	0.000	7.6017	5.2322	1.598	
0.50960E+10	1.700	3.704	0.323	0.000	0.000	7.6165	5.2768	1.698	
0.51059E+10	1.800	3.699	0.323	0.000	0.000	7.6322	5.3197	1.798	
0.51141E+10	1.900	3.695	0.323	0.000	0.000	7.6485	5.3613	1.898	
0.51209E+10	2.000	3.690	0.323	0.000	0.000	7.6654	5.4019	1.998	
0.51266E+10	2.100	3.685	0.323	0.000	0.000	7.6830	5.4424	2.098	
0.51317E+10	2.200	3.680	0.323	0.001	0.000	7.7022	5.4855	2.198	
0.51392E+10	2.300	3.676	0.332	0.019	0.000	7.7337	5.5575	2.298	
0.51424E+10	2.400	3.671	0.342	0.029	0.000	7.7484	5.5939	2.397	
0.51452E+10	2.500	3.665	0.354	0.044	0.000	7.7633	5.6309	2.497	
0.51476E+10	2.600	3.660	0.366	0.069	0.000	7.7787	5.6685	2.597	
0.51496E+10	2.700	3.654	0.378	0.099	0.000	7.7948	5.7069	2.697	
0.51513E+10	2.800	3.649	0.392	0.124	0.000	7.8116	5.7464	2.797	
0.51527E+10	2.900	3.643	0.407	0.155	0.000	7.8289	5.7874	2.897	
0.51539E+10	3.000	3.637	0.422	0.183	0.000	7.8468	5.8299	2.997	
0.51550E+10	3.100	3.632	0.439	0.206	0.000	7.8652	5.8745	3.096	
0.51559E+10	3.200	3.626	0.458	0.220	0.000	7.8836	5.9213	3.196	
0.51562E+10	3.236	3.624	0.466	0.142	1.014	7.8879	5.9354	3.232	

M=1.1 Z=0.001 Y=0.299

AGE	$L/L_\odot$	T_{eff}	M_{con}	M_{Sch}	X_{cen}	T_c	ρ_c	L_x	
0.00000E+00	0.443	3.893	0.127	0.051	0.700	7.2314	2.0481	0.443	
0.71424E+09	0.501	3.900	0.125	0.051	0.600	7.2563	2.1052	0.501	
0.13005E+10	0.559	3.906	0.098	0.043	0.500	7.2827	2.1732	0.559	
0.17510E+10	0.612	3.912	0.075	0.030	0.400	7.3104	2.2531	0.612	
0.22157E+10	0.670	3.915	0.113	0.041	0.300	7.3454	2.3285	0.670	
0.23137E+10	0.682	3.915	0.127	0.045	0.288	7.3517	2.3344	0.682	Te-M
0.29294E+10	0.781	3.904	0.194	0.071	0.200	7.3895	2.3498	0.782	
0.32685E+10	0.840	3.884	0.179	0.072	0.100	7.4195	2.4040	0.840	
0.34162E+10	0.870	3.874	0.166	0.069	0.050	7.4408	2.4546	0.871	
0.34750E+10	0.886	3.872	0.160	0.067	0.028	7.4557	2.4949	0.886	Te-m
0.35204E+10	0.906	3.879	0.152	0.064	0.010	7.4808	2.5702	0.904	
0.35409E+10	0.951	3.908	0.140	0.055	0.001	7.5311	2.7458	0.921	
0.35436E+10	1.020	3.934	0.715	0.000	0.000	7.5621	3.2121	0.926	Te-M
0.35439E+10	1.018	3.930	0.715	0.000	0.000	7.5600	3.3354	1.038	
0.35444E+10	1.019	3.920	0.715	0.000	0.000	7.5565	3.4372	1.068	
0.35449E+10	1.035	3.910	0.715	0.000	0.000	7.5549	3.5193	1.077	
0.35455E+10	1.052	3.900	0.715	0.000	0.000	7.5538	3.5951	1.084	
0.35463E+10	1.063	3.890	0.715	0.000	0.000	7.5529	3.6640	1.089	
0.35472E+10	1.072	3.880	0.715	0.000	0.000	7.5523	3.7283	1.092	
0.35483E+10	1.079	3.870	0.715	0.000	0.000	7.5521	3.7895	1.094	
0.35496E+10	1.084	3.860	0.715	0.000	0.000	7.5527	3.8482	1.097	
0.35511E+10	1.089	3.850	0.707	0.000	0.000	7.5540	3.9043	1.099	
0.35527E+10	1.093	3.840	0.707	0.000	0.000	7.5566	3.9584	1.101	
0.35546E+10	1.096	3.830	0.707	0.000	0.000	7.5607	4.0123	1.103	
0.35568E+10	1.099	3.820	0.707	0.000	0.000	7.5666	4.0684	1.105	
0.35593E+10	1.102	3.810	0.707	0.000	0.000	7.5750	4.1287	1.108	
0.35623E+10	1.105	3.800	0.707	0.000	0.000	7.5863	4.1961	1.110	
0.35657E+10	1.105	3.790	0.707	0.000	0.000	7.5999	4.2689	1.111	
0.35695E+10	1.103	3.780	0.707	0.000	0.000	7.6147	4.3450	1.110	
0.35739E+10	1.096	3.770	0.707	0.000	0.000	7.6297	4.4257	1.103	
0.35791E+10	1.082	3.760	0.707	0.000	0.000	7.6429	4.5071	1.091	
0.35860E+10	1.065	3.750	0.707	0.000	0.000	7.6526	4.5975	1.073	
0.35894E+10	1.063	3.747	0.707	0.000	0.000	7.6542	4.6343	1.069	L-m
0.35994E+10	1.076	3.740	0.707	0.000	0.000	7.6529	4.7216	1.077	
0.36084E+10	1.100	3.736	0.707	0.000	0.000	7.6493	4.7853	1.100	
0.36360E+10	1.200	3.729	0.595	0.000	0.000	7.6334	4.9302	1.199	
0.36589E+10	1.300	3.724	0.483	0.000	0.000	7.6227	5.0214	1.299	
0.36785E+10	1.400	3.720	0.410	0.000	0.000	7.6194	5.0927	1.398	
0.36950E+10	1.500	3.716	0.373	0.000	0.000	7.6220	5.1528	1.498	
0.37088E+10	1.600	3.712	0.348	0.000	0.000	7.6288	5.2059	1.598	
0.37203E+10	1.700	3.707	0.337	0.000	0.000	7.6387	5.2548	1.698	
0.37298E+10	1.800	3.703	0.331	0.000	0.000	7.6507	5.3005	1.798	
0.37377E+10	1.900	3.698	0.330	0.000	0.000	7.6643	5.3442	1.898	
0.37443E+10	2.000	3.693	0.330	0.000	0.000	7.6792	5.3866	1.998	
0.37499E+10	2.100	3.688	0.330	0.000	0.000	7.6951	5.4280	2.098	
0.37546E+10	2.200	3.683	0.330	0.000	0.000	7.7120	5.4696	2.198	
0.37621E+10	2.300	3.679	0.333	0.015	0.000	7.7465	5.5515	2.297	
0.37653E+10	2.400	3.674	0.343	0.023	0.000	7.7605	5.5884	2.397	
0.37681E+10	2.500	3.668	0.354	0.034	0.000	7.7746	5.6259	2.497	
0.37704E+10	2.600	3.663	0.366	0.055	0.000	7.7891	5.6640	2.597	
0.37724E+10	2.700	3.657	0.379	0.084	0.000	7.8042	5.7028	2.697	
0.37740E+10	2.800	3.652	0.392	0.109	0.000	7.8200	5.7426	2.797	
0.37755E+10	2.900	3.646	0.407	0.142	0.000	7.8365	5.7837	2.897	
0.37767E+10	3.000	3.640	0.423	0.172	0.000	7.8536	5.8265	2.997	
0.37777E+10	3.100	3.635	0.440	0.196	0.000	7.8712	5.8714	3.096	
0.37786E+10	3.200	3.629	0.458	0.196	0.000	7.8886	5.9180	3.196	
0.37788E+10	3.219	3.628	0.463	0.120	1.168	7.8894	5.9236	3.215	

M=1.2 Z=0.001 Y=0.299

AGE	$L/L_\odot$	T_{eff}	M_{con}	M_{Sch}	X_{cen}	T_c	ρ_c	L_x	
0.00000E+00	0.607	3.929	0.166	0.071	0.700	7.2581	2.0448	0.607	
0.57165E+09	0.668	3.936	0.159	0.067	0.600	7.2835	2.1000	0.668	
0.10338E+10	0.727	3.942	0.139	0.055	0.500	7.3105	2.1647	0.728	
0.14377E+10	0.785	3.946	0.160	0.057	0.400	7.3406	2.2291	0.785	
0.16491E+10	0.822	3.946	0.195	0.067	0.360	7.3569	2.2475	0.822	Te-M
0.19605E+10	0.884	3.943	0.235	0.081	0.300	7.3790	2.2621	0.885	
0.22823E+10	0.948	3.929	0.227	0.089	0.200	7.4040	2.2964	0.948	
0.25373E+10	1.008	3.906	0.201	0.086	0.100	7.4322	2.3491	1.009	
0.26456E+10	1.038	3.895	0.185	0.080	0.050	7.4532	2.3997	1.039	
0.26900E+10	1.054	3.893	0.177	0.077	0.027	7.4689	2.4423	1.054	Te-m
0.27217E+10	1.073	3.900	0.172	0.073	0.010	7.4936	2.5135	1.071	
0.27368E+10	1.116	3.930	0.160	0.067	0.001	7.5457	2.6870	1.082	
0.27387E+10	1.184	3.959	0.813	0.000	0.000	7.5835	3.1500	1.082	Te-M
0.27390E+10	1.164	3.950	0.813	0.000	0.000	7.5761	3.3024	1.232	
0.27393E+10	1.162	3.940	0.813	0.000	0.000	7.5739	3.3739	1.231	
0.27396E+10	1.182	3.930	0.805	0.000	0.000	7.5736	3.4464	1.239	
0.27399E+10	1.201	3.920	0.805	0.000	0.000	7.5735	3.5148	1.247	
0.27404E+10	1.214	3.910	0.805	0.000	0.000	7.5736	3.5760	1.251	
0.27408E+10	1.223	3.900	0.805	0.000	0.000	7.5740	3.6328	1.254	
0.27414E+10	1.230	3.890	0.805	0.000	0.000	7.5750	3.6866	1.256	
0.27419E+10	1.236	3.880	0.805	0.000	0.000	7.5765	3.7374	1.258	
0.27426E+10	1.241	3.870	0.805	0.000	0.000	7.5785	3.7861	1.260	
0.27433E+10	1.244	3.860	0.805	0.000	0.000	7.5811	3.8323	1.261	
0.27440E+10	1.247	3.850	0.805	0.000	0.000	7.5843	3.8762	1.262	
0.27448E+10	1.249	3.840	0.805	0.000	0.000	7.5882	3.9183	1.263	
0.27456E+10	1.251	3.830	0.805	0.000	0.000	7.5926	3.9584	1.264	
0.27465E+10	1.253	3.820	0.805	0.000	0.000	7.5981	3.9996	1.264	
0.27475E+10	1.253	3.810	0.805	0.000	0.000	7.6048	4.0433	1.264	
0.27486E+10	1.253	3.800	0.805	0.000	0.000	7.6133	4.0919	1.265	
0.27500E+10	1.251	3.790	0.805	0.000	0.000	7.6245	4.1486	1.263	
0.27516E+10	1.246	3.780	0.805	0.000	0.000	7.6382	4.2111	1.260	
0.27533E+10	1.237	3.770	0.805	0.000	0.000	7.6540	4.2793	1.252	
0.27554E+10	1.221	3.760	0.805	0.000	0.000	7.6722	4.3559	1.237	
0.27579E+10	1.203	3.750	0.805	0.000	0.000	7.6922	4.4412	1.218	
0.27594E+10	1.199	3.746	0.805	0.000	0.000	7.7029	4.4894	1.210	L-m
0.27621E+10	1.208	3.740	0.805	0.000	0.000	7.7185	4.5681	1.212	
0.27740E+10	1.300	3.730	0.721	0.000	0.000	7.7531	4.8208	1.295	
0.27852E+10	1.400	3.724	0.559	0.000	0.000	7.7529	4.9653	1.397	
0.27961E+10	1.500	3.719	0.466	0.000	0.000	7.7417	5.0627	1.498	
0.28062E+10	1.600	3.715	0.401	0.000	0.000	7.7309	5.1373	1.598	
0.28155E+10	1.700	3.710	0.367	0.000	0.000	7.7242	5.2011	1.698	
0.28238E+10	1.800	3.706	0.351	0.000	0.000	7.7222	5.2575	1.798	
0.28309E+10	1.900	3.701	0.343	0.000	0.000	7.7246	5.3087	1.898	
0.28370E+10	2.000	3.696	0.341	0.000	0.000	7.7304	5.3565	1.998	
0.28422E+10	2.100	3.691	0.341	0.000	0.000	7.7390	5.4020	2.098	
0.28467E+10	2.200	3.686	0.341	0.000	0.000	7.7499	5.4461	2.197	
0.28504E+10	2.300	3.681	0.341	0.000	0.000	7.7626	5.4897	2.297	
0.28567E+10	2.400	3.676	0.346	0.002	0.000	7.7908	5.5768	2.397	
0.28593E+10	2.500	3.671	0.357	0.015	0.000	7.8022	5.6154	2.497	
0.28615E+10	2.600	3.666	0.368	0.029	0.000	7.8141	5.6547	2.597	
0.28635E+10	2.700	3.660	0.381	0.053	0.000	7.8267	5.6946	2.697	
0.28651E+10	2.800	3.655	0.394	0.083	0.000	7.8402	5.7353	2.797	
0.28665E+10	2.900	3.649	0.408	0.115	0.000	7.8544	5.7773	2.897	
0.28677E+10	3.000	3.643	0.424	0.146	0.000	7.8694	5.8208	2.997	
0.28688E+10	3.100	3.638	0.441	0.172	0.000	7.8852	5.8663	3.096	
0.28695E+10	3.173	3.633	0.455	0.083	1.423	7.8930	5.8952	3.169	

M=1.3 Z=0.001 Y=0.299

AGE	$L/L_\odot$	T_{eff}	M_{con}	M_{Sch}	X_{cen}	T_c	ρ_c	L_x	
0.00000E+00	0.754	3.962	0.210	0.086	0.700	7.2819	2.0397	0.754	
0.46500E+09	0.817	3.968	0.198	0.081	0.600	7.3072	2.0919	0.817	
0.85468E+09	0.878	3.973	0.208	0.077	0.500	7.3344	2.1461	0.878	
0.11818E+10	0.942	3.975	0.256	0.085	0.420	7.3604	2.1800	0.942	Te-M
0.12628E+10	0.959	3.974	0.266	0.088	0.400	7.3666	2.1863	0.959	
0.15864E+10	1.033	3.967	0.275	0.104	0.300	7.3926	2.2154	1.034	
0.18338E+10	1.098	3.951	0.257	0.105	0.200	7.4161	2.2478	1.099	
0.20287E+10	1.159	3.927	0.226	0.097	0.100	7.4432	2.2981	1.160	
0.21141E+10	1.189	3.914	0.208	0.091	0.050	7.4639	2.3478	1.190	
0.21444E+10	1.203	3.912	0.198	0.088	0.030	7.4772	2.3842	1.204	Te-m
0.21729E+10	1.225	3.918	0.189	0.085	0.010	7.5047	2.4644	1.223	
0.21844E+10	1.265	3.950	0.181	0.076	0.001	7.5579	2.6346	1.231	
0.21859E+10	1.335	3.981	0.902	0.000	0.000	7.6016	3.0749	1.178	Te-M
0.21861E+10	1.305	3.970	0.902	0.000	0.000	7.5923	3.2518	1.387	
0.21863E+10	1.298	3.960	0.902	0.000	0.000	7.5908	3.3154	1.381	
0.21865E+10	1.315	3.950	0.902	0.000	0.000	7.5913	3.3807	1.387	
0.21867E+10	1.337	3.940	0.902	0.000	0.000	7.5921	3.4449	1.396	
0.21869E+10	1.351	3.930	0.902	0.000	0.000	7.5931	3.5027	1.401	
0.21872E+10	1.362	3.920	0.902	0.000	0.000	7.5945	3.5557	1.405	
0.21875E+10	1.370	3.910	0.902	0.000	0.000	7.5962	3.6058	1.407	
0.21878E+10	1.377	3.900	0.902	0.000	0.000	7.5984	3.6526	1.409	
0.21882E+10	1.382	3.890	0.902	0.000	0.000	7.6009	3.6969	1.410	
0.21886E+10	1.386	3.880	0.902	0.000	0.000	7.6038	3.7391	1.412	
0.21889E+10	1.389	3.870	0.902	0.000	0.000	7.6072	3.7792	1.412	
0.21893E+10	1.391	3.860	0.902	0.000	0.000	7.6108	3.8171	1.413	
0.21897E+10	1.393	3.850	0.902	0.000	0.000	7.6148	3.8531	1.413	
0.21901E+10	1.394	3.840	0.902	0.000	0.000	7.6191	3.8871	1.414	
0.21905E+10	1.395	3.830	0.902	0.000	0.000	7.6237	3.9196	1.414	
0.21909E+10	1.395	3.820	0.902	0.000	0.000	7.6286	3.9511	1.413	
0.21914E+10	1.394	3.810	0.902	0.000	0.000	7.6342	3.9839	1.413	
0.21919E+10	1.393	3.800	0.902	0.000	0.000	7.6408	4.0199	1.412	
0.21925E+10	1.390	3.790	0.902	0.000	0.000	7.6493	4.0622	1.410	
0.21932E+10	1.383	3.780	0.902	0.000	0.000	7.6602	4.1118	1.406	
0.21940E+10	1.373	3.770	0.902	0.000	0.000	7.6731	4.1673	1.399	
0.21949E+10	1.354	3.760	0.902	0.000	0.000	7.6883	4.2289	1.386	
0.21960E+10	1.331	3.750	0.902	0.000	0.000	7.7053	4.2958	1.366	
0.21968E+10	1.324	3.744	0.902	0.000	0.000	7.7181	4.3467	1.353	L-m
0.22002E+10	1.400	3.730	0.836	0.000	0.000	7.7577	4.5225	1.400	
0.22032E+10	1.500	3.723	0.638	0.000	0.000	7.7826	4.6485	1.495	
0.22065E+10	1.600	3.718	0.510	0.000	0.000	7.8050	4.7681	1.593	
0.22125E+10	1.700	3.714	0.435	0.000	0.000	7.8357	4.9470	1.692	
0.22220E+10	1.800	3.709	0.411	0.000	0.000	7.8492	5.1470	1.796	
0.22274E+10	1.900	3.704	0.385	0.000	0.000	7.8437	5.2258	1.897	
0.22322E+10	2.000	3.699	0.369	0.000	0.000	7.8386	5.2902	1.997	
0.22364E+10	2.100	3.694	0.363	0.000	0.000	7.8357	5.3466	2.097	
0.22402E+10	2.200	3.689	0.361	0.000	0.000	7.8357	5.3990	2.197	
0.22436E+10	2.300	3.684	0.361	0.000	0.000	7.8386	5.4488	2.297	
0.22465E+10	2.400	3.679	0.361	0.000	0.000	7.8440	5.4970	2.397	
0.22492E+10	2.500	3.674	0.361	0.000	0.000	7.8523	5.5474	2.497	
0.22534E+10	2.600	3.669	0.374	0.001	0.000	7.8664	5.6337	2.597	
0.22552E+10	2.700	3.663	0.385	0.017	0.000	7.8738	5.6762	2.697	
0.22568E+10	2.800	3.658	0.398	0.039	0.000	7.8824	5.7192	2.797	
0.22582E+10	2.900	3.652	0.412	0.068	0.000	7.8921	5.7632	2.897	
0.22594E+10	3.000	3.646	0.428	0.039	0.000	7.9069	5.8064	2.996	
0.22595E+10	3.012	3.646	0.430	0.009	1.417	7.9205	5.8068	3.009	

M=1.5 Z=0.001 Y=0.299

AGE	$L/L_\odot$	T_{eff}	M_{con}	M_{Sch}	X_{cen}	T_c	ρ_c	L_x	
0.00000E+00	1.012	4.019	0.285	0.120	0.700	7.3231	2.0289	1.012	
0.34166E+09	1.076	4.022	0.331	0.120	0.600	7.3464	2.0600	1.077	
0.66534E+09	1.151	4.024	0.368	0.128	0.500	7.3719	2.0889	1.151	
0.67473E+09	1.153	4.024	0.369	0.128	0.497	7.3727	2.0898	1.153	
0.92519E+09	1.223	4.020	0.367	0.140	0.400	7.3943	2.1122	1.224	
0.11326E+10	1.295	4.009	0.347	0.142	0.300	7.4151	2.1340	1.295	
0.12949E+10	1.364	3.991	0.313	0.135	0.200	7.4361	2.1606	1.364	
0.14228E+10	1.427	3.964	0.273	0.120	0.100	7.4621	2.2082	1.428	
0.14766E+10	1.459	3.950	0.246	0.113	0.050	7.4827	2.2597	1.459	
0.14993E+10	1.475	3.947	0.236	0.109	0.026	7.4998	2.3055	1.475	Te-m
0.15138E+10	1.493	3.953	0.229	0.104	0.010	7.5241	2.3742	1.490	
0.15212E+10	1.532	3.984	0.218	0.098	0.001	7.5785	2.5460	1.495	
0.15221E+10	1.598	4.016	1.077	0.000	0.000	7.6265	3.0032	1.498	Te-M
0.15222E+10	1.574	4.010	1.077	0.000	0.000	7.6187	3.1105	1.658	
0.15222E+10	1.551	4.000	1.077	0.000	0.000	7.6153	3.1736	1.653	
0.15223E+10	1.547	3.990	1.077	0.000	0.000	7.6153	3.2286	1.648	
0.15224E+10	1.564	3.980	1.077	0.000	0.000	7.6166	3.2858	1.654	
0.15225E+10	1.585	3.970	1.077	0.000	0.000	7.6183	3.3412	1.662	
0.15227E+10	1.601	3.960	1.077	0.000	0.000	7.6202	3.3923	1.668	
0.15228E+10	1.612	3.950	1.077	0.000	0.000	7.6224	3.4391	1.672	
0.15229E+10	1.620	3.940	1.077	0.000	0.000	7.6250	3.4828	1.674	
0.15231E+10	1.627	3.930	1.077	0.000	0.000	7.6278	3.5241	1.676	
0.15232E+10	1.633	3.920	1.077	0.000	0.000	7.6308	3.5634	1.678	
0.15233E+10	1.637	3.910	1.077	0.000	0.000	7.6340	3.6001	1.680	
0.15235E+10	1.641	3.900	1.077	0.000	0.000	7.6373	3.6349	1.681	
0.15236E+10	1.643	3.890	1.077	0.000	0.000	7.6408	3.6675	1.681	
0.15238E+10	1.645	3.880	1.077	0.000	0.000	7.6444	3.6985	1.682	
0.15240E+10	1.647	3.870	1.077	0.000	0.000	7.6482	3.7279	1.682	
0.15241E+10	1.648	3.860	1.077	0.000	0.000	7.6520	3.7557	1.682	
0.15243E+10	1.648	3.850	1.077	0.000	0.000	7.6558	3.7821	1.682	
0.15244E+10	1.648	3.840	1.077	0.000	0.000	7.6596	3.8069	1.681	
0.15245E+10	1.647	3.830	1.077	0.000	0.000	7.6635	3.8307	1.681	
0.15247E+10	1.646	3.820	1.077	0.000	0.000	7.6674	3.8533	1.680	
0.15248E+10	1.645	3.810	1.077	0.000	0.000	7.6714	3.8755	1.679	
0.15250E+10	1.643	3.800	1.077	0.000	0.000	7.6759	3.8991	1.677	
0.15252E+10	1.640	3.790	1.077	0.000	0.000	7.6811	3.9256	1.675	
0.15254E+10	1.635	3.780	1.077	0.000	0.000	7.6878	3.9578	1.672	
0.15257E+10	1.627	3.770	1.077	0.000	0.000	7.6969	3.9984	1.667	
0.15260E+10	1.612	3.760	1.077	0.000	0.000	7.7081	4.0458	1.657	
0.15264E+10	1.589	3.750	1.077	0.000	0.000	7.7226	4.1030	1.643	
0.15269E+10	1.572	3.740	1.077	0.000	0.000	7.7404	4.1696	1.625	L-m
0.15274E+10	1.600	3.731	1.077	0.000	0.000	7.7599	4.2420	1.628	
0.15284E+10	1.700	3.722	0.888	0.000	0.000	7.7901	4.3599	1.700	
0.15294E+10	1.800	3.716	0.702	0.000	0.000	7.8159	4.4638	1.794	
0.15305E+10	1.900	3.711	0.576	0.000	0.000	7.8406	4.5620	1.892	
0.15315E+10	2.000	3.706	0.501	0.000	0.000	7.8657	4.6589	1.992	
0.15326E+10	2.100	3.700	0.455	0.000	0.000	7.8916	4.7547	2.091	
0.15338E+10	2.200	3.695	0.426	0.000	0.000	7.9191	4.8534	2.192	
0.15351E+10	2.300	3.690	0.411	0.000	0.000	7.9502	4.9570	2.292	
0.15361E+10	2.364	3.686	0.404	0.000	0.000	8.0129	5.0007	2.356	L-M
0.17247E+10	2.400	3.690	0.565	0.081	0.000	8.1534	5.4810	0.776	

=0.7 Y=0.2

AGE	$L/L_\odot$	T_{eff}	M_{con}	M_{Sch}	X_{cen}	T_c	ρ_c	L_x
0.00000E+00	−0.712	3.710	0.000	0.009	0.799	7.0363	1.9576	−0.712
0.30835E+10	−0.680	3.715	0.000	0.000	0.700	7.0485	2.0139	−0.680
0.60572E+10	−0.645	3.720	0.000	0.000	0.600	7.0607	2.0758	−0.645
0.90688E+10	−0.608	3.725	0.000	0.000	0.500	7.0764	2.1468	−0.608
0.12105E+11	−0.565	3.730	0.000	0.000	0.400	7.0930	2.2272	−0.565
0.15188E+11	−0.517	3.735	0.000	0.000	0.300	7.1144	2.3223	−0.517
0.18410E+11	−0.459	3.742	0.000	0.000	0.200	7.1398	2.4404	−0.459
0.22487E+11	−0.366	3.750	0.000	0.000	0.100	7.1759	2.6308	−0.366
0.25836E+11	−0.264	3.758	0.000	0.000	0.050	7.2138	2.8407	−0.264
0.29017E+11	−0.127	3.765	0.000	0.000	0.010	7.2906	3.0963	−0.127
0.29740E+11	−0.088	3.766	0.000	0.000	0.001	7.2993	3.1869	−0.088
0.31037E+11	0.000	3.765	0.313	0.000	0.000	7.3080	3.4423	0.000
0.32023E+11	0.100	3.758	0.313	0.000	0.000	7.3318	3.8027	0.100
0.32597E+11	0.200	3.742	0.313	0.000	0.000	7.3733	4.1954	0.201
0.32901E+11	0.300	3.729	0.313	0.000	0.000	7.4037	4.4679	0.300
0.33104E+11	0.400	3.723	0.313	0.000	0.000	7.4184	4.6411	0.399
0.33277E+11	0.500	3.720	0.313	0.000	0.000	7.4272	4.7693	0.499
0.33427E+11	0.600	3.718	0.313	0.000	0.000	7.4362	4.8697	0.599
0.33556E+11	0.700	3.716	0.313	0.000	0.000	7.4467	4.9519	0.699
0.33663E+11	0.800	3.713	0.313	0.000	0.000	7.4586	5.0223	0.799
0.33749E+11	0.900	3.711	0.308	0.000	0.000	7.4709	5.0835	0.899
0.33819E+11	1.000	3.709	0.299	0.000	0.000	7.4838	5.1381	0.999
0.33876E+11	1.100	3.706	0.295	0.000	0.000	7.4969	5.1875	1.099
0.33921E+11	1.200	3.703	0.295	0.000	0.000	7.5107	5.2335	1.199
0.33958E+11	1.300	3.700	0.295	0.000	0.000	7.5248	5.2769	1.299
0.33988E+11	1.400	3.697	0.295	0.000	0.000	7.5390	5.3175	1.399
0.34012E+11	1.500	3.693	0.295	0.000	0.000	7.5539	5.3566	1.498
0.34032E+11	1.600	3.689	0.295	0.000	0.000	7.5689	5.3939	1.598
0.34048E+11	1.700	3.685	0.295	0.000	0.000	7.5845	5.4306	1.698
0.34062E+11	1.800	3.681	0.294	0.006	0.000	7.6019	5.4697	1.798
0.34073E+11	1.900	3.677	0.302	0.020	0.000	7.6173	5.5037	1.898
0.34081E+11	2.000	3.672	0.311	0.044	0.000	7.6327	5.5368	1.998
0.34088E+11	2.100	3.668	0.321	0.064	0.000	7.6486	5.5698	2.098
0.34094E+11	2.200	3.663	0.331	0.087	0.000	7.6653	5.6031	2.198
0.34099E+11	2.300	3.658	0.341	0.113	0.000	7.6826	5.6370	2.298
0.34103E+11	2.400	3.653	0.352	0.131	0.000	7.7004	5.6714	2.398
0.34106E+11	2.500	3.648	0.364	0.150	0.000	7.7186	5.7067	2.498
0.34109E+11	2.600	3.642	0.377	0.170	0.000	7.7372	5.7427	2.597
0.34111E+11	2.700	3.637	0.390	0.186	0.000	7.7562	5.7799	2.697
0.34113E+11	2.800	3.632	0.404	0.207	0.000	7.7754	5.8185	2.797
0.34115E+11	2.900	3.626	0.419	0.226	0.000	7.7949	5.8587	2.897
0.34116E+11	3.000	3.621	0.435	0.240	0.000	7.8147	5.9006	2.997
0.34117E+11	3.100	3.616	0.453	0.263	0.000	7.8346	5.9452	3.097
0.34119E+11	3.200	3.611	0.472	0.283	0.000	7.8547	5.9926	3.196
0.34119E+11	3.300	3.606	0.493	0.235	0.000	7.8731	6.0415	3.296
0.34119E+11	3.302	3.606	0.494	0.216	0.000	7.8726	6.0416	3.298

M=0.8 Y=0.2

AGE	$L/L_\odot$	T_{eff}	M_{con}	M_{Sch}	X_{cen}	T_c	ρ_c	L_x
0.00000E+00	-0.435	3.750	0.000	0.005	0.799	7.0724	1.9652	-0.435
0.20501E+10	-0.401	3.754	0.000	0.000	0.700	7.0858	2.0219	-0.401
0.40126E+10	-0.365	3.758	0.000	0.000	0.600	7.1002	2.0843	-0.365
0.59353E+10	-0.327	3.762	0.000	0.000	0.500	7.1165	2.1535	-0.327
0.78163E+10	-0.285	3.766	0.000	0.000	0.400	7.1345	2.2313	-0.285
0.96745E+10	-0.239	3.770	0.000	0.000	0.300	7.1553	2.3218	-0.239
0.11654E+11	-0.182	3.774	0.000	0.000	0.200	7.1799	2.4386	-0.182
0.14321E+11	-0.084	3.780	0.000	0.000	0.100	7.2174	2.6413	-0.084
0.16301E+11	0.015	3.785	0.000	0.000	0.050	7.2588	2.8404	0.015
0.17545E+11	0.091	3.787	0.000	0.000	0.010	7.3078	2.9805	0.091
0.18065E+11	0.128	3.787	0.000	0.000	0.001	7.3134	3.0761	0.128
0.19451E+11	0.269	3.780	0.389	0.000	0.000	7.3334	3.5284	0.269
0.19847E+11	0.332	3.770	0.389	0.000	0.000	7.3550	3.8064	0.332
0.20033E+11	0.369	3.760	0.389	0.000	0.000	7.3767	4.0069	0.370
0.20378E+11	0.500	3.731	0.389	0.000	0.000	7.4418	4.5125	0.500
0.20500E+11	0.600	3.725	0.389	0.000	0.000	7.4568	4.6791	0.599
0.20598E+11	0.700	3.721	0.389	0.000	0.000	7.4658	4.7985	0.699
0.20682E+11	0.800	3.718	0.381	0.000	0.000	7.4750	4.8924	0.799
0.20752E+11	0.900	3.715	0.347	0.000	0.000	7.4852	4.9702	0.899
0.20811E+11	1.000	3.713	0.326	0.000	0.000	7.4967	5.0372	0.999
0.20859E+11	1.100	3.710	0.311	0.000	0.000	7.5093	5.0970	1.099
0.20899E+11	1.200	3.707	0.300	0.000	0.000	7.5224	5.1512	1.199
0.20933E+11	1.300	3.703	0.297	0.000	0.000	7.5368	5.2033	1.298
0.20961E+11	1.400	3.700	0.297	0.000	0.000	7.5516	5.2524	1.398
0.20984E+11	1.500	3.696	0.297	0.000	0.000	7.5667	5.2991	1.498
0.21003E+11	1.600	3.693	0.297	0.000	0.000	7.5821	5.3437	1.598
0.21019E+11	1.700	3.688	0.297	0.000	0.000	7.5980	5.3868	1.698
0.21033E+11	1.800	3.684	0.297	0.000	0.000	7.6154	5.4319	1.798
0.21050E+11	1.900	3.680	0.302	0.000	0.000	7.6389	5.4937	1.898
0.21058E+11	2.000	3.676	0.311	0.000	0.000	7.6509	5.5287	1.998
0.21065E+11	2.100	3.671	0.321	0.010	0.000	7.6636	5.5628	2.098
0.21071E+11	2.200	3.666	0.331	0.042	0.000	7.6777	5.5970	2.198
0.21076E+11	2.300	3.662	0.341	0.075	0.000	7.6930	5.6317	2.298
0.21080E+11	2.400	3.656	0.352	0.107	0.000	7.7092	5.6666	2.398
0.21083E+11	2.500	3.651	0.364	0.133	0.000	7.7261	5.7021	2.498
0.21086E+11	2.600	3.646	0.376	0.152	0.000	7.7438	5.7387	2.597
0.21088E+11	2.700	3.641	0.390	0.176	0.000	7.7619	5.7761	2.697
0.21090E+11	2.800	3.635	0.404	0.198	0.000	7.7804	5.8148	2.797
0.21092E+11	2.900	3.630	0.419	0.218	0.000	7.7993	5.8551	2.897
0.21093E+11	3.000	3.624	0.435	0.241	0.000	7.8185	5.8974	2.997
0.21094E+11	3.100	3.619	0.452	0.258	0.000	7.8380	5.9419	3.097
0.21095E+11	3.200	3.614	0.471	0.279	0.000	7.8576	5.9894	3.197
0.21096E+11	3.294	3.609	0.491	0.231	0.000	7.8744	6.0352	3.291

M=0.9 Y=0.200

AGE	$L/L_\odot$	T_{eff}	M_{con}	M_{Sch}	X_{cen}	T_c	ρ_c	L_x
0.00000E+00	-0.191	3.782	0.021	0.009	0.799	7.1088	1.9741	-0.191
0.15341E+10	-0.152	3.785	0.001	0.000	0.700	7.1245	2.0324	-0.152
0.28194E+10	-0.117	3.788	0.000	0.000	0.600	7.1395	2.0931	-0.117
0.40435E+10	-0.080	3.791	0.000	0.000	0.500	7.1558	2.1592	-0.080
0.52177E+10	-0.041	3.794	0.000	0.000	0.400	7.1736	2.2331	-0.041
0.63899E+10	0.002	3.797	0.000	0.000	0.300	7.1934	2.3210	0.002
0.76991E+10	0.059	3.800	0.000	0.000	0.200	7.2170	2.4405	0.059
0.94846E+10	0.158	3.805	0.000	0.000	0.100	7.2566	2.6476	0.159
0.10454E+11	0.227	3.808	0.000	0.000	0.050	7.2937	2.7824	0.227
0.11090E+11	0.276	3.808	0.000	0.000	0.010	7.3231	2.8878	0.277
0.11493E+11	0.314	3.808	0.000	0.000	0.001	7.3281	2.9883	0.314
0.12493E+11	0.443	3.800	0.479	0.000	0.000	7.3459	3.3984	0.443
0.12784E+11	0.498	3.790	0.479	0.000	0.000	7.3624	3.6423	0.499
0.12926E+11	0.531	3.780	0.479	0.000	0.000	7.3793	3.8272	0.532
0.13018E+11	0.553	3.770	0.479	0.000	0.000	7.3988	3.9879	0.555
0.13087E+11	0.569	3.760	0.479	0.000	0.000	7.4205	4.1349	0.571
0.13147E+11	0.584	3.750	0.479	0.000	0.000	7.4430	4.2785	0.587
0.13188E+11	0.600	3.743	0.479	0.000	0.000	7.4577	4.3773	0.602
0.13307E+11	0.700	3.729	0.479	0.000	0.000	7.4865	4.6405	0.700
0.13384E+11	0.800	3.723	0.479	0.000	0.000	7.4962	4.7790	0.799
0.13447E+11	0.900	3.720	0.426	0.000	0.000	7.5042	4.8821	0.899
0.13500E+11	1.000	3.717	0.379	0.000	0.000	7.5132	4.9655	0.999
0.13545E+11	1.100	3.714	0.342	0.000	0.000	7.5236	5.0365	1.099
0.13581E+11	1.200	3.710	0.324	0.000	0.000	7.5329	5.0974	1.199
0.13612E+11	1.300	3.707	0.311	0.000	0.000	7.5456	5.1533	1.299
0.13638E+11	1.400	3.704	0.305	0.000	0.000	7.5593	5.2047	1.398
0.13659E+11	1.500	3.700	0.305	0.000	0.000	7.5739	5.2532	1.498
0.13676E+11	1.600	3.696	0.303	0.000	0.000	7.5891	5.2993	1.598
0.13691E+11	1.700	3.692	0.303	0.000	0.000	7.6048	5.3435	1.698
0.13703E+11	1.800	3.688	0.303	0.000	0.000	7.6211	5.3868	1.798
0.13713E+11	1.900	3.684	0.303	0.000	0.000	7.6389	5.4316	1.898
0.13731E+11	2.000	3.680	0.312	0.000	0.000	7.6706	5.5176	1.998
0.13738E+11	2.100	3.675	0.321	0.000	0.000	7.6811	5.5537	2.098
0.13744E+11	2.200	3.670	0.331	0.008	0.000	7.6928	5.5895	2.198
0.13748E+11	2.300	3.665	0.341	0.041	0.000	7.7057	5.6249	2.298
0.13752E+11	2.400	3.660	0.352	0.072	0.000	7.7200	5.6606	2.398
0.13756E+11	2.500	3.655	0.364	0.106	0.000	7.7354	5.6967	2.498
0.13758E+11	2.600	3.650	0.376	0.135	0.000	7.7517	5.7336	2.597
0.13761E+11	2.700	3.644	0.389	0.161	0.000	7.7687	5.7715	2.697
0.13763E+11	2.800	3.639	0.403	0.182	0.000	7.7863	5.8105	2.797
0.13764E+11	2.900	3.633	0.418	0.212	0.000	7.8044	5.8511	2.897
0.13766E+11	3.000	3.628	0.434	0.227	0.000	7.8228	5.8935	2.997
0.13767E+11	3.100	3.622	0.452	0.252	0.000	7.8416	5.9384	3.097
0.13768E+11	3.200	3.617	0.471	0.274	0.000	7.8606	5.9859	3.196
0.13769E+11	3.291	3.612	0.491	0.201	1.790	7.8748	6.0280	3.288

M=1.0 Z=0.02 Y=0.28

AGE	$L/L_\odot$	T_{eff}	M_{con}	M_{Sch}	X_{cen}	T_c	ρ_c	L_x
0.00000E+00	-0.010	3.780	0.003	0.001	0.700	7.1573	2.0025	-0.010
0.96072E+09	0.023	3.782	0.000	0.000	0.600	7.1720	2.0613	0.023
0.18389E+10	0.055	3.783	0.000	0.000	0.500	7.1872	2.1238	0.055
0.26602E+10	0.088	3.784	0.000	0.000	0.400	7.2032	2.1923	0.088
0.34551E+10	0.122	3.785	0.000	0.000	0.300	7.2201	2.2715	0.122
0.42468E+10	0.159	3.786	0.000	0.000	0.200	7.2400	2.3653	0.159
0.48892E+10	0.189	3.785	0.000	0.000	0.100	7.2654	2.4528	0.189
0.51432E+10	0.200	3.784	0.000	0.000	0.050	7.2761	2.4970	0.200
0.54913E+10	0.218	3.784	0.000	0.000	0.010	7.2784	2.5704	0.218
0.58890E+10	0.243	3.783	0.000	0.000	0.001	7.2768	2.6483	0.243
0.68455E+10	0.315	3.780	0.532	0.000	0.000	7.2803	2.8674	0.315
0.77402E+10	0.398	3.770	0.532	0.000	0.000	7.2932	3.2424	0.398
0.80554E+10	0.424	3.760	0.532	0.000	0.000	7.3067	3.5142	0.425
0.82209E+10	0.429	3.750	0.532	0.000	0.000	7.3264	3.7476	0.431
0.86235E+10	0.500	3.710	0.532	0.000	0.000	7.4187	4.5208	0.500
0.87352E+10	0.600	3.705	0.437	0.000	0.000	7.4251	4.6694	0.600
0.88194E+10	0.700	3.701	0.359	0.000	0.000	7.4321	4.7682	0.699
0.88870E+10	0.800	3.698	0.308	0.000	0.000	7.4420	4.8469	0.799
0.89409E+10	0.900	3.695	0.279	0.000	0.000	7.4527	4.9121	0.899
0.89841E+10	1.000	3.692	0.263	0.000	0.000	7.4643	4.9682	0.999
0.90195E+10	1.100	3.688	0.255	0.000	0.000	7.4771	5.0194	1.099
0.90482E+10	1.200	3.684	0.251	0.000	0.000	7.4910	5.0662	1.199
0.90716E+10	1.300	3.679	0.251	0.000	0.000	7.5055	5.1099	1.299
0.90910E+10	1.400	3.674	0.251	0.000	0.000	7.5208	5.1516	1.398
0.91072E+10	1.500	3.669	0.251	0.000	0.000	7.5369	5.1925	1.498
0.91232E+10	1.600	3.663	0.251	0.000	0.000	7.5571	5.2401	1.598
0.91495E+10	1.700	3.658	0.260	0.000	0.000	7.5883	5.3242	1.698
0.91585E+10	1.800	3.652	0.268	0.000	0.000	7.5983	5.3567	1.798
0.91660E+10	1.900	3.645	0.275	0.000	0.000	7.6096	5.3885	1.898
0.91723E+10	2.000	3.638	0.283	0.000	0.000	7.6225	5.4197	1.998
0.91775E+10	2.100	3.632	0.292	0.000	0.000	7.6368	5.4509	2.098
0.91818E+10	2.200	3.625	0.301	0.002	0.000	7.6522	5.4820	2.198
0.91854E+10	2.300	3.618	0.310	0.028	0.000	7.6686	5.5135	2.298
0.91885E+10	2.400	3.611	0.320	0.056	0.000	7.6858	5.5454	2.398
0.91910E+10	2.500	3.603	0.330	0.078	0.000	7.7037	5.5776	2.498
0.91931E+10	2.600	3.595	0.341	0.101	0.000	7.7223	5.6107	2.597
0.91949E+10	2.700	3.588	0.353	0.124	0.000	7.7415	5.6445	2.697
0.91964E+10	2.800	3.580	0.365	0.142	0.000	7.7614	5.6794	2.797
0.91977E+10	2.900	3.572	0.378	0.159	0.000	7.7822	5.7162	2.897
0.91988E+10	3.000	3.565	0.393	0.183	0.000	7.8035	5.7546	2.997
0.91998E+10	3.100	3.558	0.409	0.196	0.000	7.8257	5.7953	3.096
0.92005E+10	3.174	3.552	0.421	0.208	0.000	7.8425	5.8268	3.170

M=1.1 Z=0.02 Y=0.28

AGE	$L/L_\odot$	T_{eff}	M_{con}	M_{Sch}	X_{cen}	T_c	ρ_c	L_x	
0.00000E+00	0.188	3.800	0.026	0.011	0.700	7.1902	2.0059	0.188	
0.80809E+09	0.226	3.801	0.025	0.011	0.600	7.2082	2.0633	0.226	
0.15502E+10	0.263	3.802	0.030	0.012	0.500	7.2275	2.1239	0.263	
0.21100E+10	0.293	3.802	0.031	0.013	0.417	7.2445	2.1786	0.293	Te-M
0.22268E+10	0.299	3.802	0.032	0.013	0.400	7.2485	2.1903	0.299	
0.39860E+10	0.383	3.792	0.151	0.048	0.300	7.2943	2.2128	0.383	
0.48247E+10	0.412	3.781	0.161	0.051	0.200	7.3145	2.2374	0.412	
0.54611E+10	0.424	3.770	0.141	0.049	0.100	7.3360	2.2928	0.425	
0.57498E+10	0.432	3.764	0.128	0.046	0.050	7.3535	2.3456	0.432	
0.58906E+10	0.443	3.763	0.122	0.044	0.025	7.3698	2.3951	0.443	Te-m
0.59677E+10	0.463	3.764	0.118	0.043	0.010	7.3903	2.4578	0.461	
0.60114E+10	0.536	3.773	0.112	0.041	0.001	7.4402	2.6211	0.503	
0.60164E+10	0.633	3.782	0.627	0.000	0.000	7.4672	3.0844	0.543	Te-M
0.60171E+10	0.607	3.780	0.627	0.000	0.000	7.4556	3.2174	0.675	
0.60191E+10	0.581	3.770	0.627	0.000	0.000	7.4452	3.4060	0.651	
0.60232E+10	0.587	3.760	0.627	0.000	0.000	7.4390	3.5826	0.622	
0.60326E+10	0.573	3.750	0.627	0.000	0.000	7.4372	3.7775	0.589	
0.60499E+10	0.553	3.740	0.627	0.000	0.000	7.4532	3.9814	0.563	
0.60755E+10	0.541	3.728	0.627	0.000	0.000	7.4901	4.2090	0.547	L-m
0.61453E+10	0.600	3.714	0.627	0.000	0.000	7.5264	4.5944	0.600	
0.62143E+10	0.700	3.707	0.463	0.000	0.000	7.4931	4.7583	0.700	
0.62792E+10	0.800	3.703	0.370	0.000	0.000	7.4710	4.8573	0.799	
0.63344E+10	0.900	3.700	0.312	0.000	0.000	7.4659	4.9291	0.899	
0.63794E+10	1.000	3.696	0.282	0.000	0.000	7.4695	4.9866	0.999	
0.64162E+10	1.100	3.692	0.266	0.000	0.000	7.4782	5.0369	1.099	
0.64459E+10	1.200	3.688	0.260	0.000	0.000	7.4897	5.0824	1.199	
0.64700E+10	1.300	3.683	0.257	0.000	0.000	7.5027	5.1244	1.299	
0.64896E+10	1.400	3.679	0.257	0.000	0.000	7.5170	5.1642	1.399	
0.65057E+10	1.500	3.673	0.257	0.000	0.000	7.5322	5.2025	1.498	
0.65193E+10	1.600	3.668	0.257	0.000	0.000	7.5485	5.2405	1.598	
0.65426E+10	1.700	3.663	0.260	0.000	0.000	7.5848	5.3205	1.698	
0.65521E+10	1.800	3.656	0.267	0.000	0.000	7.5979	5.3547	1.798	
0.65596E+10	1.900	3.650	0.275	0.000	0.000	7.6100	5.3864	1.898	
0.65659E+10	2.000	3.643	0.283	0.000	0.000	7.6232	5.4178	1.998	
0.65711E+10	2.100	3.637	0.292	0.000	0.000	7.6375	5.4491	2.098	
0.65754E+10	2.200	3.630	0.300	0.001	0.000	7.6529	5.4806	2.198	
0.65791E+10	2.300	3.622	0.310	0.023	0.000	7.6693	5.5123	2.298	
0.65821E+10	2.400	3.615	0.320	0.050	0.000	7.6866	5.5444	2.398	
0.65846E+10	2.500	3.608	0.330	0.076	0.000	7.7046	5.5769	2.498	
0.65868E+10	2.600	3.600	0.341	0.102	0.000	7.7231	5.6099	2.597	
0.65885E+10	2.700	3.592	0.352	0.120	0.000	7.7423	5.6439	2.697	
0.65901E+10	2.800	3.584	0.365	0.142	0.000	7.7622	5.6792	2.797	
0.65914E+10	2.900	3.577	0.378	0.165	0.000	7.7827	5.7158	2.897	
0.65925E+10	3.000	3.569	0.393	0.177	0.000	7.8041	5.7542	2.997	
0.65934E+10	3.100	3.562	0.408	0.197	0.000	7.8263	5.7949	3.097	
0.65943E+10	3.200	3.554	0.426	0.217	0.000	7.8493	5.8385	3.197	
0.65951E+10	3.300	3.547	0.445	0.230	0.000	7.8728	5.8851	3.296	
0.65956E+10	3.367	3.543	0.461	0.149	3.847	7.8820	5.9080	3.361	

M=1.2 Z=0.02 Y=0.28

AGE	$L/L_\odot$	T_{eff}	M_{con}	M_{Sch}	X_{cen}	T_c	ρ_c	L_x	
0.00000E+00	0.367	3.820	0.069	0.029	0.700	7.2197	2.0033	0.367	
0.72650E+09	0.409	3.820	0.088	0.035	0.600	7.2403	2.0549	0.410	
0.15112E+10	0.457	3.819	0.120	0.046	0.500	7.2644	2.1041	0.457	
0.24199E+10	0.512	3.812	0.178	0.058	0.400	7.2903	2.1303	0.513	
0.31576E+10	0.553	3.800	0.202	0.063	0.300	7.3093	2.1438	0.554	
0.37346E+10	0.576	3.787	0.185	0.063	0.200	7.3257	2.1765	0.576	
0.42070E+10	0.586	3.774	0.158	0.056	0.100	7.3464	2.2341	0.587	
0.44204E+10	0.592	3.768	0.142	0.052	0.050	7.3637	2.2892	0.593	
0.45363E+10	0.605	3.766	0.134	0.050	0.022	7.3833	2.3497	0.605	Te-m
0.45817E+10	0.623	3.767	0.131	0.049	0.010	7.4010	2.4033	0.621	
0.46147E+10	0.698	3.777	0.126	0.047	0.001	7.4525	2.5631	0.664	
0.46183E+10	0.798	3.786	0.728	0.000	0.000	7.4847	3.0076	0.697	Te-M
0.46192E+10	0.719	3.780	0.728	0.000	0.000	7.4640	3.2192	0.830	
0.46204E+10	0.719	3.770	0.728	0.000	0.000	7.4608	3.3592	0.809	
0.46225E+10	0.721	3.760	0.728	0.000	0.000	7.4604	3.5057	0.779	
0.46263E+10	0.705	3.750	0.728	0.000	0.000	7.4646	3.6640	0.742	
0.46442E+10	0.666	3.728	0.728	0.000	0.000	7.5075	4.0454	0.683	L-m
0.46576E+10	0.700	3.717	0.719	0.000	0.000	7.5431	4.2394	0.709	
0.46745E+10	0.800	3.709	0.499	0.000	0.000	7.5730	4.4272	0.801	
0.46897E+10	0.900	3.704	0.388	0.000	0.000	7.5915	4.5635	0.898	
0.47082E+10	1.000	3.700	0.318	0.000	0.000	7.6067	4.7008	0.997	
0.47533E+10	1.100	3.697	0.300	0.000	0.000	7.6129	4.9437	1.097	
0.47765E+10	1.200	3.692	0.282	0.000	0.000	7.5978	5.0217	1.199	
0.47968E+10	1.300	3.688	0.271	0.000	0.000	7.5877	5.0820	1.298	
0.48143E+10	1.400	3.683	0.267	0.000	0.000	7.5844	5.1333	1.398	
0.48288E+10	1.500	3.677	0.267	0.000	0.000	7.5863	5.1779	1.498	
0.48411E+10	1.600	3.672	0.267	0.000	0.000	7.5921	5.2192	1.598	
0.48515E+10	1.700	3.666	0.267	0.000	0.000	7.6012	5.2590	1.698	
0.48698E+10	1.800	3.661	0.270	0.000	0.000	7.6274	5.3416	1.798	
0.48773E+10	1.900	3.654	0.277	0.000	0.000	7.6376	5.3762	1.898	
0.48836E+10	2.000	3.647	0.285	0.000	0.000	7.6483	5.4099	1.998	
0.48887E+10	2.100	3.641	0.293	0.000	0.000	7.6599	5.4424	2.098	
0.48930E+10	2.200	3.634	0.302	0.000	0.000	7.6729	5.4748	2.198	
0.48966E+10	2.300	3.626	0.311	0.000	0.000	7.6872	5.5072	2.298	
0.48996E+10	2.400	3.619	0.321	0.013	0.000	7.7027	5.5398	2.398	
0.49021E+10	2.500	3.612	0.331	0.043	0.000	7.7191	5.5729	2.497	
0.49043E+10	2.600	3.604	0.342	0.068	0.000	7.7364	5.6064	2.597	
0.49060E+10	2.700	3.596	0.353	0.097	0.000	7.7543	5.6405	2.697	
0.49076E+10	2.800	3.589	0.366	0.119	0.000	7.7731	5.6760	2.797	
0.49089E+10	2.900	3.581	0.379	0.142	0.000	7.7928	5.7129	2.897	
0.49100E+10	3.000	3.573	0.393	0.165	0.000	7.8133	5.7517	2.997	
0.49109E+10	3.100	3.566	0.409	0.183	0.000	7.8345	5.7926	3.096	
0.49118E+10	3.200	3.559	0.426	0.207	0.000	7.8566	5.8362	3.196	
0.49120E+10	3.228	3.556	0.432	0.207	0.000	7.8628	5.8486	3.225	

M=1.3 Z=0.02 Y=0.28

AGE	$L/L_\odot$	T_{eff}	M_{con}	M_{Sch}	X_{cen}	T_c	ρ_c	L_x	
0.00000E+00	0.524	3.842	0.126	0.049	0.700	7.2449	1.9938	0.524	
0.66793E+09	0.570	3.841	0.159	0.060	0.600	7.2659	2.0351	0.570	
0.13547E+10	0.620	3.836	0.207	0.071	0.500	7.2871	2.0613	0.620	
0.20018E+10	0.665	3.824	0.238	0.075	0.400	7.3048	2.0725	0.666	
0.25506E+10	0.700	3.810	0.231	0.075	0.300	7.3198	2.0913	0.701	
0.29997E+10	0.724	3.795	0.206	0.071	0.200	7.3354	2.1242	0.725	
0.33685E+10	0.735	3.779	0.173	0.063	0.100	7.3558	2.1839	0.736	
0.35350E+10	0.739	3.771	0.156	0.058	0.050	7.3730	2.2396	0.740	
0.36312E+10	0.754	3.770	0.147	0.055	0.019	7.3956	2.3092	0.753	Te-m
0.36584E+10	0.769	3.771	0.144	0.054	0.010	7.4107	2.3540	0.767	
0.36837E+10	0.847	3.781	0.140	0.053	0.001	7.4631	2.5127	0.811	
0.36864E+10	0.946	3.792	0.834	0.000	0.000	7.4978	2.9450	0.839	Te-M
0.36868E+10	0.904	3.790	0.834	0.000	0.000	7.4807	3.0850	1.002	
0.36874E+10	0.842	3.780	0.834	0.000	0.000	7.4750	3.2194	0.971	
0.36883E+10	0.852	3.770	0.834	0.000	0.000	7.4749	3.3414	0.950	
0.36897E+10	0.847	3.760	0.834	0.000	0.000	7.4781	3.4700	0.920	
0.36918E+10	0.827	3.750	0.834	0.000	0.000	7.4857	3.6056	0.884	
0.37000E+10	0.786	3.730	0.834	0.000	0.000	7.5211	3.9152	0.815	L-m
0.37149E+10	0.900	3.711	0.593	0.000	0.000	7.5840	4.2593	0.906	
0.37220E+10	1.000	3.706	0.442	0.000	0.000	7.6074	4.3833	1.001	
0.37288E+10	1.100	3.701	0.359	0.000	0.000	7.6270	4.4890	1.098	
0.37356E+10	1.200	3.696	0.312	0.000	0.000	7.6458	4.5859	1.197	
0.37426E+10	1.300	3.692	0.287	0.000	0.000	7.6637	4.6788	1.297	
0.37500E+10	1.400	3.687	0.272	0.000	0.000	7.6822	4.7739	1.396	
0.37600E+10	1.500	3.681	0.267	0.000	0.000	7.7046	4.8938	1.496	
0.37926E+10	1.600	3.676	0.267	0.000	0.000	7.7118	5.1667	1.598	
0.38029E+10	1.700	3.671	0.267	0.000	0.000	7.7051	5.2289	1.698	
0.38178E+10	1.800	3.665	0.274	0.000	0.000	7.6990	5.3146	1.798	
0.38247E+10	1.900	3.659	0.281	0.000	0.000	7.6981	5.3539	1.898	
0.38305E+10	2.000	3.652	0.288	0.000	0.000	7.7006	5.3909	1.998	
0.38354E+10	2.100	3.645	0.296	0.000	0.000	7.7060	5.4260	2.098	
0.38396E+10	2.200	3.638	0.304	0.000	0.000	7.7140	5.4604	2.198	
0.38431E+10	2.300	3.631	0.313	0.000	0.000	7.7241	5.4945	2.298	
0.38460E+10	2.400	3.623	0.323	0.000	0.000	7.7359	5.5286	2.398	
0.38485E+10	2.500	3.616	0.333	0.000	0.000	7.7491	5.5626	2.498	
0.38506E+10	2.600	3.608	0.344	0.018	0.000	7.7638	5.5972	2.597	
0.38523E+10	2.700	3.601	0.355	0.045	0.000	7.7794	5.6323	2.697	
0.38538E+10	2.800	3.593	0.367	0.081	0.000	7.7959	5.6681	2.797	
0.38551E+10	2.900	3.585	0.381	0.106	0.000	7.8137	5.7058	2.897	
0.38562E+10	3.000	3.577	0.395	0.135	0.000	7.8323	5.7451	2.997	
0.38572E+10	3.100	3.570	0.411	0.156	0.000	7.8518	5.7866	3.096	
0.38580E+10	3.200	3.562	0.428	0.183	0.000	7.8721	5.8307	3.196	
0.38587E+10	3.283	3.556	0.443	0.187	-0.416	7.8892	5.8691	3.280	

M=1.5 Z=0.02 Y=0.280

AGE	$L/L_\odot$	T_{eff}	M_{con}	M_{Sch}	X_{cen}	T_c	ρ_c	L_x	
0.00000E+00	0.790	3.897	0.262	0.093	0.700	7.2835	1.9572	0.790	
0.53270E+09	0.836	3.890	0.309	0.102	0.600	7.2989	1.9670	0.836	
0.10463E+10	0.886	3.877	0.333	0.106	0.500	7.3123	1.9675	0.887	
0.14735E+10	0.932	3.859	0.316	0.106	0.400	7.3250	1.9778	0.933	
0.18241E+10	0.972	3.836	0.287	0.100	0.300	7.3383	1.9964	0.973	
0.21070E+10	1.001	3.811	0.249	0.091	0.200	7.3533	2.0295	1.002	
0.23392E+10	1.014	3.788	0.208	0.079	0.100	7.3736	2.0896	1.015	
0.24413E+10	1.017	3.778	0.186	0.072	0.050	7.3901	2.1452	1.018	
0.24992E+10	1.030	3.775	0.173	0.069	0.021	7.4108	2.2106	1.030	Te-m
0.25185E+10	1.047	3.776	0.170	0.067	0.010	7.4281	2.2609	1.045	
0.25341E+10	1.123	3.790	0.168	0.066	0.001	7.4817	2.4195	1.087	
0.25358E+10	1.217	3.805	0.995	0.000	0.000	7.5172	2.8649	1.185	Te-M
0.25360E+10	1.161	3.800	0.995	0.000	0.000	7.5003	2.9914	1.278	
0.25362E+10	1.100	3.790	0.995	0.000	0.000	7.4970	3.0853	1.255	
0.25365E+10	1.095	3.780	0.995	0.000	0.000	7.4976	3.1725	1.241	
0.25369E+10	1.099	3.770	0.995	0.000	0.000	7.5002	3.2639	1.223	
0.25375E+10	1.088	3.760	0.995	0.000	0.000	7.5058	3.3639	1.197	
0.25383E+10	1.066	3.750	0.995	0.000	0.000	7.5151	3.4726	1.164	
0.25408E+10	1.028	3.731	0.995	0.000	0.000	7.5462	3.7115	1.092	L-m
0.25451E+10	1.100	3.715	0.826	0.000	0.000	7.5920	3.9797	1.117	
0.25484E+10	1.200	3.708	0.619	0.000	0.000	7.6261	4.1410	1.205	
0.25513E+10	1.300	3.702	0.491	0.000	0.000	7.6551	4.2652	1.301	
0.25541E+10	1.400	3.697	0.415	0.000	0.000	7.6817	4.3746	1.398	
0.25567E+10	1.500	3.691	0.375	0.000	0.000	7.7065	4.4730	1.496	
0.25593E+10	1.600	3.685	0.350	0.000	0.000	7.7299	4.5640	1.596	
0.25619E+10	1.700	3.679	0.331	0.000	0.000	7.7540	4.6544	1.695	
0.25644E+10	1.800	3.672	0.318	0.000	0.000	7.7776	4.7404	1.795	
0.25667E+10	1.900	3.666	0.311	0.000	0.000	7.7999	4.8203	1.895	
0.25690E+10	2.000	3.659	0.310	0.000	0.000	7.8215	4.8966	1.995	
0.25712E+10	2.100	3.652	0.310	0.000	0.000	7.8432	4.9725	2.095	
0.25736E+10	2.200	3.645	0.310	0.000	0.000	7.8675	5.0561	2.195	
0.25892E+10	2.300	3.638	0.331	0.000	0.000	7.8947	5.4146	2.297	
0.25916E+10	2.400	3.631	0.339	0.000	0.000	7.8929	5.4588	2.397	
0.25937E+10	2.500	3.624	0.348	0.000	0.000	7.8934	5.5013	2.497	
0.25955E+10	2.600	3.616	0.357	0.000	0.000	7.8962	5.5427	2.597	
0.25971E+10	2.700	3.608	0.367	0.000	0.000	7.9010	5.5836	2.697	
0.25985E+10	2.800	3.601	0.379	0.000	0.000	7.9136	5.6235	2.797	
0.25991E+10	2.848	3.597	0.385	0.000	3.286	8.0445	5.6064	2.836	

Figure 4.1) The relevant RGB luminosity distribution for Z = 0.01 Each histogram is labelled with age in billion years (from Barbaro and Pigatto 1984)

Figure 4.2) The magnitude $M_{b,RG}$ of the faintest red stars against the colour index of the MS turnoff point. Lines show theoretical relations for the base of the RGB for standard models (from Barbaro and Pigatto 1984)

Figure 4.3) The same of Figure 4.2 but with theoretical relations from VandenBerg 1985, without overshooting (dashed lines) and from models with overshooting. (From Pigatto 1986)

Figure 4.4) Size of the convective core versus central Hydrogen abundance by mass for the following models (set 1):
X = 0.700, Y = 0.28, Z = 0.02 Λ = 1 and mass of
1.5, 1.4, 1.3, 1.1 M_o

Figure 4.5) Same of Figure 4.4 but for (set 2):
X = 0.700, Y = 0.299, Z = 0.001, Λ = 1 and mass of
1.5, 1.3, 1.2, 1.2, 1.1, 1.0, 0.9 M_o

Figure 4.6) HR diagram for the models of set 1 above and mass of
1.5, 1.4, 1.3, 1.1, 1.0 M_o

Figure 4.7) HR diagram for the models of set 2 above and mass of
1.5, 1.3, 1.2, 1.1, 1.0, 0.9, 0.8, 0.7.

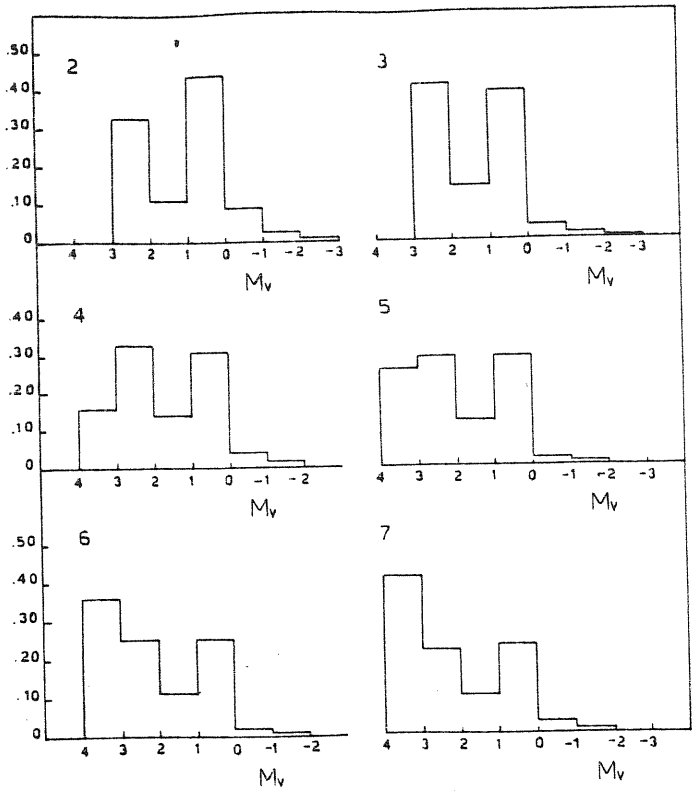

4.1

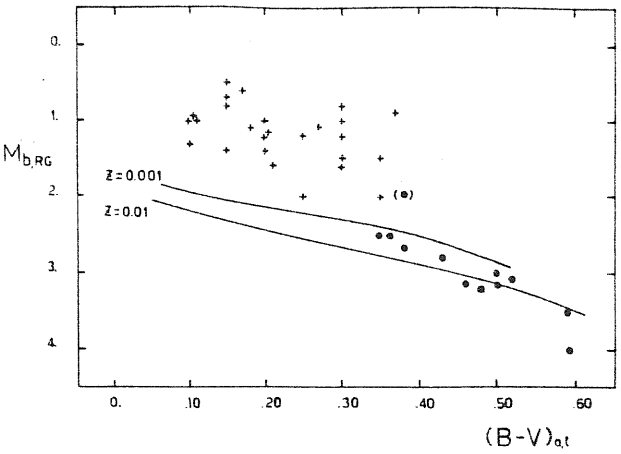

4.2

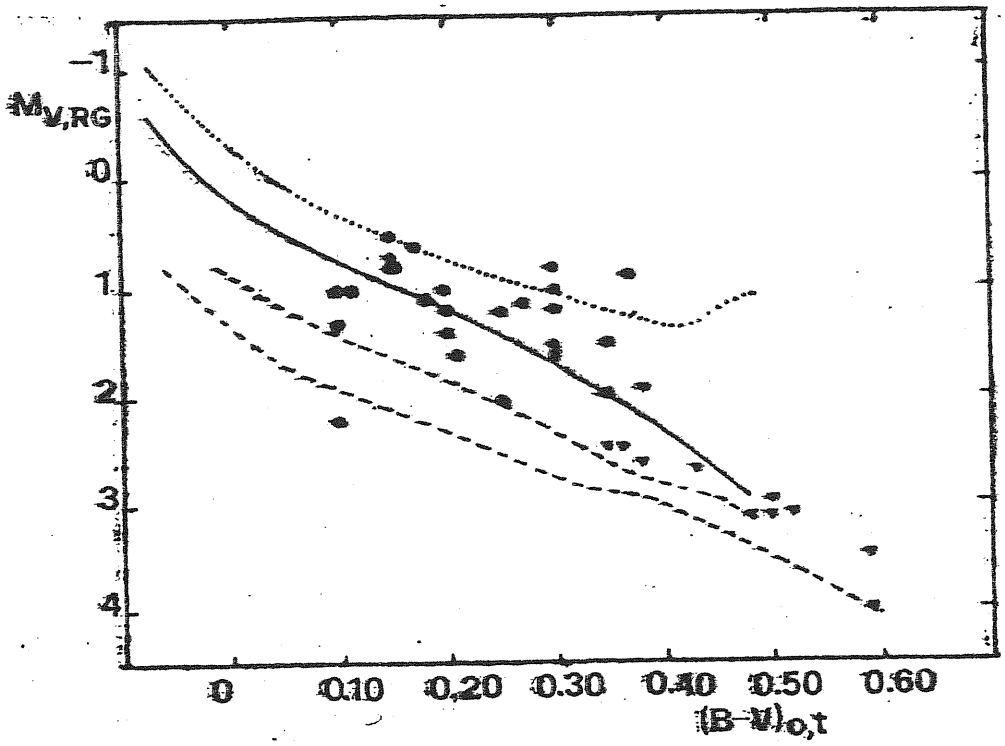

4.3

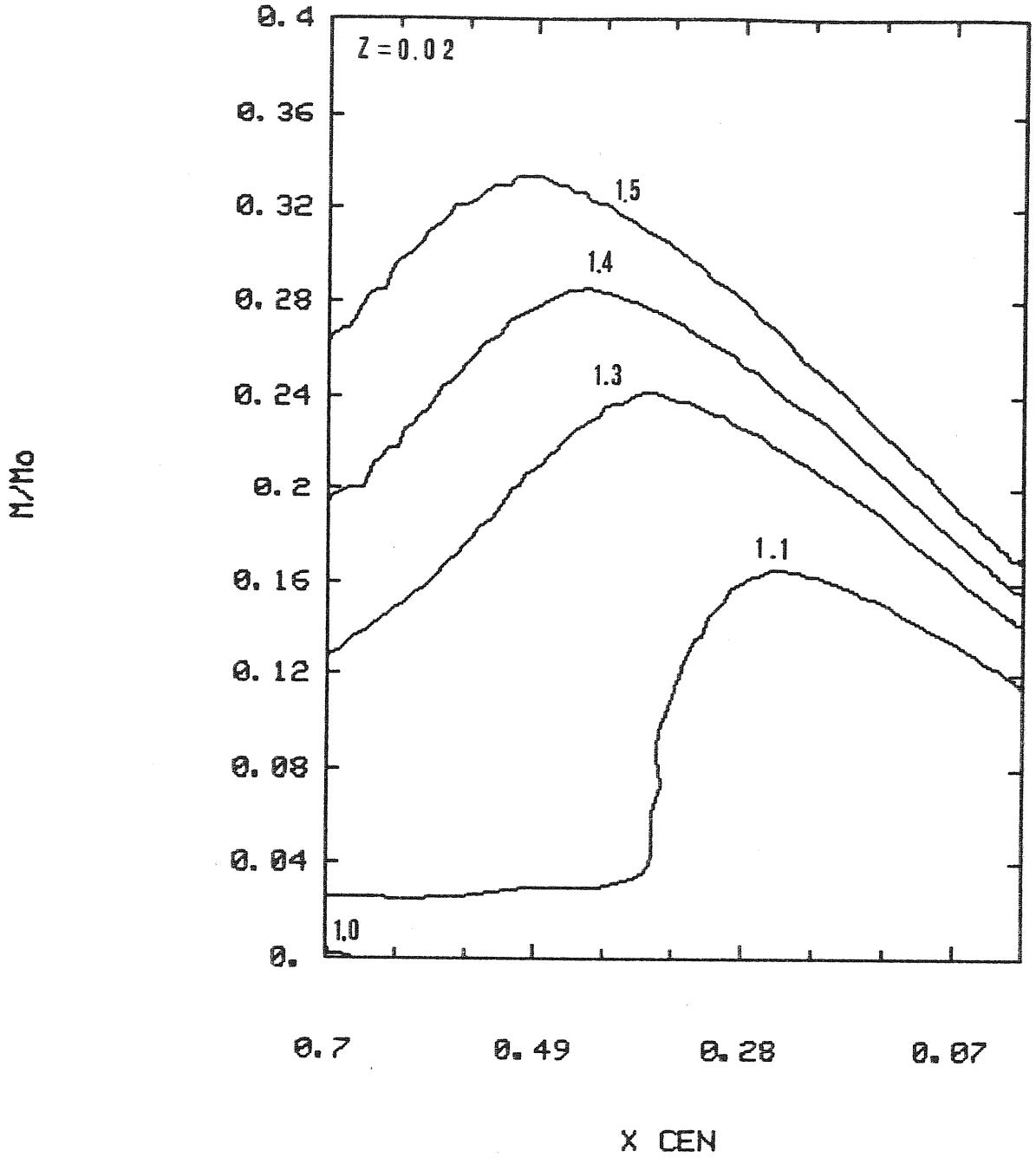
0.4
Z = 0.02
0.36
0.32
0.28
0.24
0.2
0.16
0.12
0.08
0.04
0.
1.5
1.4
1.3
1.1
1.0
M/Mo
0.7
0.49
0.28
0.07
X CEN

4.4

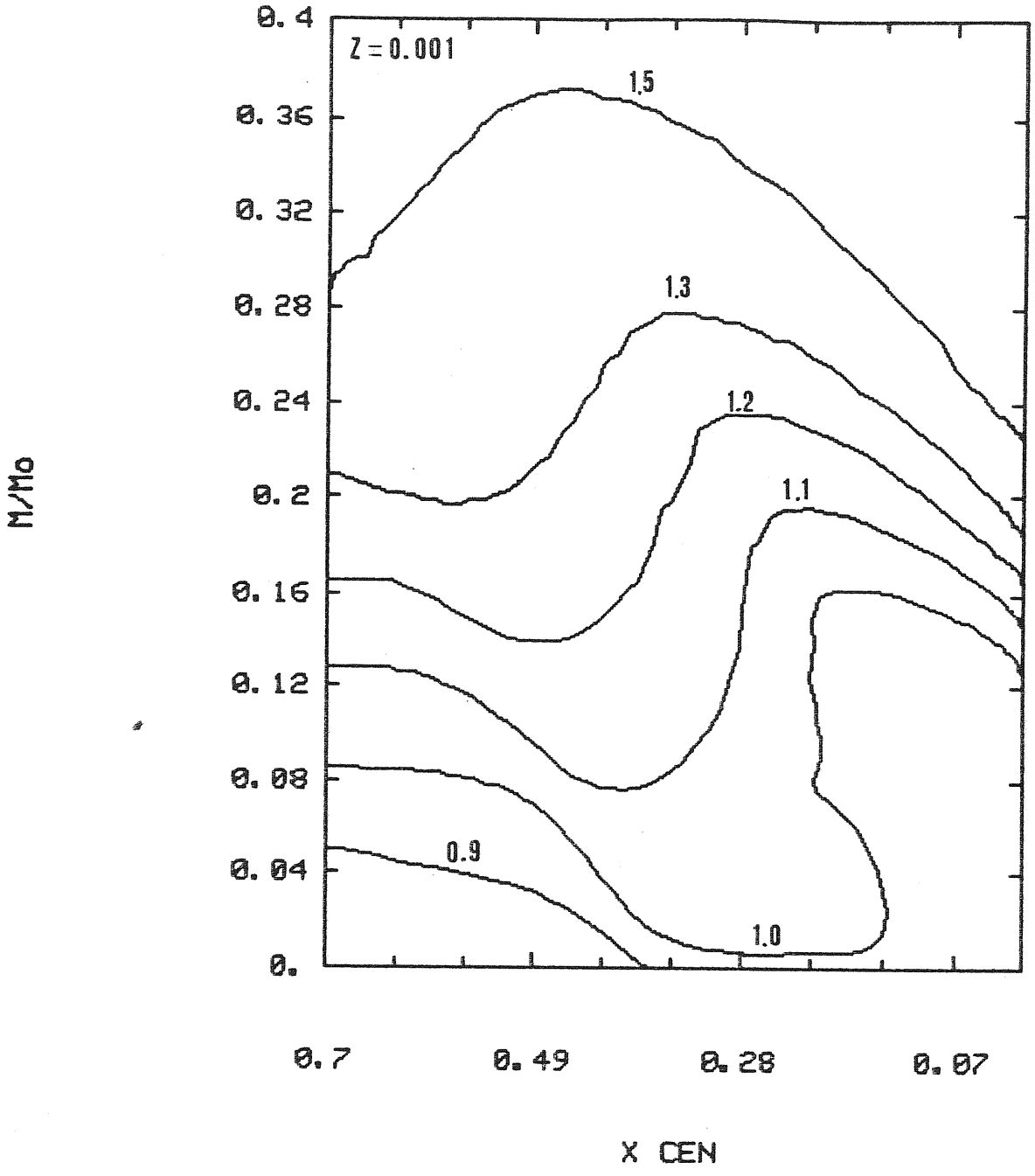
Z = 0.001
1.5
1.3
1.2
1.1
1.0
0.9
0. 4
0. 36
0. 32
0. 28
0. 24
0. 2
0. 16
0. 12
0. 08
0. 04
0.
M/Mo
0.7
0. 49
0. 28
0. 07
X CEN

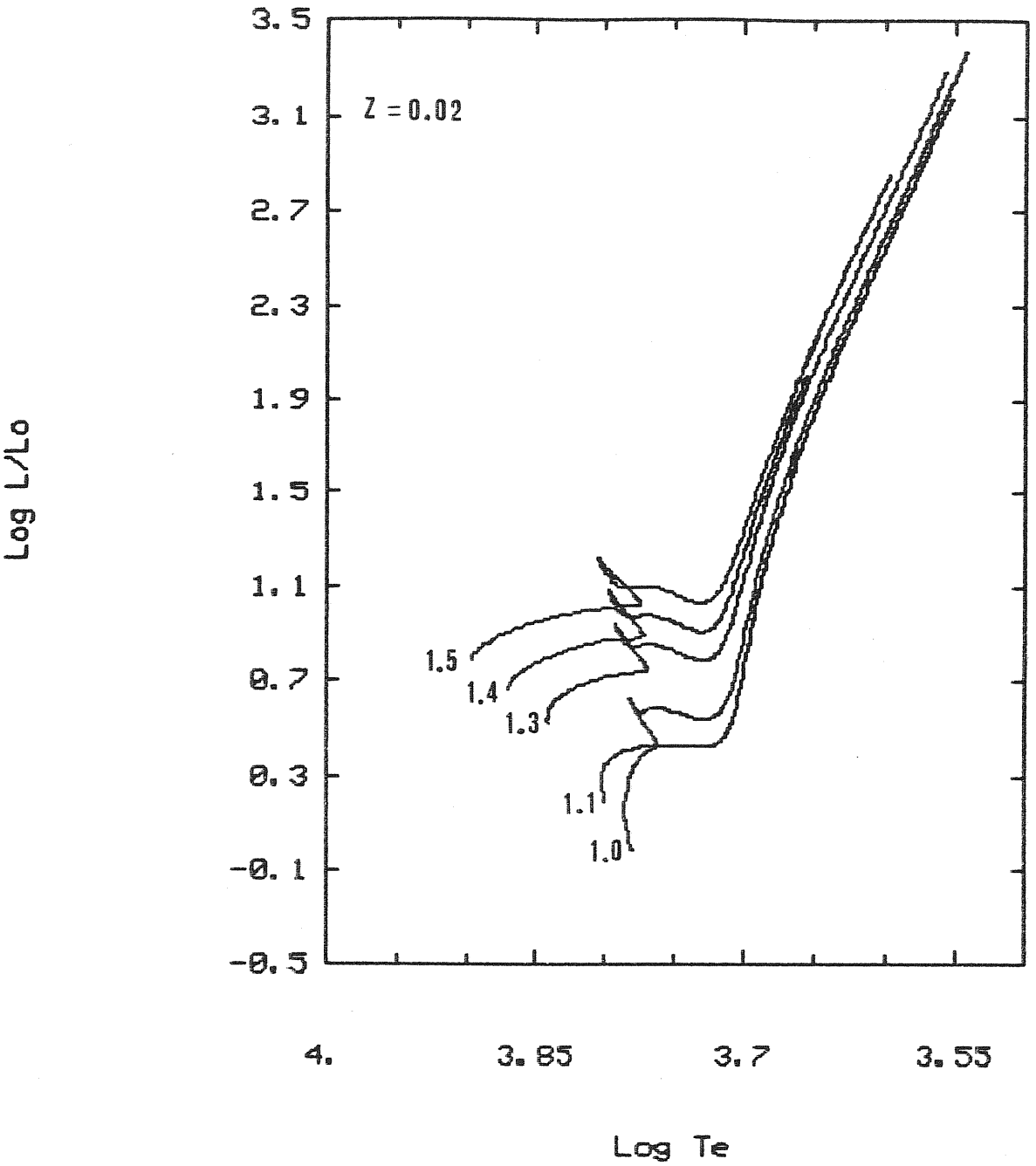
3.5
3.1
2.7
2.3
1.9
1.5
1.1
0.7
0.3
-0.1
-0.5
Z = 0.02
1.5
1.4
1.3
1.1
1.0
4.
3.85
3.7
3.55
Log L/Lo
Log Te

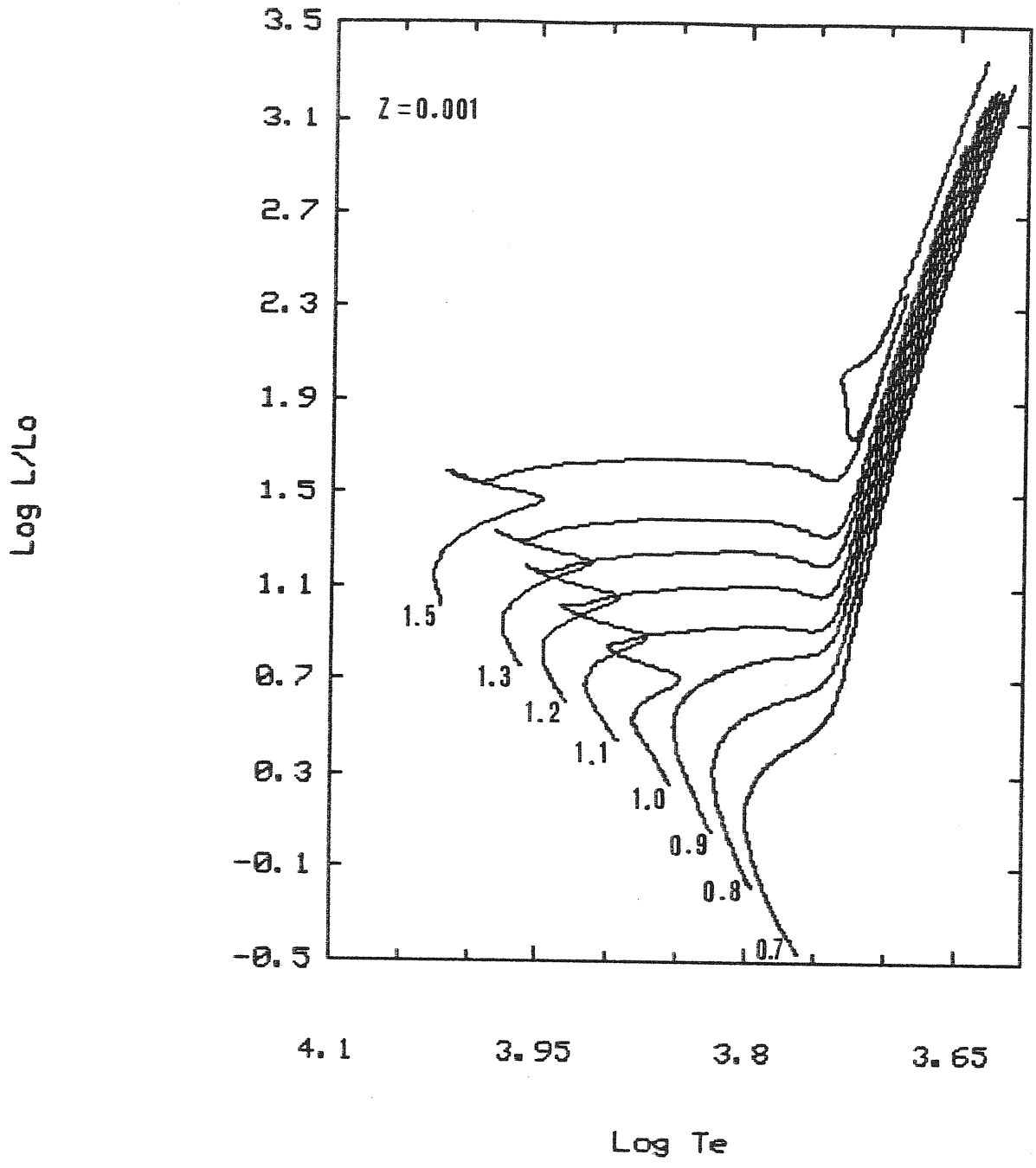
3.5
3.1
2.7
2.3
1.9
1.5
1.1
0.7
0.3
-0.1
-0.5
Z=0.001
1.5
1.3
1.2
1.1
1.0
0.9
0.8
0.7
4.1
3.95
3.8
3.65
Log L/Lo
Log Te

CHAPTER V

5.1 Horizontal branch stars

In recent years a great deal of theoretical work has been carried out in stellar evolution theory, thanks to many recent developments in the basic stellar physics and observational information on star clusters.

Among others, convective mixing during major phases of nuclear burning has been found to be perhaps the most uncertain and important physical process in the theory of stellar evolution.

The inclusion of "overshooting and induced semiconvection" (Castellani et al 1971a,b) in models of core Helium burning horizontal branch stars, and of "non local overshooting" in main sequence stars (Maeder 1975, Roxburgh 1978; Bressan et al 1981) are, among others, important attempts to interpret observational data by means of a more consistent physical treatment of convection.

In the preceding chapters I have analysed the effects of overshooting on the stellar structure over different ranges of mass, and pointed out that a substantial mixing beyond the standard convective core, as defined by the Schwarzschild criterion, ought to occur in model stars in order to account for several observational facts. Among others I recall:

1) The width of the main sequence band, which appears larger than predicted by standard models, and the number ratio of evolved to

unevolved stars in galactic clusters (Maeder & Mermilliod 1981) and in populous young globular clusters, like NGC1866 in LMC (cf. Becker & Mathews 1983).

2) The long lasting discrepancy between evolutionary and pulsational mass of Cepheid stars (cf. the recent study by Schmidt 1984).

3) The lack of very luminous asymptotic giant branch (AGB) stars in several clusters of the Magellanic Clouds, where they are expected to occur on the basis of the cluster turn-off mass (see the populous young cluster NGC1866 as prototype). This fact strongly indicates that M_{up} (upper mass limit for non degenerate carbon ignition) is much lower than the classical value.

4) The discrepancy between ages derived from the observed terminal AGB luminosity (Mould & Aaronson 1982 a,b; Mould 1983) and those derived from the turn-off and/or main sequence termination luminosity (Hodge 1983) for clusters of the Magellanic Clouds.

5) The "anomalous" behaviour of several old open clusters which, in spite of a turn-off mass of about 1.5 $M_{\odot}$, seem not to develop an extended red giant branch (RGB) and in turn to miss the stage of core Helium flash (Barbaro & Pigatto 1984; Pigatto 1986).

However, in spite of the much better agreement between theory and observations nowadays possible with models incorporating convective overshooting (Bressan et al. 1981; Bertelli et al 1984, 1985, 1986a,b; Chiosi et al 1986), still there are some

aspects of those evolutionary models that are not fully clarified.

Firstly, the scheme devised to describe convective overshooting rests on the mixing length theory of convection and contains the ratio Λ of the mean free path of convective elements to the pressure scale height as a free parameter.

Secondly, part of the above discrepancies can be also cured by other, completely different, mixing mechanisms. In fact, as I have anticipated in Chapter III, Castellani et al (1985a) were able to show that a lower value of M_{UP} can be obtained as a result of the so-called "breathing pulses of convection" which seem to be the natural consequence of the local treatment of convection during central Helium burning.

Fortunately, the above schemes rely on very different basic physical assumptions, and perhaps we may decide which of those schemes ought to be preferred looking at model predictions on a wider context, and not limited to the problem of M_{UP} alone.

In particular, induced semiconvection and breathing pulses of convection are driven by local mixing. The former occurs during central Helium burning because of the increase in the opacity of the carbon-oxygen rich mixture, whereas the latter develops in the very late stages of the same phase, because of the enhanced energy generation.

On the contrary, the non-local description of overshooting I have discussed at the beginning leads to the onset of "full

convection" outside the unstable core, as a consequence of inertia of motions. In this case, the major task of the theory is the determination of the velocity field, in that contrary to local treatments which consider only the acceleration field. As a consequence of this, overshooting have turned out to be more efficient than in the acceleration schemes.

Differences in the final evolutionary results may arise not only because of the different prescriptions used in model construction, but also because of the fact that non local overshooting is efficient starting from central Hydrogen burning, if the star mass is large enough for a convective core to develop. We have already seen that these stars terminate the core Hydrogen burning phase having much larger Hydrogen exhausted cores.

In the case of central convection being present already starting from the core Hydrogen burning phase, the comparison of the two methods in question is somewhat difficult, even though observational constraints such as (1) and (2), which are related to core Hydrogen burning models (see also (4) and (5)), cannot be easily reproduced by models based on local theories of convection.

Stars in old globular clusters are a better laboratory, since core Hydrogen burning is known to occur in a radiative core, and central convection is present only during the Helium burning phase in horizontal branches. Furthermore, globular clusters are

normally well populated, so that star counts there possess statistical significance and the comparison with their theoretical counterparts, lifetimes, is meaningful. In addition to this, stars in globular cluster are confined in a rather narrow range of basic parameters, such as the turn-off mass, the mass at the tip of RGB and in the horizontal branch. Finally, star counts in different areas of C-M diagrams of several globular clusters led Buzzoni et al (1983) and Buonanno et al (1985) to assess that "semiconvection" has to be fully efficient during Helium burning; in particular the above authors stressed the high sensitivity of the ratio of AGB stars to horizontal branch (HB) stars ($R_2 = N_{AGB}/N_{HB}$) to the adopted mixing criterion.

In this Chapter I present evolutionary computations for HB stars followed from core Helium ignition till the start of the thermally pulsing AGB phase (TP-AGB). Overshooting by the non-local scheme is taken into account in all phases with convective cores, and beside the value $\Lambda = 1$ used in the previous chapters a slightly larger one, $\Lambda = 1.25$, is also used in order to get a precise indication from observations. The results of these calculations are compared with similar models based on the classical scheme (semiconvection and accompanying breathing convection) followed by many authors (cf. Castellani et al 1985 and references therein), and tested against star counts by Buzzoni et al (1983) to cast light on which kind of mixing better

reproduces the observational data. The following table 5.1 contains the initial parameters which characterize the models computed.

Table 5.1

Helium burning

Z = 0.02	M_c = 0.475	Y = 0.280
Λ = 1	M_i = 0.6,0.7,0.8,0.9,1.0,1.1,1.2,1.3,1.4	
Z = 0.001	M_c = 0.475	Y = 0.299
Λ = 1	M_i = 0.6,0.65,0.7,0.8,0.9,1.0,1.1,1.2,1.3,1.4	
Λ = 1.25	M_i = 0.6,0.65,0.7,0.8	
Z = 0.001	M_c = 0.500	Y = 0.200
Λ = 1.25	M_i = 0.6,0.65,0.7,0.8	

M_c = initial Helium core mass in solar masses
M_i = total mass in solar units

As can be seen from the table an additional set of models with Z = 0.001, Y = 0.200, M_c = 0.500 and Λ = 1.25 has been computed to test the dependence of the quantity R_2 - discussed below - on the He content in the envelope. All other details of the input physics are as in previous Chapters.

5.2 The effects of a gradient in molecular weight (μ).

As the evolution proceeds, the kinetic energy of motions grows

and elements enter the region of discontinuity in molecular weight surrounding the Helium core. As shown by Bressan et al (1981), the effect of gradients of molecular weight must be treated separately from the equation of motion because the deceleration imparted to convective elements may be several orders of magnitude greater than the contribution given by the temperature term. Therefore, an extreme fine mass and time grid (cf. Renzini 1977 for some characteristic dimensions), would be required to follow the mixing, which would imply an enormous computational effort far beyond the scope of the present study. Following Castellani et al (1971a) and Renzini (1977), I evaluate the characteristic scale of penetration of convective motion inside a molecular barrier, as given by the velocity of propagation of convection

$$v_p = v^2 / [2g\ (\Delta\mu/\mu)] * (v_{max}/l) \qquad (5.1)$$

into the time step of the model

$$\Delta R_c = \Delta t * V_p \quad . \qquad (5.2)$$

The maximum increase of the convective core at each time step is chosen to be the minimum value between ΔR_c and the amount of penetration determined by the velocity field neglecting the molecular term.

The quantities that define relation (5.1) are the molecular weight and size of its discontinuity, μ and $\delta\mu$ respectively, the acceleration of gravity, g, the maximum value of the velocity field, V_{max}, the distance l over which the molecular weight has to be smeared out (corresponding to the linear size of the convective core), and finally the local value, v, of the velocity field in the region undergoing mixing. Relation (5.1) provides only an indicative estimate of the effect of molecular weight.

The validity of the above expression has been criticized by Renzini (1977), in the sense that, owing to the finite dimensions of the elements or effects of ionic diffusion, the true velocity V_p may be greater by several orders of magnitude. However, I think that the relation in question is indeed fairly appropriate owing to the very different physical conditions we are dealing with. In fact, relation (5.1) is not applied to regions near which the maximum of the velocity field is located, and velocities are almost radially directed, nor near the point where $\nabla_R \simeq \nabla_A$, at which effects by ionic diffusion are expected to be important. On the contrary, relation (5.1) is applied to external stable ($\nabla_R < \nabla_A$) regions, in which the velocity is dropping to zero and mixing is likely driven by tangential shear, and controlled by a relation almost identical to relation (5.1).

Finally I anticipate that relation (5.1) has no effect in constraining the size of the convective core during all but the very end of Helium burning, when the time scale for penetrative

convection overwhelms that of nuclear burning.

5.3 The evolutionary results

The main results obtained here can be summarized as follows:

1) Overshooting versus semiconvection

In models of low mass stars with non-local treatment of convective overshooting, semiconvection at the border of the convective core never develops. This confirms the similar result found long ago in massive stars (Cloutmann & Whitaker 1980; Bressan et al 1981).

Figures (5.1) and (5.2) show the run as a function of the interior mass of the adiabatic and radiative temperature gradients together with the velocity field and the Helium content, inside the core of the 0.7 $M_{\odot}$ model at different evolutionary stages. The convective core steady increases during evolution as a natural consequence of the growth of the unstable region (which is about half sized) and extension of the velocity field beyond the chemical discontinuity. However, contrary to standard models, the region above the convective core is definitely stable in all models.

2) Overshooting versus breathing convection

A second result concerns the occurrence of the so called breathing pulses of convection known to take place at the end of central Helium burning. As extensively described by Castellani et al (1985a,b) when the central helium abundance gets very low (< 0.1) further mixing of fresh helium through the growth of the

convective core may give rise to an excess of nuclear energy release, which in turn enhances convective instability and induces further mixing. The net result is a convective pulse that considerably increases the size of the mixed region and consequently the lifetime of the Helium burning phase. Other important implications of this phenomenon are described by Castellani et al (1985a,b). Here I notice that, toward the end of central Helium burning the unstable region starts growing at a larger rate (cf. Figure (5.3)), but not as a consequence of the sole increase in opacity as suggested by Castellani et al (1985a,b). In fact, the linear perturbation of the radiative transport equation, at fixed mass coordinate around the unstable core, gives the following relation

$$\delta\nabla_R/\nabla_R = \delta(L/M)/(L/M) + (\delta\kappa/\kappa) + \delta\beta/(1-\beta) \qquad (5.3)$$

where all symbols have their usual meaning and variations are taken with respect of time. An inspection of the models shows that the opacity term balances the luminosity term of opposite sign. On the contrary, since β is very close to unity, the factor $1/(1-\beta)$ gets very large and a small increase in the gas pressure (partly because of the incipient electron degeneracy) is responsible of the starting of a breathing pulse. Once more, another important difference between local and non local treatments of convection can be seen. In standard models, in which the steep Helium profile is located where $\nabla_R = \nabla_A$, once

the above mechanism has started , enough fresh helium is mixed into the core to produce the breathing pulse. On the contrary, in models with non local overshooting the above mechanism is no longer sufficient, as mixing is driven by the velocity field through relation (5.1). The low velocities ($\rightarrow 0$) existing at the border of the core delay mixing for a time sufficient to the core to adjust itself without undergoing an enhanced energy production and thus to proceed toward a quiet exhaustion of helium. To carefully delineate the space of parameters in which this phenomenon may occur, test models were arbitrarily perturbed by allowing for enhanced mixing. The result was that the sharp discontinuity in molecular weight always dumps any breathing pulse of convection that may tend to develop.

One may conclude therefore that breathing convection is a mere consequence of the local treatment of convection (Castellani et al 1985a,b), and it disappears when a more physical approach is undertaken.

5.4 The HR diagram

Figures (5.4a), (5.4b) and (5.4c) show the HR diagram for a few HB models up to the starting of the TP phase with $\Lambda = 1$, $Y = 0.299$ and $Z = 0.001$; $\Lambda = 1.25$, $Z = 0.001$ and two values for the helium abundance, $Y = 0.299$ and $Y = 0.200$ respectively. For purposes of completeness, in the same figures we also show a few

evolutionary tracks, whose initial masses are compatible with the mass in the horizontal branch. These tracks are evolved from the zero age main sequence till the tip of the red giant branch. The models with Z = 0.02 will not be discussed here. The value of the initial mass, horizontal branch mass and He core mass are indicated in the figures. From Figures (5.4a), (5.4b) and (5.4c) one sees that convective overshooting does not appreciably change the overall morphology of the HR diagram for Helium burning low mass stars. Minor differences with respect to other evolutionary models in literature (cf. Sweigart & Gross 1976) are mainly due to differences in the treatment of the outer envelope: grey atmospheres instead of the T-τ relation used by Sweigart & Gross (1976), a mixing length of 1.5 in outer layers, and finally different opacities and their interpolations.

Table 5.2 contains some characteristic quantities of the HB models shown in the above Figures as a function of the evolutionary stage. Lastly, we would like to comment on the abundance of ^{12}C that is built up in the core at the end of the Helium burning phase. With the new rate for the $^{12}C(\alpha,\gamma)^{16}O$ reaction (here assumed to be from 2 to 3 times the old value) carbon is much less abundant than oxygen, its final value being about 0.18 - 0.19 (by mass).

5.5 The ratio R2

Since the major goal in this chapter is to investigate on the

effects given by different kinds of mixing, I will not address here the problem of how well these models reproduce the HR diagrams of real globular clusters. On the contrary, I will concentrate on the ratio $R_2 = t_{AGB}/t_{HB} = N_{AGB}/N_{HB}$, which according to Buonanno et al (1985) is particularly sensitive to the kind of mixing taking place in central regions during core Helium burning. It is worth recalling here that t_{HB} is the lifetime spent in the HB up to the relative maximum in the luminosity, whereas t_{AGB} is the lifetime elapsed from the relative maximum luminosity up to 2.5 magnitudes above the RR Lyrae luminosity (cf. Caputo et al 1978).

Figure (5.5) shows the luminosity versus age relationship for the 0.7 M_0 model (M_{He} = 0.475, Y= 0.299) with two different values of the overshooting parameter Λ = 1 and Λ = 1.25. The figure clearly illustrates the effects by the adopted type of mixing. In fact, while the total lifetime does not change with Λ, the lifetime t_{HB} increases while the lifetime t_{AGB} decreases with increasing Λ: thus the ratio R_2 turns out to be a very sensitive function of the mixing parameter. Table 5.3 contains the lifetimes t_{HB}, t_{AGB} and the ratio R_2 derived from our models. An inspection of Table 5.3 shows that in addition to mixing, for Y = 0.299 these quantities are sensitive functions of the total mass M_{HB}. On the contrary, for Y = 0.200 only the HB lifetime shows such a dependence, whereas the AGB lifetime and the ratio R_2 are almost constant over the range of masses considered here.

Furthermore, the data of Table 5.3 indicate that if consistency with the previous RGB phase is imposed - by assuming the appropriate initial He core mass M_{He} - then R_2 turns out to be almost independent of the He abundance in the envelope. In this way once the range of masses pertinent to the horizontal branches of globular clusters is known, observations of the parameter R_2 yield a straightforward indication of the extension of mixing during core Helium burning, at least for the metal content under consideration.

Table 5.3 (a)

	Λ = 1 (b)			Λ = 1.25 (b)			L = 1.25 (c)		
M_{HB}/M_O	t_{HB}	t_{AGB}	R_2	t_{HB}	t_{AGB}	R_2	t_{HB}	t_{AGB}	R_2
0.60	108.46	24.34	0.22	116.78	20.52	0.18	107.76	17.77	0.16
0.65	104.10	22.37	0.21	112.05	18.42	0.16	104.65	17.80	0.17
0.70	103.50	19.03	0.18	109.37	16.93	0.15	102.96	17.47	0.17
0.80	99.68	18.19	0.18	106.04	15.22	0.14	100.57	16.81	0.17
0.90	97.83	16.68	0.17	103.80	13.67	0.13	--	--	--

(a) ages in units of 10^6 yrs

(b) models with Y = 0.299 and M_{He} = 0.475 M_O

(c) models with Y = 0.200 and M_{He} = 0.500 M_O

5.6 Comparison with the observations

Table 5.4 presents a list of values R_2 obtained by different authors together with our theoretical predictions and compares them with the more recent data derived by Buzzoni et al (1983) for a sample of 15 well observed globular clusters.

For the purposes of this study, we assume $M_{HB} = 0.65\ M_0$, as a value in between 0.6 and 0.7 M_0 is indicated by the overall morphology of globular clusters (Renzini 1977) and it has been adopted in previous studies.

The value of $R_2 = 0.12$ given by Gingold (1976) deserves a short discussion as it is often taken as representative of the AGB lifetime of low mass stars. This particular value refers to an evolutionary track with $M_{HB} = 0.6\ M_0$, $M_{He}=0.466\ M_0$, Y= 0.300, Z=0.001, and computed with the canonical prescription for local overshooting and semiconvection (Gingold 1976). Due to the dependence of R_2 on total mass M_{HB} and He core mass, the normalization of these parameters to 0.65 M_0 and 0.475 M_0 respectively, would lower the quoted value below 0.10, in closer agreement with the estimates given by other authors under the same physical assumptions (e.g. Caputo et al 1978). Furthermore, models by Gingold (1976) of the same set encounter sooner or later the problem of breathing convection (e.g. $M_{HB}=0.6\ M_0$ and Y=0.200 in Gingold 1976) in analogy with most updated

computations which show that this phenomenon constitutes a constant characteristic of the so-called "canonical" prescription for the treatment of core convection (Sweigart & Gross 1976; Castellani et al 1985a,b; Iben 1986; Lattanzio 1986).

Table 5.4 (a)

Theoretical and observational ratios R_2

Y	Z	M_{He}	M_{HB}	Model	R_2	Reference
0.3	0.001	0.475	0.625	I1	0.65	Iben & Rood (1970)
0.3	0.001	0.475	0.600	I2	0.71	Iben & Rood (1970)
0.3	0.001	0.466	0.600	G	0.12	Gingold (1976)
0.3	0.001	0.475	0.660	C1	0.05	Caputo et al (1978)
0.2	0.001	0.498	0.660	C2	0.06	Caputo et al (1978)
0.2	0.001	0.500	0.650	C3	0.06	Castellani et al (1985b)
0.299	0.001	0.475	0.650	B1	0.21	Bressan et al (1986)
0.299	0.001	0.475	0.650	B2	0.16	Bressan et al (1986)
0.200	0.001	0.500	0.650	B3	0.17	This thesis
Observed value				A	0.15	Buzzoni et al (1983)

Legend:
Model I1: without overshooting and/or semiconvection
Model I2: without overshooting and/or semiconvection
Model G: local overshooting and semiconvection
Model C1: local overshooting and semiconvection
Model C2: local overshooting and semiconvection
Model C3: local overshooting, semiconvection and breathing pulses of convection
Model B1: non local overshooting, $\Lambda = 1$
Model B2: non local overshooting, $\Lambda = 1.25$
Model B3: non local overshooting, $\Lambda = 1.25$

Notes
(a) : masses in solar units
A : average value of 15 clusters (0.15 ± 0.03)

The last entry of Table 5.4 (R_2 = 0.15) is the mean value from the data for 15 globular clusters given by Buzzoni et al (1983). Considering the error of each observational ratio to be 0.07 (Buonanno et al 1985), the error on the mean value is about 0.03. The data of Buzzoni et al (1983) are shown in the histogram of Figure (5.6) (number of clusters versus R_2) together with the theoretical values of Table 5.4. The dispersion in these latter is by far larger than in the observed ones, thus emphasizing once more the high sensitivity of the ratio R_2 with respect to the mixing prescription adopted during central Helium burning. It is soon evident that models which strictly follow the standard criterion for convection ($\nabla_R < \nabla_A$, Iben and Rood 1970) predict too large a ratio (> 0.6). Indeed, the observations seem to suggest that mixing outside the formal boundary effectively takes place at full efficiency. However models that, instead of the simple Schwarzschild condition, consider local overshooting and semiconvection, predict on the contrary too low a value, as indicated by cases G, C1, C2 of Table 5.4 or even lower when breathing convection is considered (case C3). Therefore, observations seem to indicate that mixing ought not to be as efficient as imposed by these local prescriptions. On the other hand, since the above schemes neglect any detailed description of convective motions, the suggestion arises that only by knowing the velocity field one may adequately reproduce the effects of internal convection. This is evident in our models with non local

overshooting, which not only eliminate the problem of breathing convection but also provide a good agreement with observations. The best result is obtained for Λ about 1.25 independently from the helium abundance of the envelope: 0.16 or 0.17 versus the observational value of 0.15. The value of Λ =1 was invoked by Bertelli et al (1984, 1985) and Chiosi et al (1986) to bring theory and observations into agreement in other areas of the HR diagram (cf. points 1 to 5 above). A value slightly greater than 1 will not change the main conclusions reached in the previous chapters. Indeed an even lower M_{up} would result as perhaps indicated by recent data on the AGB star luminosity function in LMC (Mould & Aaronson 1986).

Legend to Table 5.2.

AGE: age in units of 10^6 years; L/Lo: the logarithm of luminosity in solar units; Teff: logarithm of the effective temperature; Mcon: mass of the convective core ; Msch: mass of the unstable region ; Mhe: mass of the helium core. All masses are in solar units. Ycen: central abundance by mass of helium ; Lx and Ly: logarithm of the luminosity of the H and He-burning shells in solar units.

Te-m: minimum effective temperature; Te-M: maximum effective temperature; L-M: relative maximum luminosity at the end of core He-burning; L-m: minimum luminosity in AGB; Lx-m: minimum luminosity by the H-burning shell in AGB; 2.5m indicates the model along the AGB 2.5 bolometric magnitudes brighter than its zero age horizontal branch luminosity; Lx=y: stage at which the luminosity of the H-burning shell equals that of He-burning shell; STP: starting of the thermally pulsing regime of the He-burning shell

TABLE 5.2

M=0.6 Y=0.299 Λ = 1

AGE	L/L_o	T_{eff}	M_{con}	M_{sch}	M_{HE}	Y	XC	L_x	L_y	
0.000	1.620	3.957	0.195	0.090	0.475	0.999	0.000	1.425	1.179	
7.922	1.640	3.950	0.193	0.093	0.475	0.937	0.060	1.441	1.207	Te-m
12.322	1.643	3.955	0.195	0.093	0.475	0.900	0.093	1.436	1.224	
24.066	1.623	3.994	0.198	0.097	0.475	0.800	0.175	1.365	1.277	
35.394	1.598	4.027	0.200	0.100	0.475	0.700	0.245	1.268	1.327	
46.155	1.580	4.047	0.203	0.103	0.476	0.600	0.302	1.164	1.372	
56.219	1.569	4.057	0.205	0.106	0.478	0.500	0.347	1.055	1.413	
64.487	1.567	4.059	0.204	0.108	0.480	0.418	0.373	0.963	1.446	Te-M
66.198	1.568	4.059	0.205	0.108	0.480	0.400	0.378	0.944	1.452	
75.831	1.576	4.054	0.205	0.109	0.481	0.300	0.391	0.845	1.489	
85.304	1.595	4.045	0.205	0.112	0.482	0.200	0.382	0.783	1.523	
95.132	1.630	4.031	0.207	0.114	0.483	0.100	0.336	0.833	1.554	
100.523	1.670	4.016	0.207	0.117	0.483	0.050	0.284	0.990	1.564	
106.465	1.791	3.942	0.203	0.116	0.485	0.010	0.198	1.403	1.541	
107.993	1.955	3.746	0.174	0.084	0.486	0.001	0.173	1.752	1.356	
108.463	2.167	3.700	0.000	0.000	0.487	0.000	0.170	2.034	1.464	L-M
109.930	1.994	3.731	0.000	0.000	0.491	0.000	0.170	1.451	1.848	L-m
128.972	2.354	3.682	0.000	0.000	0.500	0.000	0.170	0.929	2.334	Lx-m
132.803	2.622	3.661	0.000	0.000	0.504	0.000	0.170	1.760	2.548	2.5m
134.018	2.832	3.647	0.000	0.000	0.508	0.000	0.170	2.524	2.521	Lx=y
135.090	3.054	3.633	0.000	0.000	0.518	0.000	0.170	2.880	2.918	STP

M=0.65 Y=0.299 Λ = 1

AGE	L/L_o	T_{eff}	M_{con}	M_{sch}	M_{HE}	Y	XC	Lx	Ly	
0.000	1.699	3.764	0.193	0.090	0.475	0.999	0.000	1.545	1.172	
7.528	1.722	3.756	0.194	0.092	0.475	0.940	0.057	1.568	1.202	Te-m
12.330	1.726	3.759	0.194	0.094	0.475	0.900	0.093	1.563	1.224	
24.176	1.714	3.807	0.200	0.097	0.475	0.800	0.175	1.513	1.285	
35.002	1.700	3.858	0.201	0.102	0.479	0.700	0.245	1.453	1.341	
45.703	1.687	3.897	0.205	0.104	0.482	0.600	0.303	1.382	1.392	
55.625	1.676	3.923	0.208	0.107	0.485	0.500	0.348	1.302	1.440	
64.958	1.671	3.938	0.208	0.110	0.488	0.400	0.379	1.217	1.484	
74.074	1.672	3.942	0.210	0.112	0.489	0.301	0.393	1.136	1.525	Te-M
74.205	1.672	3.942	0.210	0.112	0.489	0.300	0.393	1.135	1.526	
82.904	1.685	3.936	0.208	0.114	0.491	0.200	0.386	1.077	1.563	
92.047	1.717	3.915	0.209	0.117	0.493	0.100	0.340	1.105	1.595	
97.433	1.759	3.884	0.212	0.119	0.494	0.050	0.283	1.220	1.607	
102.254	1.868	3.764	0.210	0.119	0.496	0.010	0.208	1.528	1.583	
103.678	2.003	3.717	0.178	0.088	0.497	0.001	0.183	1.804	1.402	
104.103	2.188	3.694	0.000	0.000	0.499	0.000	0.179	2.046	1.503	L-M
105.687	2.033	3.712	0.000	0.000	0.503	0.000	0.179	1.447	1.902	L-m
123.432	2.443	3.673	0.000	0.000	0.511	0.000	0.179	0.698	2.430	Lx-m
126.473	2.706	3.654	0.000	0.000	0.514	0.000	0.179	1.793	2.638	2.5m
127.423	2.905	3.641	0.000	0.000	0.518	0.000	0.179	2.593	2.593	Lx=y
128.359	3.221	3.621	0.000	0.000	0.529	0.000	0.179	3.141	3.015	STP

M=0.7 Y=0.299 Λ = 1

AGE	L/L_o	T_{eff}	M_{con}	M_{sch}	M_{HE}	Y	XC	Lx	Ly	
0.000	1.737	3.736	0.191	0.090	0.475	0.999	0.000	1.599	1.170	
7.922	1.761	3.732	0.195	0.091	0.475	0.938	0.059	1.623	1.201	Te-m
12.514	1.765	3.733	0.196	0.093	0.475	0.900	0.093	1.618	1.224	
24.076	1.761	3.741	0.199	0.098	0.476	0.800	0.175	1.584	1.289	
35.204	1.756	3.751	0.203	0.101	0.481	0.700	0.245	1.543	1.348	
45.581	1.750	3.768	0.207	0.104	0.486	0.600	0.303	1.493	1.403	
55.168	1.744	3.794	0.208	0.108	0.490	0.500	0.349	1.434	1.454	
64.599	1.740	3.818	0.211	0.109	0.493	0.400	0.380	1.367	1.503	
73.215	1.741	3.829	0.212	0.111	0.495	0.300	0.395	1.303	1.547	
76.687	1.744	3.831	0.213	0.114	0.496	0.262	0.394	1.278	1.564	Te-M
81.882	1.752	3.827	0.211	0.116	0.498	0.200	0.387	1.250	1.588	
90.608	1.781	3.800	0.213	0.118	0.500	0.100	0.342	1.265	1.623	
95.324	1.819	3.765	0.211	0.121	0.502	0.050	0.291	1.352	1.634	
100.509	1.917	3.729	0.209	0.121	0.504	0.010	0.204	1.597	1.614	
101.840	2.037	3.708	0.182	0.089	0.505	0.001	0.179	1.840	1.436	
102.248	2.212	3.690	0.000	0.000	0.507	0.000	0.176	2.053	1.745	L-M
103.505	2.064	3.705	0.000	0.000	0.510	0.000	0.176	1.480	1.933	L-m
120.026	2.497	3.668	0.000	0.000	0.518	0.000	0.176	0.530	2.487	Lx-m
122.539	2.736	3.652	0.000	0.000	0.520	0.000	0.176	1.612	2.690	2.5m
123.568	2.958	3.638	0.000	0.000	0.526	0.000	0.176	2.649	2.644	Lx=y
124.288	3.125	3.627	0.000	0.000	0.535	0.000	0.176	2.904	3.005	STP

M=0.8 Y=0.299 Λ = 1

AGE	L/L_o	T_{eff}	M_{con}	M_{sch}	M_{HE}	Y	XC	Lx	Ly	
0.000	1.780	3.723	0.189	0.091	0.475	0.999	0.000	1.659	1.169	
8.973	1.806	3.720	0.194	0.092	0.475	0.929	0.068	1.682	1.206	Te-m
12.497	1.809	3.721	0.197	0.093	0.475	0.900	0.093	1.678	1.225	
23.935	1.813	3.724	0.198	0.099	0.478	0.800	0.175	1.658	1.294	
34.944	1.817	3.728	0.204	0.101	0.485	0.700	0.245	1.633	1.356	
44.967	1.819	3.732	0.206	0.107	0.490	0.600	0.304	1.602	1.416	
54.434	1.820	3.735	0.209	0.108	0.495	0.500	0.349	1.565	1.470	
63.536	1.822	3.739	0.213	0.108	0.499	0.400	0.381	1.520	1.524	
71.814	1.826	3.741	0.214	0.110	0.503	0.300	0.397	1.475	1.572	
76.628	1.830	3.741	0.216	0.111	0.505	0.242	0.396	1.449	1.599	Te-M
79.987	1.835	3.741	0.215	0.116	0.506	0.200	0.390	1.435	1.617	
88.282	1.861	3.736	0.217	0.120	0.510	0.100	0.345	1.438	1.655	
92.732	1.892	3.729	0.215	0.124	0.512	0.050	0.295	1.495	1.667	
98.086	1.977	3.714	0.214	0.122	0.515	0.010	0.196	1.681	1.652	
99.323	2.083	3.701	0.186	0.090	0.516	0.001	0.171	1.891	1.477	
99.685	2.247	3.687	0.000	0.000	0.518	0.000	0.168	2.096	1.630	L-M
101.169	2.104	3.699	0.000	0.000	0.522	0.000	0.168	1.454	1.994	L-m
115.624	2.541	3.666	0.000	0.000	0.528	0.000	0.168	0.297	2.533	Lx-m
117.880	2.781	3.651	0.000	0.000	0.530	0.000	0.168	1.330	2.754	2.5m
118.945	3.022	3.635	0.000	0.000	0.536	0.000	0.168	2.707	2.712	Lx=y
119.595	3.279	3.619	0.000	0.000	0.546	0.000	0.168	3.175	3.142	STP

M=0.6 Y=0.299 Λ = 1.25

AGE	L/L_o	T_{eff}	M_{con}	M_{sch}	M_{HE}	Y	XC	L_x	L_y	
0.000	1.620	3.958	0.215	0.083	0.475	0.999	0.000	1.430	1.176	
7.922	1.640	3.950	0.217	0.083	0.475	0.945	0.052	1.453	1.189	Te-m
14.180	1.644	3.959	0.218	0.084	0.475	0.900	0.093	1.445	1.212	
27.369	1.618	4.006	0.219	0.088	0.475	0.800	0.175	1.360	1.273	
40.015	1.593	4.040	0.223	0.091	0.476	0.700	0.244	1.256	1.327	
51.577	1.575	4.058	0.224	0.093	0.478	0.600	0.302	1.144	1.376	
62.855	1.566	4.067	0.224	0.096	0.480	0.500	0.346	1.024	1.421	
67.814	1.565	4.068	0.225	0.096	0.481	0.453	0.363	0.968	1.440	Te-M
73.390	1.566	4.067	0.226	0.097	0.482	0.400	0.377	0.906	1.462	
83.529	1.578	4.061	0.224	0.099	0.483	0.300	0.391	0.798	1.501	
93.495	1.598	4.050	0.224	0.100	0.483	0.200	0.382	0.728	1.537	
103.691	1.635	4.034	0.222	0.102	0.484	0.100	0.335	0.771	1.570	
109.284	1.673	4.021	0.221	0.104	0.485	0.050	0.284	0.931	1.583	
114.690	1.786	3.957	0.221	0.105	0.486	0.010	0.207	1.359	1.562	
116.262	1.949	3.760	0.196	0.078	0.488	0.001	0.182	1.729	1.391	
116.782	2.208	3.695	0.000	0.000	0.489	0.000	0.179	2.084	1.262	L-M
118.512	2.026	3.724	0.000	0.000	0.493	0.000	0.179	1.374	1.917	L-m
133.558	2.356	3.682	0.000	0.000	0.500	0.000	0.179	0.968	2.334	Lx-m
137.393	2.626	3.661	0.000	0.000	0.504	0.000	0.179	1.779	2.549	2.5m
138.605	2.835	3.647	0.000	0.000	0.508	0.000	0.179	2.527	2.524	Lx=y
139.695	3.049	3.634	0.000	0.000	0.518	0.000	0.179	2.855	3.030	STP

M=0.65 Y=0.299 Λ = 1.25

AGE	L/L_o	T_{eff}	M_{con}	M_{sch}	M_{HE}	Y	XC	L_x	L_y	
0.000	1.699	3.764	0.215	0.083	0.475	0.999	0.000	1.549	1.173	
7.528	1.723	3.756	0.215	0.083	0.475	0.948	0.050	1.577	1.185	Te-m
14.087	1.727	3.762	0.217	0.085	0.475	0.900	0.093	1.568	1.215	
27.366	1.714	3.822	0.221	0.088	0.476	0.800	0.175	1.514	1.282	
39.731	1.699	3.877	0.226	0.091	0.481	0.700	0.244	1.450	1.343	
50.996	1.686	3.915	0.226	0.095	0.485	0.600	0.302	1.372	1.400	
61.864	1.675	3.940	0.229	0.097	0.488	0.500	0.347	1.285	1.451	
71.691	1.670	3.953	0.229	0.100	0.490	0.400	0.379	1.191	1.498	
78.511	1.671	3.956	0.231	0.100	0.492	0.331	0.391	1.126	1.528	Te-M
81.394	1.673	3.955	0.230	0.101	0.492	0.300	0.393	1.099	1.541	
90.566	1.688	3.947	0.226	0.103	0.494	0.200	0.386	1.030	1.581	
99.945	1.721	3.925	0.228	0.105	0.495	0.100	0.340	1.054	1.615	
105.106	1.761	3.896	0.226	0.107	0.496	0.050	0.289	1.172	1.628	
110.112	1.867	3.782	0.226	0.108	0.498	0.010	0.212	1.495	1.608	
111.555	2.001	3.719	0.201	0.081	0.500	0.001	0.187	1.787	1.441	
112.050	2.233	3.690	0.000	0.000	0.501	0.000	0.184	2.087	1.653	L-M
113.308	2.067	3.709	0.000	0.000	0.505	0.000	0.184	1.422	1.956	L-m
127.328	2.434	3.674	0.000	0.000	0.511	0.000	0.184	0.731	2.421	Lx-m
130.467	2.702	3.655	0.000	0.000	0.514	0.000	0.184	1.739	2.640	2.5m
131.508	2.914	3.641	0.000	0.000	0.519	0.000	0.184	2.604	2.602	Lx=y
132.406	3.128	3.627	0.000	0.000	0.530	0.000	0.184	2.947	3.094	STP

M=0.7 Y=0.299 Λ = 1.25

AGE	L/L_o	T_{eff}	M_{con}	M_{sch}	M_{HE}	Y	XC	L_x	L_y	
0.000	1.737	3.736	0.215	0.082	0.475	0.999	0.000	1.604	1.168	
7.922	1.762	3.732	0.217	0.082	0.475	0.946	0.052	1.631	1.183	Te-m
14.276	1.766	3.734	0.217	0.084	0.475	0.900	0.093	1.623	1.217	
27.451	1.763	3.743	0.223	0.088	0.478	0.800	0.175	1.588	1.287	
39.414	1.759	3.756	0.225	0.092	0.484	0.700	0.245	1.544	1.352	
50.842	1.752	3.781	0.229	0.095	0.489	0.600	0.302	1.489	1.412	
61.113	1.746	3.814	0.231	0.098	0.493	0.500	0.348	1.425	1.467	
71.012	1.743	3.837	0.231	0.099	0.496	0.400	0.380	1.351	1.519	
80.101	1.744	3.847	0.233	0.101	0.499	0.300	0.395	1.277	1.565	
82.232	1.746	3.847	0.234	0.102	0.499	0.278	0.395	1.261	1.575	Te-M
89.070	1.755	3.842	0.232	0.105	0.501	0.200	0.388	1.216	1.609	
97.927	1.786	3.814	0.230	0.107	0.503	0.100	0.343	1.225	1.646	
102.841	1.823	3.775	0.231	0.109	0.505	0.050	0.292	1.316	1.658	
107.548	1.918	3.732	0.229	0.111	0.507	0.010	0.215	1.571	1.640	
108.913	2.037	3.710	0.203	0.084	0.508	0.001	0.190	1.825	1.475	
109.368	2.256	3.687	0.000	0.000	0.510	0.000	0.187	2.106	1.683	L-M
110.446	2.095	3.702	0.000	0.000	0.513	0.000	0.187	1.451	1.985	L-m
123.612	2.483	3.670	0.000	0.000	0.519	0.000	0.187	0.548	2.473	Lx-m
126.303	2.736	3.653	0.000	0.000	0.522	0.000	0.187	1.554	2.695	2.5m
127.390	2.969	3.637	0.000	0.000	0.528	0.000	0.187	2.656	2.658	Lx=y
128.198	3.349	3.613	0.000	0.000	0.539	0.000	0.187	3.307	3.028	STP

M=0.8 Y=0.299 Λ = 1.25

AGE	L/L_o	T_{eff}	M_{con}	M_{sch}	M_{HE}	Y	XC	L_x	L_y	
0.000	1.781	3.723	0.212	0.083	0.475	0.999	0.000	1.663	1.166	
8.954	1.807	3.720	0.213	0.084	0.475	0.938	0.059	1.688	1.190	Te-m
14.059	1.811	3.721	0.215	0.086	0.475	0.900	0.093	1.683	1.219	
27.297	1.818	3.725	0.224	0.088	0.481	0.800	0.175	1.665	1.292	
39.078	1.822	3.729	0.225	0.093	0.488	0.700	0.245	1.639	1.362	
49.757	1.825	3.733	0.227	0.097	0.494	0.600	0.304	1.605	1.426	
60.375	1.827	3.737	0.234	0.097	0.499	0.500	0.348	1.564	1.487	
69.621	1.829	3.741	0.234	0.099	0.503	0.400	0.381	1.515	1.542	
78.178	1.833	3.743	0.235	0.101	0.507	0.300	0.398	1.463	1.593	
83.264	1.837	3.743	0.236	0.102	0.509	0.242	0.397	1.434	1.621	Te-M
87.039	1.843	3.743	0.237	0.105	0.510	0.200	0.389	1.416	1.641	
95.407	1.868	3.737	0.235	0.109	0.514	0.100	0.346	1.412	1.681	
99.923	1.900	3.730	0.232	0.112	0.516	0.050	0.295	1.470	1.695	
104.374	1.980	3.715	0.236	0.113	0.518	0.010	0.218	1.661	1.679	
105.644	2.083	3.702	0.209	0.086	0.520	0.001	0.192	1.877	1.517	
106.040	2.282	3.685	0.000	0.000	0.521	0.000	0.189	2.136	1.494	L-M
107.270	2.134	3.697	0.000	0.000	0.525	0.000	0.189	1.408	2.044	L-m
119.169	2.554	3.666	0.000	0.000	0.530	0.000	0.189	0.310	2.546	Lx-m
121.262	2.782	3.651	0.000	0.000	0.531	0.000	0.189	1.215	2.759	2.5m
122.416	3.042	3.634	0.000	0.000	0.539	0.000	0.189	2.729	2.730	Lx=y
123.042	3.244	3.621	0.000	0.000	0.548	0.000	0.189	3.082	3.187	STP

M=0.6 Y=0.2 Λ = 1.25

AGE	L/L_o	T_{eff}	M_{con}	M_{sch}	M_{HE}	Y	XC	L_x	L_y	
0.000	1.423	4.054	0.230	0.087	0.499	0.999	0.000	0.895	1.272	
9.031	1.434	4.048	0.229	0.090	0.499	0.924	0.072	0.863	1.301	
11.833	1.435	4.046	0.229	0.090	0.499	0.900	0.094	0.843	1.310	
23.087	1.440	4.041	0.230	0.092	0.499	0.800	0.176	0.746	1.345	
34.138	1.449	4.032	0.229	0.093	0.499	0.700	0.247	0.633	1.380	
44.757	1.462	4.019	0.230	0.094	0.499	0.600	0.305	0.510	1.413	
55.135	1.480	4.001	0.228	0.097	0.499	0.500	0.351	0.379	1.447	
65.160	1.502	3.980	0.228	0.098	0.499	0.400	0.382	0.250	1.480	
74.468	1.527	3.957	0.225	0.099	0.499	0.306	0.395	0.138	1.511	
75.072	1.529	3.955	0.225	0.099	0.499	0.300	0.395	0.131	1.513	
84.814	1.558	3.927	0.224	0.100	0.499	0.200	0.386	0.045	1.546	
94.881	1.593	3.901	0.221	0.102	0.499	0.100	0.338	0.064	1.579	
100.383	1.614	3.894	0.223	0.104	0.499	0.050	0.287	0.224	1.592	
105.752	1.666	3.881	0.223	0.106	0.499	0.010	0.209	0.785	1.582	
107.259	1.782	3.764	0.199	0.080	0.499	0.001	0.183	1.349	1.419	
107.763	2.043	3.700	0.000	0.000	0.499	0.000	0.180	1.832	1.384	L-M
108.494	1.931	3.713	0.000	0.000	0.499	0.000	0.180	1.097	1.872	L-m
121.689	2.240	3.681	0.000	0.000	0.499	0.000	0.180	0.538	2.228	Lx-m
125.529	2.428	3.667	0.000	0.000	0.500	0.000	0.180	0.752	2.413	2.5m
129.210	2.811	3.641	0.000	0.000	0.508	0.000	0.180	2.503	2.499	Lx=y
130.050	2.983	3.631	0.000	0.000	0.514	0.000	0.180	2.826	2.962	STP

M=0.65 Y=0.2 Λ = 1.25

AGE	L/L_o	T_{eff}	M_{con}	M_{sch}	M_{HE}	Y	XC	L_x	L_y	
0.000	1.540	3.859	0.229	0.087	0.500	0.999	0.000	1.209	1.268	
11.867	1.549	3.854	0.229	0.090	0.500	0.900	0.094	1.181	1.310	
13.468	1.550	3.854	0.229	0.091	0.500	0.886	0.106	1.174	1.317	Te-m
23.084	1.551	3.857	0.231	0.092	0.500	0.800	0.176	1.123	1.350	
34.023	1.549	3.862	0.230	0.094	0.500	0.700	0.247	1.037	1.392	
43.414	1.548	3.863	0.232	0.095	0.500	0.609	0.301	0.942	1.427	Te-M
44.435	1.548	3.862	0.232	0.096	0.500	0.600	0.306	0.930	1.431	
54.426	1.552	3.855	0.230	0.098	0.500	0.500	0.352	0.806	1.469	
64.062	1.562	3.839	0.231	0.099	0.500	0.400	0.383	0.674	1.504	
73.499	1.579	3.812	0.229	0.100	0.500	0.300	0.398	0.542	1.539	
82.759	1.602	3.780	0.225	0.102	0.500	0.200	0.389	0.437	1.573	
92.345	1.634	3.759	0.226	0.103	0.500	0.100	0.342	0.444	1.604	
97.592	1.660	3.751	0.224	0.106	0.500	0.050	0.290	0.590	1.617	
102.682	1.727	3.736	0.227	0.107	0.500	0.010	0.213	1.054	1.603	
104.139	1.841	3.716	0.201	0.081	0.500	0.001	0.188	1.479	1.438	
104.654	2.090	3.690	0.000	0.000	0.500	0.000	0.185	1.871	1.695	L-M
119.189	2.331	3.671	0.000	0.000	0.505	0.000	0.185	0.483	2.322	Lx-m
122.448	2.538	3.658	0.000	0.000	0.506	0.000	0.185	0.968	2.519	2.5m
124.889	2.854	3.637	0.000	0.000	0.513	0.000	0.185	2.542	2.543	Lx=y
125.618	2.941	3.632	0.000	0.000	0.519	0.000	0.185	2.655	2.832	STP

M=0.7 y=0.2 Λ = 1.25

AGE	L/L_o	T_{eff}	M_{con}	M_{sch}	M_{HE}	Y	XC	L_x	L_y	
0.000	1.594	3.751	0.229	0.087	0.500	0.999	0.000	1.319	1.266	
11.839	1.608	3.747	0.229	0.090	0.500	0.900	0.094	1.309	1.309	
13.468	1.609	3.747	0.229	0.090	0.500	0.886	0.106	1.305	1.315	Te-m
23.186	1.611	3.749	0.231	0.091	0.500	0.800	0.176	1.267	1.352	
33.963	1.607	3.752	0.232	0.094	0.500	0.700	0.247	1.194	1.397	
44.333	1.602	3.756	0.232	0.097	0.500	0.600	0.306	1.099	1.441	
54.097	1.601	3.757	0.233	0.098	0.500	0.500	0.352	0.991	1.481	
54.505	1.600	3.757	0.234	0.098	0.500	0.496	0.352	0.987	1.482	
63.671	1.605	3.755	0.232	0.099	0.500	0.400	0.384	0.868	1.520	
72.733	1.616	3.749	0.230	0.102	0.500	0.300	0.399	0.741	1.556	
81.805	1.634	3.743	0.230	0.103	0.500	0.200	0.391	0.633	1.590	
91.069	1.664	3.735	0.226	0.105	0.500	0.100	0.344	0.617	1.622	
96.135	1.690	3.731	0.227	0.106	0.500	0.050	0.292	0.743	1.634	
101.042	1.758	3.721	0.226	0.109	0.501	0.010	0.215	1.140	1.619	
102.459	1.865	3.708	0.200	0.083	0.502	0.001	0.190	1.517	1.454	
102.960	2.105	3.687	0.000	0.000	0.503	0.000	0.187	1.884	1.722	L-M
103.547	1.985	3.696	0.000	0.000	0.504	0.000	0.187	1.261	1.904	L-m
116.727	2.343	3.670	0.000	0.000	0.508	0.000	0.187	0.422	2.334	Lx-m
120.427	2.597	3.654	0.000	0.000	0.510	0.000	0.187	1.093	2.575	2.5m
122.394	2.885	3.635	0.000	0.000	0.518	0.000	0.187	2.575	2.571	Lx=y
123.110	3.081	3.623	0.000	0.000	0.524	0.000	0.187	2.960	2.927	STP

M=0.8 Y=0.2 Λ = 1.25

AGE	L/L_o	T_{eff}	M_{con}	M_{sch}	M_{HE}	Y	XC	L_x	L_y	
0.000	1.651	3.727	0.228	0.087	0.500	0.999	0.000	1.424	1.263	
11.954	1.668	3.725	0.230	0.089	0.500	0.900	0.094	1.422	1.308	
14.577	1.670	3.725	0.229	0.091	0.500	0.877	0.114	1.417	1.319	Te-m
23.105	1.671	3.726	0.228	0.093	0.500	0.800	0.176	1.386	1.357	
33.593	1.668	3.728	0.230	0.096	0.500	0.700	0.248	1.327	1.405	
44.009	1.664	3.730	0.235	0.097	0.500	0.600	0.306	1.256	1.451	
53.617	1.663	3.731	0.233	0.096	0.501	0.500	0.353	1.171	1.496	
60.050	1.663	3.731	0.231	0.099	0.502	0.429	0.377	1.102	1.526	Te-M
62.638	1.664	3.731	0.231	0.100	0.502	0.400	0.385	1.073	1.538	
71.411	1.669	3.730	0.234	0.100	0.503	0.300	0.401	0.969	1.576	
80.223	1.682	3.727	0.233	0.105	0.504	0.200	0.393	0.866	1.612	
89.128	1.707	3.723	0.229	0.107	0.505	0.100	0.347	0.834	1.644	
93.973	1.733	3.719	0.227	0.109	0.506	0.050	0.296	0.926	1.656	
98.751	1.799	3.712	0.230	0.110	0.507	0.010	0.218	1.246	1.639	
100.114	1.899	3.702	0.205	0.083	0.508	0.001	0.192	1.572	1.476	
100.574	2.128	3.684	0.000	0.000	0.509	0.000	0.190	1.925	1.578	L-M
101.348	2.010	3.693	0.000	0.000	0.510	0.000	0.190	1.171	1.948	L-m
114.053	2.393	3.667	0.000	0.000	0.514	0.000	0.190	0.337	2.385	Lx-m
117.383	2.652	3.651	0.000	0.000	0.516	0.000	0.190	1.132	2.629	2.5m
119.054	2.924	3.634	0.000	0.000	0.523	0.000	0.190	2.612	2.612	Lx=y
119.834	3.298	3.611	0.000	0.000	0.533	0.000	0.190	3.270	2.834	STP

Figure 5.1) Radiative, ∇_R and adiabatic, ∇_A, temperature gradients, convective velocity, v, and He profile as a function of interior mass for the model with $M_{HB} = 0.7\ M_\odot$, $M_c = 0.475\ M_\odot$, and $\Lambda = 1$ at the age of 22×10^6 yr. The velocity is in units of 104 cm/sec

Figure 5.2) The same as in Fig. 1 but for the model with age of 99×10^6 yr

Figure 5.3) The mass of the convective core M_{con} and of the unstable region M_{sch} as a function of time during the central He-burning phase of the model with $M_{HB} = 0.7\ M_\odot$, $Y = 0.299$, $M_c = 0.475\ M_\odot$ and $\Lambda = 1$

Figure 5.4a) The HR diagram of HB stars with mass 0.60, 0.65, 0.70, 0.80 $M_\odot$, core mass $M_c = 0.475\ M_\odot$, $Y = 0.299$, $Z = 0.001$, and $\Lambda = 1$. For purposes of completeness also shown are the evolutionary tracks of initial mass 0.7 and 0.8 $M_\odot$ from the zero age main sequence up to the RGB tip

Figure 5.4b) The HR diagram of HB stars with mass 0.60, 0.65, 0.70, 0.80 $M_\odot$, core mass $M_{He} = 0.475\ M_\odot$, $Y = 0.299$, $Z = 0.001$, and $\Lambda = 1.25$. For purposes of completeness also shown are the evolutionary tracks of initial mass 0.7 and 0.8 $M_\odot$ from the zero age main sequence up to the RGB tip

Figure 5.4c) The same as in Figure 4a, but for $Y = 0.200$ and $M_{He} = 0.500\ M_\odot$ for the HB models. Evolutionary tracks for H-burning models of $M = 0.7, 0.8, 0.9\ M_\odot$ are also shown

Figure 5.5) The luminosity of the models with $M_{HB} = 0.70\ M_\odot$, $M_{He} = 0.475\ M_\odot$, $Y = 0.299$, and $\Lambda = 1$ and 1.25 as a function of time

Figure 5.6) The number of clusters as a function of R_2 from Buzzoni et al (1983). B1, B2, B3 C1, C2, C3, G, I1 and I2 indicate the theoretical predictions for R_2 contained in Table 4. Finally, A gives the average observational value for R_2 estimated by Buzzoni et al (1983)

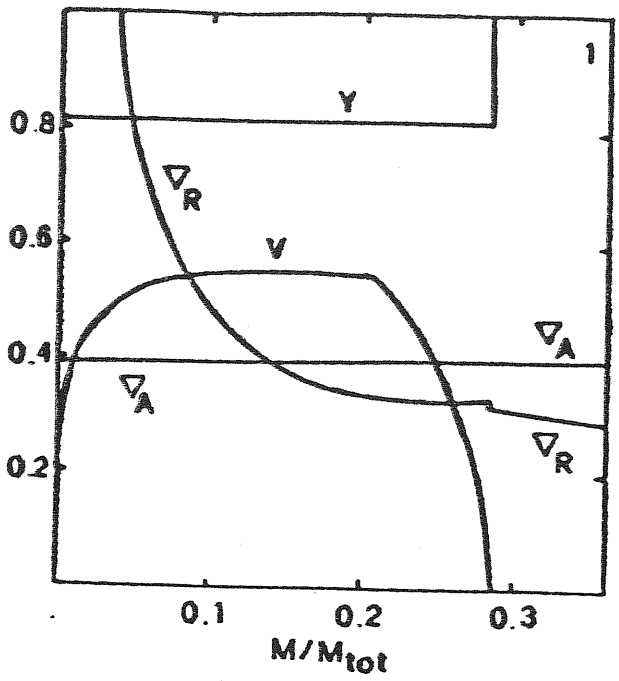
1
Y
0.8
∇_R
V
0.6
∇_A
0.4
∇_A
∇_R
0.2
0.1
0.2
0.3
M/M_{tot}

5.1

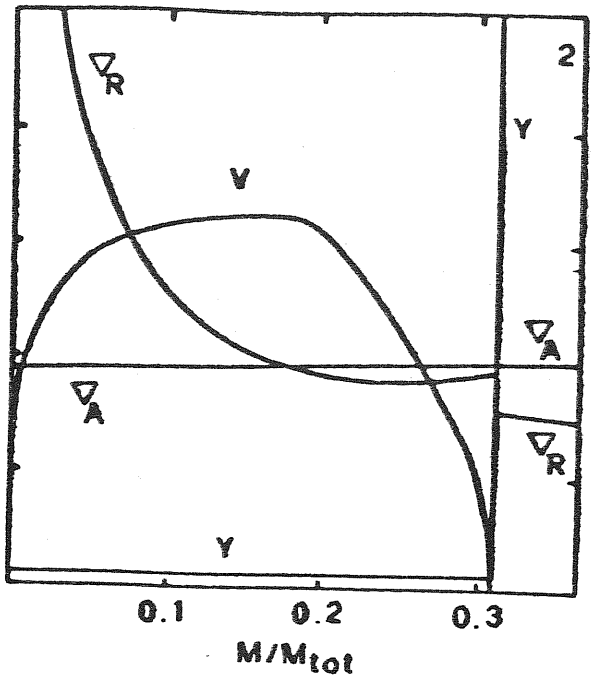
2
∇_R
Y
V
∇_A
∇_A
∇_R
Y
0.1
0.2
0.3
M/M_{tot}

5.2

5.3

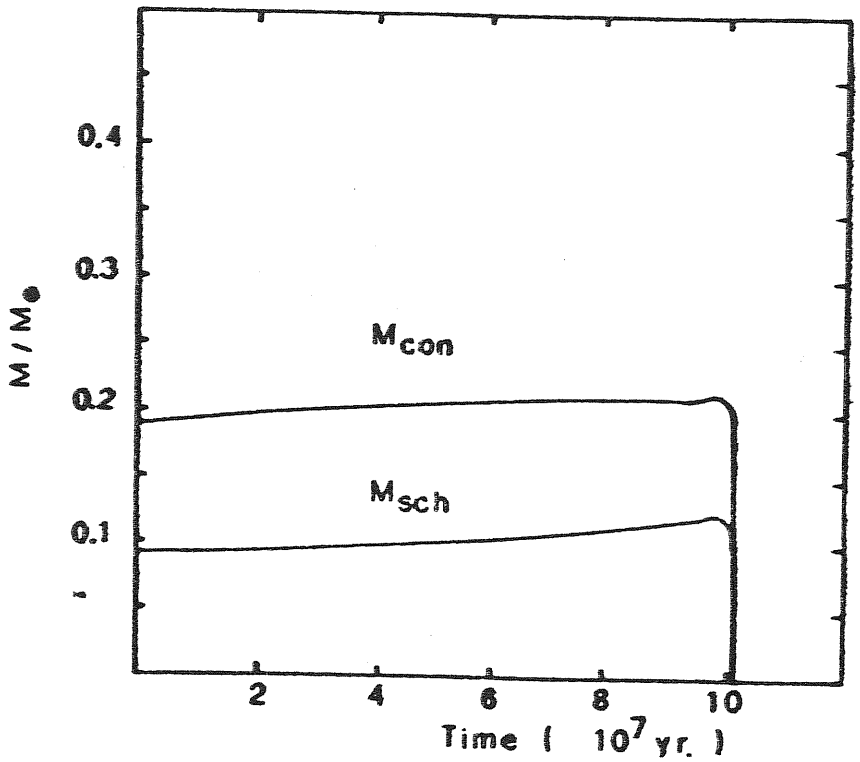
0.4
0.3
$M/M_\odot$
M_{con}
0.2
M_{sch}
0.1
2
4
6
8
10
Time (10^7 yr.)

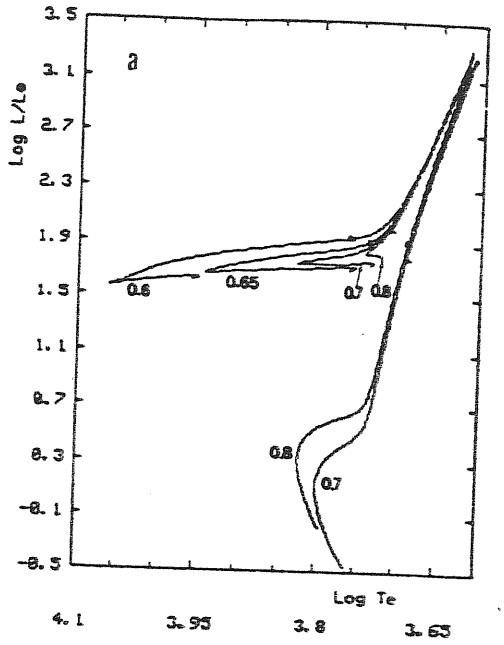
a
Log L/Le
3.5
3.1
2.7
2.3
1.9
1.5
1.1
0.7
0.3
-0.1
-0.5
0.6
0.65
0.7
0.8
0.8
0.7
Log Te
4.1
3.95
3.8
3.65

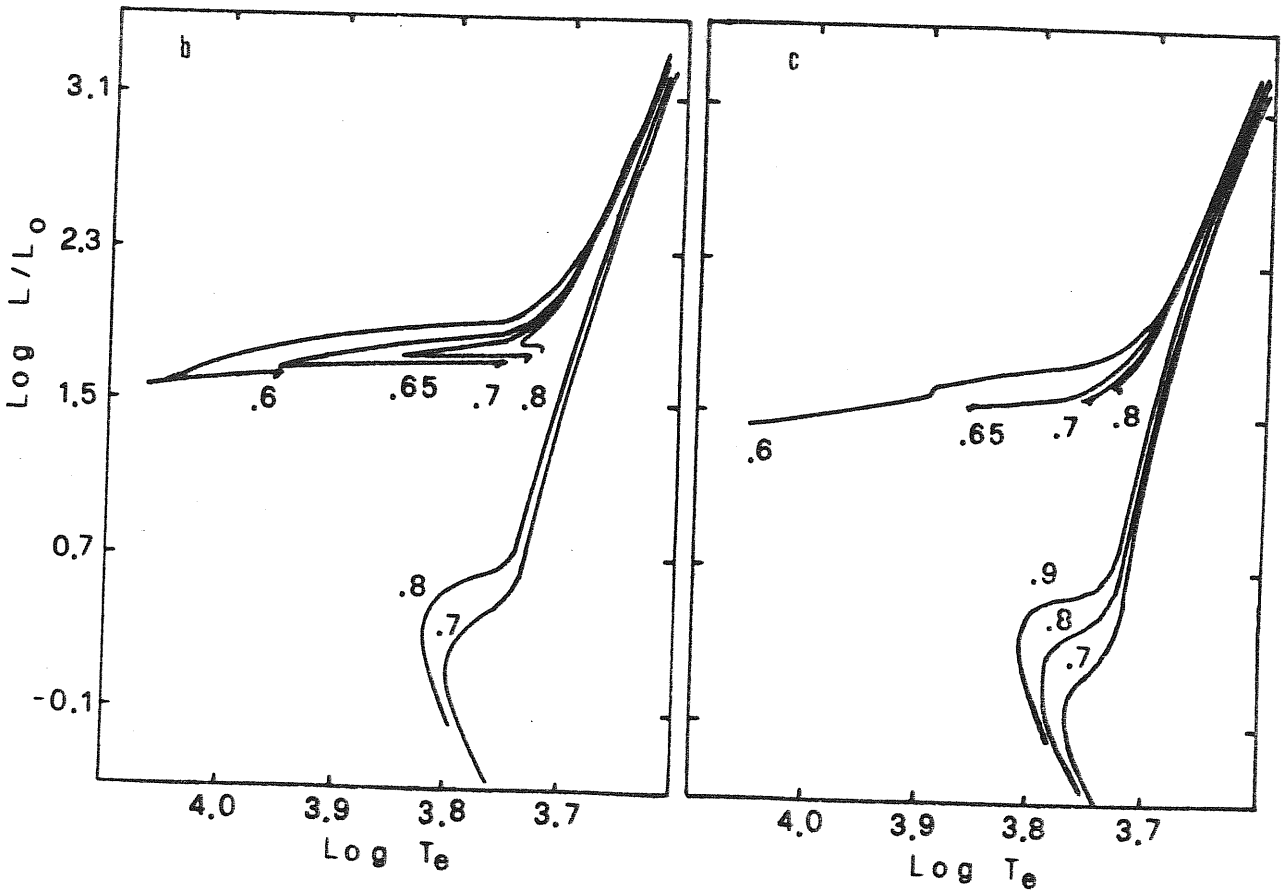
b
3.1
2.3
1.5
0.7
-0.1
Log L/Lo
.6
.65
.7
.8
.8
.7
4.0
3.9
3.8
3.7
Log Te
c
.6
.65
.7
.8
.9
.8
.7
4.0
3.9
3.8
3.7
Log Te

5.5

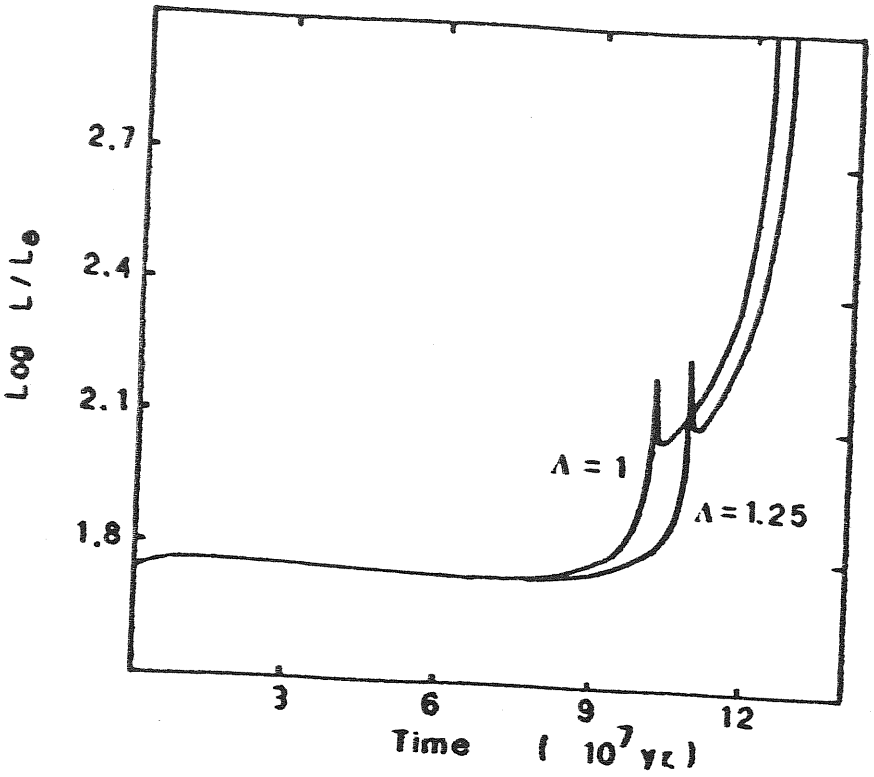
Log L/L⊙
2.7
2.4
2.1
1.8
Λ = 1
Λ = 1.25
3
6
9
12
Time (10⁷ yr)

5.6

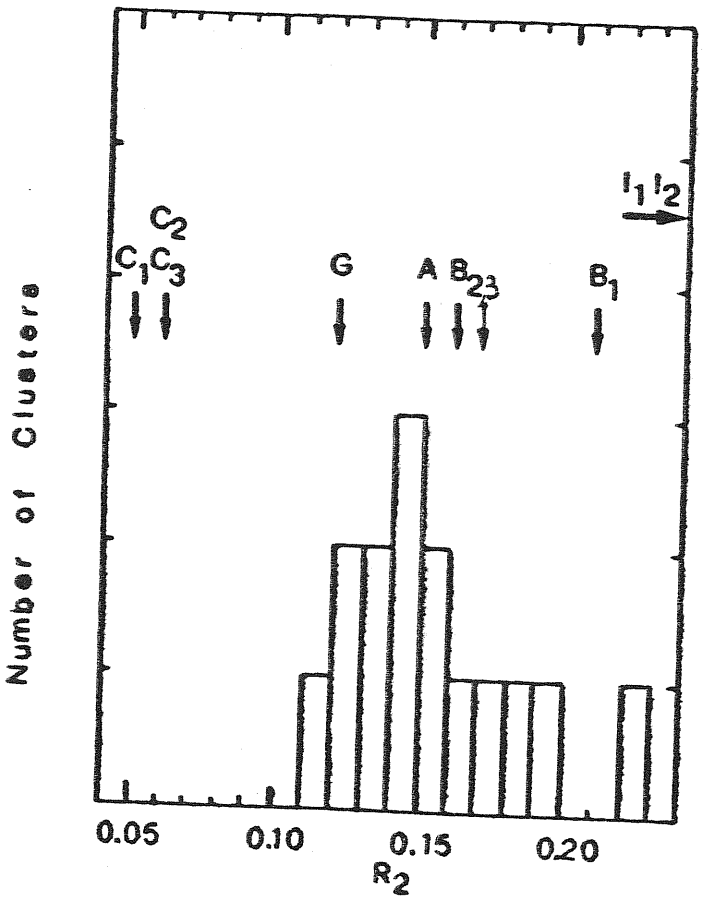
Number of Clusters
C2
C1C3
G
A
B23
B1
I1 I2
0.05
0.10
0.15
0.20
R2

Chapter VI

Conclusions.

In this thesis I have investigated on the effects of the overshooting from convective stellar cores all across the HR diagram. Making use of a new criterion which can be easily applied to stellar model computations, some relevant results have been obtained, demonstrating that, if overshooting exists, then it strongly affects the evolution of the stars and produces a series of consequences which allow the comparison with experimental data. On the other hand observations show some features that might be explained only invoking a more extended internal mixing.

Several independent evidences have been illustrated among which I recall the widening of the main sequence band for massive and intermediate mass stars; the peculiar morphology the HR diagram of galactic clusters in the age range of Pleiades to Hyades and of populous young globular clusters in LMC; the discrepancy between the masses of the Cepheid stars inferred from pulsational and from evolutionary properties; the absence of luminous asymptotic giant branch stars brighter than $M_{bol} = -6$ in the Magellanic Clouds; the discrepancy between turnoff and red giant populations in old open clusters.

To reconcile theory with observations various ways out have been proposed, but none of them are equally efficient in the different

areas described above.

Non-local overshooting only shows the remarkable property of alleviating all those independent discrepancies with about the same value of the mixing length parameter.

To compare non local overshooting with other models of convection (semiconvection, breathing convection) and to better estimate the free parameter Λ, I have calculated evolutionary tracks of horizontal branch stars up to the start of the thermally pulsing phase. The new models turned out to be similar to the classical ones, however with some important differences.

No semiconvection is found to develop at the border of the core, but mixing is complete up to where the convective velocities get zero. However the total amount of matter mixed during central Helium burning turned out to be less than that given by models with semiconvection.

Furthermore, by following the velocity field and requiring that velocities are actually sufficient to mix matter, in a consistent way one may rule out the occurrence of breathing convection at the end of central Helium exhaustion. Major attention has been paid by Castellani et al (1985a) to breathing convection (found to occur in all the previous studies of the subject) as a possible mechanism improving the agreement between theory and observations in LMC intermediate age clusters. On the contrary, the analysis of observational data and, in particular, the ratio R_2 suggest that this mechanism likely does not occur in real

stars, otherwise the expected number of AGB stars should be approximately lower than the observed one by a factor of two.

Thus one may conclude that both semiconvection and breathing convection are merely a consequence of the local treatment of convective instability and that they do not occur when a more physically sound description is assumed. Models with overshooting contain the parameter Λ to be determined by the comparison with the observational data. The comparison of theoretical versus observational R_2 ratios indicates that the value of Λ=1.25 ought to be preferred. The uncertainty is mainly due to the observational data, as the ratio in question is very sensitive to Λ, and almost independent of the He abundance of the models and the initial mass M_{HB} in the narrow range pertinent to globular clusters. This optimal value of 1.25 is slightly larger than the one adopted for interpret the previously recalled discrepancies. However, none of the above observational constraints is able to contrive the amount of overshooting by as much as observations in old globular clusters. The estimate of Λ inferred from those constraints ought to be taken as a lower limit, so that slightly larger values could be even more appropriate.

Finally it is worth mentioning that in a very recent work on massive stars, in which the dynamic behaviour of turbulent fields is studied in detail, Xiong (1986) confirms all the above conclusions and in particular the extension of the stable region which is mixed by convective overshooting.

APPENDIX

A1 The Roxburgh criterion.

Roxburgh's criterion rests upon the averaged form of the thermal energy conservation equation of fluidodynamics;and its derivation proceeds as follows. The mass,momentum and total energy conservation equations in which gravity, nuclear energy sources,radiative flux are accounted for, while viscosity,conductive flux and composition changes are neglected can be written in cartesian coordinates (Ledoux and Walraven 1958)

$$\partial\rho/\partial t + \partial/\partial_i(\rho v_i) = 0 \qquad (A1)$$

$$\partial/_{\partial t}(\rho v_i) + \partial/\partial_j(\rho v_i v_j) = -\partial p/\partial x_i - \rho g_i \qquad (A2)$$

$$\partial/_{\partial t}\rho(e+v^2/2) + \partial/\partial_i[\ \rho v_i(W+v^2/2)] = \varepsilon\rho - \partial F_i/\partial x_i - \rho g_i v_i \qquad (A3)$$

where summation is intended on repeated indices,and symbols have the following meaning:

$W = e + p/\rho$ = enthalpy per unit mass

e =internal energy per unit mass

ε =rate of nuclear energy production per unit mass

p, T, ρ =pressure,density,temperature

F_i, g_i, v_i = i-component of radiative flux,gravitational acceleration and velocity.

Multiplying eq. (A2) by v_i one obtains the mechanical energy conservation equation

$$\frac{\partial}{\partial t}\left(\rho\frac{v^2}{2}\right)+\frac{\partial}{\partial x_i}\left(\rho v_i\frac{v^2}{2}\right)=-v_i\frac{\partial p}{\partial x_i}-\rho v_i g_i \qquad \text{(A4)}$$

Subtracting eq. (A4) from eq. (A3) and using the thermodynamic identity

$$dW=T\,dS+\frac{dp}{\rho} \qquad \text{(A5)}$$

one obtains the thermal energy conservation equation(Ledoux and Walraven 1958)

$$\frac{\partial}{\partial t}(\rho S)+\frac{\partial}{\partial x_i}(\rho S v_i)=-\frac{1}{T}\frac{\partial F_i}{\partial x_i}+\frac{\varepsilon\rho}{T}\equiv\frac{A}{T} \qquad \text{(A6)}$$

Following Roxburgh(1978) I now specify the above equation for the case of a turbulent medium. If the characteristic scales of turbulence are much shorter than the characteristic scales of the convective medium ,it is possible to separate thermodynamic quantities $f(x_i,t)$ in a mean part independent of time $f_o(x_i)$ and a fluctuating time dependent part $f_1(x_i,t)$ in such a way that

$$f(x_i,t) = f_o(x_i) + f_1(x_i,t)$$

$$f_1 / f_o \ll 1$$

$$\overline{f(x_i,t)} = f_0(x_i) \qquad \text{(A7)}$$

where the bar denotes an average process over fluctuations. In particular note that conservation of mass requires (no net transport of mass):

$$\overline{\rho v_i} = 0 \qquad \text{(A9)}$$

and then for any thermodynamic quantity f

$$\overline{\rho v_i f} = \overline{\rho v_i f_0} + \overline{\rho v_i f_1} = \overline{\rho v_i} f_1$$

Furthermore from eq. (A1) one gets

$$\overline{\rho v_i \frac{\partial f}{\partial x_i}} \simeq \overline{\frac{\partial}{\partial x_i} \rho v_i f_1}$$

With the aid of the above equations the Roxburgh condition can be easily derived. Equation (A5) writes in the averaged form

$$\overline{\frac{\partial}{\partial t}(\rho_1 S_1)} + \overline{\frac{\partial}{\partial x_i}(\rho v_i S_1)} = \overline{\frac{A_0}{T_0}} - \overline{\frac{A_1 T_1}{T_0}} \qquad \text{(A10)}$$

and neglecting the first and last term

$$\overline{\frac{\partial}{\partial x_i} T_0 \rho v_i S_1} - \overline{\rho v_i S_1 \frac{\partial T_0}{\partial x_i}} = A_0 = -\frac{\partial F_{0i}}{\partial x_i} + \varepsilon_0 \rho_0 \qquad \text{(A11)}$$

Integrating eq. (A11) in spherical symmetry from r_1 to r_2 (the borders of the convective zone) one has

$$r^2 T_0 \rho v S_1 \Big|_{r_1}^{r_2} - \int_{r_1}^{r_2} r^2 \rho v S_1 \frac{\partial T_0}{\partial r} dr = -r^2 F_0 \Big|_{r_1}^{r_2} + \int_{r_1}^{r_2} \varepsilon_0 \rho_0 r^2 dr$$

Now $v(r_1)=v(r_2)=0$ by definition and

$$\varepsilon_0 \rho_0 r^2 = \frac{\partial}{\partial r}\left(\frac{L_N}{4\pi}\right) \qquad 4\pi r^2 F_R \Big|_{r_1}^{r_2} = L_N \Big|_{r_1}^{r_2}$$

because outside the convective region energy is supposed to be carried out by radiation alone. Then the Roxburgh condition is:

$$\int_{r_1}^{r_2} 4\pi r^2 \overline{\rho v S_1} \frac{\partial T_0}{\partial r} dr = 0 \qquad \text{(A12)}$$

This condition is integrable if one knows the temperature gradient, the run of s, v and across the convective region. Since these quantities are not known a priori, the difficulty is overcome by Roxburgh defining the convective flux to be

$$F_c = T_0 \overline{\rho v S_1}$$

Thus equation (A12) becomes

$$\int_{r_1}^{r_2} 4\pi r^2 \frac{F_c}{T_0} \frac{\partial T_0}{\partial r} dr = 0 \qquad \text{(A13)}$$

and because $\partial T_0/\partial r < 0$, inside stars Fc has to change sign (this corresponds to overshooting). Condition (A13) may easily be integrated if one estimates Fc and $\partial T_0/\partial r$ (the adiabatic one) in the convective region(Roxburgh 1978). The nature of the integrand in equation (A12) has been however recently questioned by Eggleton(1983) who mainly arose doubts about its physical nature. Doom (1984) has identified this term with the divergence of the turbulent kinetic energy flux F_t and has reobtained the same condition. However both conditions(A12) and (A13) may be subjected to some criticism,as it will be discussed in the following ,which invalidate their correctness.

First I like to clarify the role of pressure fluctuations that explicitly are said to be accounted for in obtaining condition (A12) and (A13) in Roxburgh (1978). If pressure fluctuations are not negligible , then from equation (A3) one sees that the convective flux is given by

$$F_{c_i} = \overline{\rho v_i W} = \overline{\rho v_i W_1} = T_0 \overline{\rho v_i S_1} + \overline{v_i P_1}$$

and not simply $Fc = T_o \overline{\rho v_i S_1}$ as in Roxburgh. The contribution to Fc by the turbulent kinetic energy flux is not contained in the above expression, as it is accounted for separately in the basic equations. The presence of the term $v_i p_1$ obviously invalidates the Roxburgh criterion because now the a priori knowledge of the structure variables v_i and p_1 is necessary to proceed further. On the other hand ,pressure fluctuations are negligibly small when turbulent velocities are much less than the sound velocity (Cox and Giuli 1968). As a consequence of this, the average kinetic energy flux is negligible with respect to the thermal convective flux as it may be seen on the basis of the following estimates. The turbulent kinetic energy flux Fk is

$$F_{K_i} = \frac{1}{2} \overline{\rho v^2 v_i} \simeq \rho_o \overline{v^2}\ \overline{v_i}$$

while the convective flux is (i-component)

$$Fc_i = \overline{C_p \rho T v_i} \simeq c_p T_o \rho_o \overline{v_i} \simeq \rho_o v_{SOUND}^2 \overline{v_i}$$

c_p = specific heat at constant pressure

(note that $\overline{v}$ is a very small quantity as long as ρ_1 / ρ_0 is $<< 1$)

so that

$$Fc_i / Fc_i \simeq \frac{\overline{v^2}}{v_{SOUND}} \ll 1 \quad \text{IF} \quad v \ll v_{SOUND}$$

Therefore , if pressure fluctuations are negligibly small the averaged form of the total energy conservation equation (A3) becomes

$$\frac{\partial}{\partial x_i} \overline{T_0 \rho v_i S_1} = A_0 = -\overline{\frac{\partial F_i}{\partial x_i}} + \varepsilon_0 \rho_0 \qquad \text{(A14)}$$

This equation is about equal to the average form of the thermal energy equation (A11) since mechanical terms in it turn out to be negligibly small (note that I refer to averaged quantities). Equations (A11) and (A14) must differ within the order of approximation we have been using in the derivation procedure. In fact , subtracting eq. (A11) from eq. (A14) one gets (neglecting time derivatives)

$$\overline{\rho v_i S_1 \frac{\partial T_0}{\partial x_i}} = \overline{\frac{A_1 T_1}{T_0}} \qquad \text{(A15)}$$

which explicitly shows that Roxburgh's criterion follows from a second order approximation term, while other of the same order have been neglected. Turning now to the interpretation given by Doom (1984) according to which the term of relation (A15) identifies with the divergence of the turbulent kinetic energy flux it can be argued as follows.

Averaging eq (A5) one gets

$$\frac{\partial}{\partial x_i} \overline{\rho v_i \frac{v^2}{2}} = -\overline{v_i \frac{\partial P}{\partial x_i}} \qquad \text{(A16)}$$

which may be written using the thermodynamic relation (A5)

$$\frac{\partial}{\partial x_i} \overline{\rho v_i \frac{v^2}{2}} = -\frac{\partial}{\partial x_i} \overline{\rho v_i w_1} + \frac{\partial}{\partial x_i} \overline{T_0 \rho v_i S_1} - \overline{\rho v_i S_1} \frac{\partial T_0}{\partial x_i} + \overline{\rho v_i T_1} \frac{\partial S_0}{\partial x_i}$$

inserting the following relations for the fluctuations

$$W_1 = T_0 S_1 + \frac{P_1}{P_0}$$

one gets

$$\frac{\partial}{\partial x_i} \overline{\rho v_i \frac{v^2}{2}} = -\frac{\partial}{\partial x_i} \overline{v_i P_1} - \overline{\rho v_i S_1} \frac{\partial T_0}{\partial x_i} + \overline{\rho v_i T_1} \frac{\partial S_0}{\partial x_i} \qquad \text{(A17)}$$

This equation first shows that the divergence of Fk is not simply given by $\frac{\partial F_k}{\partial x_i} = \overline{\rho v_i S_1} \frac{\partial T_0}{\partial x_i}$ but further terms have to be considered. Second, if one integrates equation (A17) from r_1 to r_2 (borders of convective region) the condition below is derived

$$\int_{r_1}^{r_2} \overline{r^2 \rho v S_1} \frac{\partial T_0}{\partial r} dr = \int_{r_1}^{r_2} \overline{r^2 \rho v T_1} \frac{\partial S_0}{\partial r} dr$$

which clearly contradicts Roxburgh's condition since the two term are independent and thus cannot be set equal to zero separately.

A2 Conclusions

The Roxburgh criterion for determining the extension of stellar convective cores result from arbitrarily retaining in first order approximation of thermal energy conservation equation, the term

$$\overline{\rho v_i S_1} \quad \frac{\partial T_0}{\partial x_i}$$

which in reality turns out to belong to the second order approximation of the same equation (involving also time

derivatives of the fluctuations) so that further terms should be included for the sake of internal consistence. Consequently the identification of the above term with the divergence of the turbulent kinetic energy flux suggested by Doom(1984) is not correct. Therefore , despite of their simplicity and lack of any free parameter those criteria are not physically consistent.

REFERENCES

Adams T.F.,Castor J.I.,Davis C.G. ,1980 in Current Problems in Stellar Pulsation Instabilities ed. D.Fischel,J.R.Lesh and W.M.Sparks p. 175

Barbaro, G., Pigatto, L. : 1984, Astron. Astrophys. 136, 355

Beaudet, G.,Petrosian,V., Salpeter, E.E. :1967, Astrophys. J. 150, 979

Baker N. H. , Kuhfuss R. 1986 Astron. Astrophys. in press

Becker S.A.,Iben I.J. 1979 Astrophys. J. 232,831

Becker, S. A., Mathews, G. J. : 1983, Astrophys. J. 270, 155

Bertelli, G., Bressan, A., Chiosi, C. :1984, Astron. Astrophys. 130,279

Bertelli, G., Bressan, A., Chiosi, C. :1985, Astron. Astrophys. 150, 33

Bertelli, G., Bressan, A., Chiosi, C., Angerer, K. : 1986a, Astron. Astrophys.in press

Bertelli, G., Bressan, A., Chiosi, C.:1986b, in preparation

Blanco V.M.,Mc Carthy M.,Blanco B.M. 1980 Astrophys. J. 242,938

Bohm-Vitense E. 1958 Zs.f.Astrophys. 46,108

Bressan, A., Bertelli, G., Chiosi, C. :1981, Astron. Astrophys. 102, 25

Bressan, A., Bertelli, G., Chiosi, C. :1986 in The Age of Stellar Systems Mem. Soc. Astron. It. in press

Bressan, A. G. 1984 :Thesis for "Magister Philosophiae" I.S.A.S. Trieste

Buonanno, R., Corsi, C.E., Fusi Pecci, F. : 1985, Astron. Astrophys. 145, 97

Buser R.,Kurucz R.L. 1978 Astron.Astrophys. 70,555

Buzzoni, A., Fusi Pecci, F., Buonanno, R., Corsi, C.E. : 1983 Astron. Astrophys. 128, 94

Calvani M. , Turolla R. , Nobili L. 1986 preprint

Canuto, V. : 1970, Astrophys. J. 159, 641

Caputo, F., Castellani, V., Wood, P.R. : 1978, Mon. Not. R. astr. Soc. 184, 377

Carson T.R. 1976 Ann.Rev.Astr.Astrophys. 14,95

Carson T.R.,Stothers R.B. 1984 Astrophys. J. 276,593

Carson 1984 preprint

Castellani, V., Giannone, P., Renzini, A. : 1971a, Astrophys. and Space Sci. 10, 340

Castellani, V., Giannone, P., Renzini, A. : 1971b, Astrophys. and Space Sci. 10, 355

Castellani, V., Chieffi, A., Pulone, L., Tornambe', A. : 1985a, Astrophys. J. Lett. 294, L31

Castellani, V., Chieffi, A., Pulone, L., Tornambe', A. : 1985b, Astrophys. J. 296, 204

Chiosi, C., Bertelli, G., Bressan, A., Nasi, E. : 1986, Astron. Astrophys. 165 , 84

Chiosi C. , Maeder A. 1986 Ann. Rev. Astron. Astrophys.

Chiosi C.,Nasi E., Sreenivasan S.R. 1978 Astron.Astrophys 68,467

Chiosi C. , Summa C. 1970 Astrophys.Sp. Sci. 8,478

Christy R.F. 1968 Q.J.R.Astron.Soc. 9,13

Christy R.F. 1974 Mem.Soc.R.Sci. Liege 8,13

Ciardullo R.B., Demarque P. 1977 Yale Trans. vol 33

Cloutmann, L. D., Whitaker, R. : 1980, Astrophys. J. 237, 900

Cloutman L.D.,Whitaker R. ,1980 A.P.J. 237,900

Cogan B.C. 1970 Astrophys. J. 162,139

Cox and Giuli ,1968 Principles of Stellar Structure.

Cox, A. N., Stewart, J. N. : 1970a, Astrophys. J. Suppl. 19, 243

Cox, A. N., Stewart, J. N. : 1970b, Astrophys. J. Suppl. 19, 261

Cox A. N. 1980 , Ann. Rev. Astron. Astrophys. 18 , 15

de Loore C.,Willis A., 1982 in "Wolf Rayet stars: Observations, Physics,Evolution" IAU Symposiumn. 99,eds. de Loore C., Willis A.

Doom C. 1982a ,Astron.Astrophys. 116,303

Doom C. 1982b ,Astron.Astrophys. 116,308

Doom C. 1985 ,Astron. Astrophys. 142, 143

Doom C., de Greeve J. P., de Loore C. 1986 Astrophys. J. 303,136

Eggleton P.P.,1983 Mon.Not.Roy.Astron.Soc.204,449

Fowler W.A.,Caughlan G.R.,Zimmerman B.A. 1975 Ann.Rev.Astron. Astrophys. 13,69

Frike K.,Stobie R.S.,Strittmatter P.A. 1971 M.N.R.A.S. 154,23

Frike K.,Stobie R.S.,Strittmatter P.A. 1972 Astrophys. J. 171,593

Frogel J.,Blanco V.M. 1983 in Observational Tests of Stellar Evolution Theory, eds. Maeder A. and Renzini A.

Garmany C.D.,Olson G.L.,Conti P.S.,Van Steenberg M. 1981
Astrophys. J. 250,660

Gingold, R. A. : 1976, Astrophys. J. 204, 116

Hanson R.B. 1977 IAU Symp.N.80 The H-R Diagram
ed. A.G.D. Philip,D.S. Hayes p. 154

Hodge, P. W. : 1983, Astrophys. J. 264, 470

Huang R.Q.,Weigert A. 1983 Astron.Astrophys. 127,309

Hubbard, W. B., Lampe, M. : 1969, Astrophys. J. Suppl. 18, 297

Humphreys R.M. 1978 Astrophys. J.Supp. 38,309

Humphreys R.M.,Davidson K. 1979 Astrophys. J. 232, 409

Iben I.J. 1967 Ann.Rev.Astron.Astrophys. 5,571

Iben I.J. 1972 Astrophys. J. 178,433

Iben I.J. 1974 R.S.Ann.Rev.Astron.Astrophys.12,215

Iben I.J. 1975 Astrophys. J. 196,525

Iben I.J. 1977 Astrophys. J. 217,788

Iben I.J. 1981 Astrophys. J. 246,278

Iben, I. J. : 1986, Astrophys. J. 304, 201

Iben I.J. ,Renzini A. 1982 a, Astrophys. J. letters 259, L 79

Iben I.J. ,Renzini A. 1982 b, Astrophys. J. letters 263, L 188

Iben I.J. ,Renzini A. 1984 , Physic Report 105, 329

Iben, I. J., Rood, R. T. : 1970 Astrophys. J. 161, 587

Iben I.J.,Tuggle R.S. 1972 a Astrophys. J. 173,135

Iben I.J.,Tuggle R.S. 1972 b Astrophys. J. 178,441

Kettner K.U.,BeckerH.W.,Buchmann L.,Gorres J.,Kravinkel H. Rolfs
C.,Schmalbrok P.,Trautvetter H.P.,Vlieks A.

Z.Phys.-Atoms and Nuclei 308,73

Lattanzio, J.C. : 1986, preprint

Lauterborn D.,Refsdal S.,Weigert A. 1971 Astron. Astrophys 10,97

Ledoux V.I.,Walraven Th.1958,Handbuch der Physik 51,447

Maeder, A. : 1975, Astron. Astrophys. 40, 303

Maeder A. 1976 Astron. Astrophys. 47,389

Maeder A. 1981 a Astron. Astrophys 99,97

Maeder A. 1981 b Astron. Astrophys 102,42

Maeder, A., Mermilliod, J. C. : 1981, Astron. Astrophys. 93, 136

Matraka B.,Wassermann C.,Waigert A.,1982 Astron.Astrophys.107,283

Meyland G., Maeder A. 1982 Astron. Astrophys. 108,148

Mould, J., Aaronson, M. : 1980 Astrophys. J. 240,464

Mould, J., Aaronson, M. : 1982a, Astrophys. J. Suppl. 48, 161

Mould, J., Aaronson, M. : 1982b, Astrophys. J. 263, 629

Mould, J., Aaronson, M. : 1986, Astrophys. J. 303, 10

Mould, J.:1983, in Structure and Evolution of the Magellanic Clouds, ed. S. van den Bergh, K. S. de Boer, p. 195. Dordrecht, Reidel

Nomoto K. 1984 in Stellar Nucleosynthesis, eds. Chiosi C. and Renzini A., p. 239

Paczynski B. 1970 Acta Astron. 20,47:20,287

Pigatto, L. : 1986 in The Age of Stellar Systems , Mem. Soc. Astron. It. in press

Reimers D. 1975 Mem.Soc.Roy.Sci. Liege 8,369

Renzini, A. : 1977, in Advanced Stages in Stellar Evolution, 7th Course of the Swiss Society of Astronomy and Astrophysics, ed. P. Bouvier and A. Maeder. p. 151. Geneva Observatory

Renzini , A. 1984 in "Stellar Nucleosynthesis" ed. C. Chiosi and A. Renzini , Dordrecht Reidel , pag. 99

Renzini , A., Bernazzani M., Buonanno R. , Corsi C.E. 1985 Astrophys. J. 294, L31

Robertson J.N. Astrophys. J. 170,353

Roxburgh I. 1965 M.N.R.A.S. 130,223

Roxburgh, I. : 1978, Astron. Astrophys. 65, 281

Sandage A.,Tamman G.A. 1969 Astrophys. J. 167,293

Saslow W.C. ,Schwarzschild M. 1965 Astrophys. J. 142,1468

Schmidt E. G. ,1984 , Astrophys. J. 285, 501

Shaviv G. ,Salpeter E.E. 1973 Astrophys. J. 184,191

Stobie R.S. 1969a M.N.R.A.S. 144,461

Stobie R.S. 1969b M.N.R.A.S. 144,485

Stobie R.S. 1969c M.N.R.A.S. 144,51

Stothers R., Chin C.W. 1984 preprint

Sweigart, A. V., Gross, P. G.:1976, Astrophys. J. Suppl. 32, 367

Sweigart A.V.,Gross P.G. 1978 Astrophys. J.Supp. 36,405

Sybesma C. H. B. 1985 Astron Astrophys 142, 171

Sybesma C. H. B. 1985 Astron Astrophys 159, 108

VandenBerg D.A.,Bridges T.J. 1984 Astrophys. J. 278,679

VandenBerg D. A. , 1985 , Astrophys. J. Suppl. 58, 561